



**Międzyuczelniany Wydział
Biotechnologii**

Uniwersytetu Gdańskiego
i Gdańskiego Uniwersytetu Medycznego

ROZPRAWA DOKTORSKA

Mgr Michał Karol Pierański

Ewaluacja potencjału fotoinaktywacji w eradykacji nosicielstwa *Streptococcus agalactiae* w układzie moczowo-płciowym

Evaluation of photoinactivation potential
in eradication of *Streptococcus agalactiae*
in the urogenital system

Praca przedstawiona
Radzie Dyscypliny Nauki Biologiczne Uniwersytetu Gdańskiego
celem uzyskania stopnia doktora
w dziedzinie nauk ścisłych i przyrodniczych
w dyscyplinie nauki biologiczne

Promotor: Dr hab. Mariusz Grinholc, prof. UG
Zakład Fotobiologii i Diagnostyki Molekularnej

GDAŃSK 2023

Podziękowania

Chciałbym podziękować dr hab. Mariuszowi Grinholc, prof. UG za przyjęcie mnie pod swoje skrzydła. Za to, że zawsze potrafił znaleźć rozwiązania moich licznych rozterek, że potrafił zapewnić mnie, że niepotrzebnie się martwię, a przede wszystkim za błyskawiczną współpracę w przypadku wszystkich goniących terminów. W dodatku dziękuję za wspieranie mnie w moim rozwoju i poszukiwaniu własnej ścieżki, a przede wszystkim za to, że zawsze można na Nim polegać.

Dziękuję również wszystkim obecnym i byłym pracownikom Zakładu Fotobiologii i Diagnostyki Molekularnej: dr hab. Joannie Nakoniecznej, prof. UG, dr Agnieszce Bernat-Wójtowskiej, dr Magdzie Rybickiej-Misiejko, dr Annie Wróblewskiej i dr Alicji Sznarkowskiej za wielokrotne dzielenie się swoim doświadczeniem, nie tylko laboratoryjnym, oraz przede wszystkim za każde dobre słowo.

Podziękowania, których nie da się ubrać w słowa należą się dr Aleksandrze Rapackiej-Zdończyk, dr Agacie Woźniak-Pawlikowskiej, dr Patrycji Ogonowskiej, Klaudii Szymczak, Beacie Kruszewskiej-Naczek i Natalii Burzyńskiej. To z nimi dzieliłem wszystkie sukcesy i porażki, spędziłem razem wiele weekendów w laboratorium, zawsze mogłem liczyć na pomoc, a przede wszystkim także na fantastyczną atmosferę.

Pragnę podziękować również wszystkim pozostałym pracownikom i doktorantom Międzyuczelnianego Wydziału Biotechnologii ze szczególnym wyróżnieniem dla dr hab. inż. Aleksandry Królickiej, prof. UG, dr Anny Kawiak, Grażyny Achramowicz, Izabeli Śmigielskiej oraz Małgorzaty Świdorskiej za nawigację w funkcjonowaniu w ramach uczelni oraz dbanie o atmosferę zachęcającą do przychodzenia do laboratorium.

Ponadto dziękuję również mojej rodzinie oraz przyjaciołom: Danielowi i Celinie za wspieranie mnie na każdym kroku oraz motywowanie do wytrwania w podjętych zobowiązaniach.

Table of content

Streszczenie.....	4
Abstract	6
Funding acknowledgements	8
Chapter I.....	9
Introduction	9
Hypothesis and aims of the work.....	12
Chapter II	13
An extended logistic model of photodynamic inactivation for various levels of irradiance using the example of <i>Streptococcus agalactiae</i>	13
1. Summary of the publication.....	13
2. Publication	14
Chapter III.....	32
Increased photoinactivation stress tolerance of <i>Streptococcus agalactiae</i> upon consecutive sublethal phototreatments	32
1. Summary of the publication.....	32
2. Publication	33
Chapter IV.....	47
Optimization of <i>Streptococcus agalactiae</i> Biofilm Culture in a Continuous Flow System for Photoinactivation Studies	47
1. Summary of the publication.....	47
2. Publication	48
Chapter V	64
Antimicrobial photodynamic inactivation: an alternative for Group B <i>Streptococcus</i> vaginal colonization in a murine experimental model.....	64
1. Summary of the publication.....	64
2. Publication	65
Summary	87
Literature.....	88
Attachments.....	92
1. Statements of contribution	92

Streszczenie

Streptococcus agalactiae – najczęstszy przedstawiciel paciorkowców grupy B (eng. Group B *Streptococcus* - GBS), mimo że jest uznawany za bakterię komensalną u dorosłych, jest głównym źródłem inwazyjnych infekcji u noworodków, a ostatnio także u kobiet w ciąży, osób starszych oraz osób z obniżoną odpornością. Infekcje wywołane przez GBS mogą wywoływać szerokie spektrum chorób takich jak: bakteriemia, posocznica, zapalenie płuc, infekcje dróg moczowych, ostre i przewlekłe zapalenie szpiku i innych. Leki pierwszego rzutu stosowane przeciwko GBS to antybiotyki β -laktamowe. Wraz z rosnącym spadkiem wrażliwości drobnoustrojów na penicylinę i opornością na inne antybiotyki istnieje ogromne zapotrzebowanie na opracowywanie alternatywnych terapii. Przeciwdrobnoustrojowa inaktywacja fotodynamiczna (eng. antimicrobial Photodynamic Inactivation - aPDI) jest jedną z proponowanych terapii, która zapewnia alternatywne rozwiązanie problemu antybiotykooporności bakterii. Wymaga jednoczesnej obecności fotosensybilizatora (eng. photosensitizer - PS), światła o określonej długości fali i tlenu. W efekcie powstają reaktywne formy tlenu (RFT), które wywołują uszkodzenia błon komórkowych, białek i kwasów nukleinowych, końcowo doprowadzając do śmierci komórek bakteryjnych.

Celem pracy była ocena bakteriobójczego działania aPDI wobec różnych serotypów *S. agalactiae* i przedstawicieli fizjologicznej flory pochwy człowieka, ocena fototoksyczności aPDI wobec ludzkich keratynocytów, stworzenie rozszerzonego modelu logistycznego aPDI dla różnych intensywności naświetlania, ocena możliwości rozwoju oporności/tolerancji na aPDI, określenie potencjału mutagennego aPDI i wreszcie ocena potencjału aPDI w dekolonizacji *S. agalactiae* z pochwy myszy.

aPDI z wykorzystaniem różu bengalskiego (RB) została wybrana jako najskuteczniejszy wariant aPDI w zmniejszaniu żywotności *S. agalactiae* *in vitro*. Wywoływała mniejszy spadek żywotności przedstawicieli fizjologicznej flory pochwy człowieka niż *S. agalactiae*. Badania modelowania komputerowego zaowocowały stworzeniem rozszerzonego modelu logistycznego aPDI, który efektywnie opisuje dynamikę śmiertelności *S. agalactiae* w całym badanym zakresie mocy naświetlania. Udowodniono, że aPDI z wykorzystaniem RB, jest skuteczna również wobec biofilmu *S. agalactiae* hodowanego w modelu stacjonarnym, jak i w warunkach ciągłego przepływu, a także wobec biofilmu wielogatunkowego. Zastosowane warunki aPDI nie wykazywały istotnego działania foto- lub cytotoksycznego wobec ludzkich keratynocytów i nie wykazywały znaczącego działania mutagennego w komórkach prokariotycznych ani eukariotycznych. Zaobserwowano jednak, że wraz z zastosowaniem kolejnych cykli subletalnych dawek aPDI następuje u *S. agalactiae* rozwój tolerancji na aPDI. Bakterie tolerancyjne mają znacząco zmieniony fenotyp i poziom ekspresji genów związanych ze stresem oksydacyjnym, ale nadal można je unieszkodliwić przy użyciu wyższego stężenia

fotosensybilizatora i wyższej dawki światła. W mysim modelu kolonizacji *S. agalactiae* zaobserwowano spadek przeżywalności *S. agalactiae*. Ponadto zbadano zmiany przeżywalności różnych grup bakterii. Badania histopatologiczne nie wykazały cytotoksycznego wpływu aPDI na tkanki pochwy. Podsumowując, aPDI z wykorzystaniem RB jest skuteczna w zmniejszaniu żywotności *S. agalactiae* zarówno *in vitro* jak i *in vivo* oraz jest bezpieczna w użyciu. Jednak jej zastosowanie w praktyce klinicznej wymaga dalszych badań.

Abstract

Streptococcus agalactiae – the most common representative of Group B *Streptococcus* (GBS) despite being a common commensal bacterium in adults, is a leading source of invasive infections in newborns, but recently also in pregnant women, the elderly and immune-compromised patients. GBS infections may appear as a wide spectrum of diseases like: bacteremia, sepsis, pneumonia, urinary tract infections, acute and chronic osteomyelitis and others. First-line antimicrobials against GBS are β -lactam antibiotics. With the rising decrease of microbial susceptibility to penicillin and resistance to other antibiotics, there is a huge need for alternative therapies. Antimicrobial Photodynamic Inactivation (aPDI) is one of the proposed therapies which provide an alternative solution for antibiotic resistance in bacteria. It requires the simultaneous presence of photosensitizer (PS), light of a specific wavelength and environmental oxygen. As a results, there are generated Reactive Oxygen Species (ROS), which cause damage in cellular membranes, proteins and nucleic acids, and finally, lead to bacterial cell death.

The aim of the study was the evaluation of aPDI bactericidal activity against *S. agalactiae* serotypes and representatives of physiological flora of the human vagina, evaluation of photo- and cytotoxicity of aPDI to human keratinocytes, creation of the extended logistic model of aPDI for various levels of irradiance, evaluation of the possibility of aPDI resistance/tolerance development, determination of the mutagenic potential of aPDI and finally evaluation of aPDI potential in the decolonization of *S. agalactiae* from the mice vagina.

Rose Bengal (RB) mediated aPDI was chosen as the most effective aPDI variant in decreasing of *S. agalactiae* viability *in vitro*. It caused a lower viability decrease in representatives of physiological flora of the human vagina than for *S. agalactiae*. Computer modelling studies resulted in the creation of an extended logistic aPDI model which effectively describes the dynamics of *S. agalactiae* mortality in the whole tested irradiation power range. RB-mediated aPDI was proven effective also against *S. agalactiae* biofilm grown in stationary and continuous flow models, as well as in multispecies biofilm culture. Used conditions of aPDI did not have significant photo- or cytotoxic effect against human keratinocytes and did not show substantial mutagenic effect in prokaryotic or eukaryotic cells. However, I observed that with the treatment of consecutive cycles of sub-lethal doses of aPDI, the aPDI tolerance development in *S. agalactiae* occurs. Tolerant bacteria have significantly altered phenotype and expression levels of oxidative stress-related genes but can still be eradicated with higher PS concentration and light dose. In the mouse model of *S. agalactiae* colonization a decrease in *S. agalactiae* viability was observed. Moreover, changes in the viability of different bacterial groups were investigated. Histopathology studies did not show any cytotoxic effect of aPDI in vaginal tissues. In conclusion, RB-mediated aPDI is effective in decreasing

Evaluation of photoinactivation potential
in eradication of *Streptococcus agalactiae* in the urogenital system

of *S. agalactiae* viability both *in vitro* and *in vivo* and is safe to use. However, its application in clinical practice requires further investigation.

Funding acknowledgements



NATIONAL SCIENCE CENTRE
POLAND

National Science Center as part of the Opus 12 program.

Grant number: 2016/23/B/NZ7/03236

Title: *Ewaluacja potencjału fotoinaktywacji w eradykacji nosicielstwa Streptococcus agalactiae w układzie moczowo-płciowym: badania in vitro i in vivo.*



University
of Gdańsk

Research Project Competition Grant for Participants of Life Sciences and
Mathematics Interdisciplinary Doctoral Studies (LISMIDOS).

Grant number: 539-N106-B932-21

Title: *Optimization of the multispecies biofilm culture of Streptococcus agalactiae and vaginal physiological flora as a model for S. agalactiae carriage studies.*

Chapter I

Introduction

Streptococcus agalactiae is a Gram-positive bacterium, the most common representative of Group B *Streptococcus* (GBS). Although considered a commensal organism of adult humans it can cause life-threatening infections in newborns. It colonizes the genitourinary and gastrointestinal tract of around 15-40% of pregnant women [1]. When transmitted during labour to the newborn it can cause pneumonia, septicaemia or meningitis [2]. To prevent these infections prenatal antibiotic prophylaxis is used, mainly with the use of penicillin. It has significantly decreased the incidence of *S. agalactiae* infections in newborns, but it is not a routine in all parts of the world [3]. Moreover, the morbidity rates of GBS infections are still very high and neurodevelopmental impairment affects up to 50% of surviving newborns [4]. Another problem is that not all women are screened for GBS before delivery, some women do not comply with the indications about taking or dosing of the antibiotics, and some are allergic to penicillin. It also has to be taken into account that penicillin-tolerant *S. agalactiae* strains have been already reported, as well as strains resistant to second-line antibiotics like erythromycin and levofloxacin, but also macrolides and fluoroquinolones [5],[6]. Moreover, GBS affects not only newborns. In recent years there is a growing number of invasive *S. agalactiae* infection cases in non-pregnant adults in example elderly, or immunocompromised patients manifested with bacteriemia, skin and soft tissue infections, urinary tract infections, pneumonia, endocarditis or meningitis [7],[8]. In addition to humans, GBS also poses a threat to animals. It causes significant economic losses in Nile tilapia aquacultures because of high mortality caused by outbreaks of disease [9]. It also affects cattle, mainly through bovine mastitis, causing reduced milk production [10]. Interestingly, *S. agalactiae* strains isolated from cattle, fish and humans often has close genetic relationship and the same isolate can cause infection outbreaks affecting for example both fish and humans [11],[12].

The emergence of antibiotic resistance has led the scientific community to pursue for alternative forms of prevention or therapy. There already are available attenuated or oral vaccines against GBS for Nile tilapia [13],[14]. As for humans intensive research is ongoing for an effective capsule polysaccharide conjugate vaccines against GBS. With polysaccharide-based vaccines being during clinical trials our concern should be: the fact that we can distinguish 10 serotypes of *S. agalactiae* including non-typeable strains, which could escape the action of the vaccine; the fact that serotype replacement was already observed for closely related *Streptococcus pneumoniae*; and that capsular switching have been already reported for GBS [15],[16],[17]. This phenomenon can make the development of a universal vaccine significantly more difficult and delayed in time.

Another way for bacteria to escape from the action of antibiotics is to form a biofilm. In a biofilm, bacteria are embedded in the extracellular matrix, which significantly reduces the penetration of antimicrobial agents. Moreover, cells embedded in biofilm multiply slower, what makes them less susceptible to especially antistatic antibiotics, and have shifted expression of multiple genes, including those connected with stress response [18]. Biofilm formation was indicated as one of the reasons for the persistence and recurrence of bacterial vaginosis [19]. And because in the vagina there is a low pH, both *S. agalactiae* and *Lactobacillus spp.* have favourable conditions for biofilm production [20],[21].

Antibiotic resistance may result from a single spontaneous mutation as it's frequently found for rifampicin, aminoglycosides and quinolones. Another possibility is the acquisition of resistance genes carried on mobile genetic elements (MGEs), i.e., plasmids or genetic alterations that result from horizontal gene transfer. Unlike antibiotics, Reactive Oxygen Species (ROS) do not have a specific molecular target for their action. They induce damage of both nucleic acids and proteins or even cell membranes. Application of ROS in concentrations far exceeding concentrations present in the environment leads to irreparable damage of bacterial cells and finally to its death. This is why ROS are produced in an oxidative burst by macrophages when pathogenic bacteria attack the human body, by some of the antibiotics i.e. chloramphenicol, by pulsed light, cold atmospheric plasma, ultraviolet light (UV), antimicrobial Blue Light (aBL) and antimicrobial Photodynamic Inactivation (aPDI) [22],[23],[24].

Antimicrobial Photodynamic Inactivation (aPDI) is one of the proposed therapies which provide an alternative solution for antibiotic resistance in bacteria. It requires the simultaneous presence of photosensitizer (PS), light of specific wavelength and environmental oxygen, so the ROS are produced only in the site of infection, what is one of its advantages. Another advantage is that resistance to aPDI has not been described yet, even though many researchers were investigating this issue [23]. When the photosensitizer absorbs a photon of light it is excited to a short-lived excited singlet electronic state. Via electronic transition, it can change into a longer-lived triplet state. PS in the triplet state can react with ground state oxygen via different photochemical pathways: Type 1 or Type 2 mechanisms. In the Type 1 mechanism electron is transferred, what results in the production of superoxide radicals and then hydroxyl radicals (HO•). In the Type 2 mechanism due to the transfer of the energy directly to oxygen, state singlet oxygen is formed [22]. Each photosensitizer undergoes transitions through both mechanisms, but in different proportion. One of the photosensitizers, which is described as mainly Type 2 – strong singlet oxygen producer is rose bengal (RB). It is a water-soluble xanthene dye, which can be activated with light of approximately 500-580 nm. RB can be used in multiple approaches including photochemical tissue bonding, photodynamic inactivation, photothrombotic animal models or sonodynamic therapy. It has been approved by FDA as a vital stain

for ocular surface assessment, so can be considered safe for humans [25]. Antimicrobial Photodynamic Inactivation has been proven to be effective against many human pathogenic bacteria, not only *in vitro*, but also *in vivo* [26]. Moreover, aPDI has been already used in the treatment of different *Streptococcus* species: *S. pyogenes*, *S. mutans*, *S. sanguinis*, *S. bovis*, *S. mitis*, *S. dysagalactiae*, *S. agalactiae*, and also closely related *Enterococcus faecalis* [27],[28],[29],[30],[31],[32],[33],[34],[35].

The best way to prevent the perinatal GBS infections would be to design a fast and safe treatment for GBS colonization, which could be administered to all pregnant women just before the labour. If this treatment would additionally have a limited effect on the physiological flora, there would be no concern for the administration of this treatment without the screening test. In my opinion, RB-mediated aPDI, has the potential to become this treatment.

Hypothesis and aims of the work

Presented doctoral thesis is based on the hypothesis, that rose bengal-mediated photoinactivation has a significant potential as a method for *Streptococcus agalactiae* eradication in the urogenital system. To verify this hypothesis several aims were determined.

1. Evaluation of the bactericidal activity of photoinactivation against *Streptococcus agalactiae*.
2. Evaluation of the bactericidal activity of photoinactivation against *Lactobacillus spp.* from human vaginal flora.
3. Evaluation of the probability of acquisition of resistance to photoinactivation due to multiple phototreatments of *S. agalactiae*.
4. Evaluation of photo- and cytotoxicity of studied photoinactivation protocol against human epithelial cells.
5. Evaluation of mutagenicity of studied photoinactivation protocol using procaryotic and eucaryotic cells.
6. Optimization of photoinactivation protocol using computer modelling.
7. Evaluation of photoinactivation in the decolonization of *S. agalactiae* in mice vagina.
8. Assessment of photoinactivation impact on microbial vaginal flora.
9. Histopathological analysis of vaginal tissues after photoinactivation.

The results of my research presented in this doctoral dissertation are attached as a set of 4 publications constituting a thematically coherent set of articles published in indexed scientific journals.

Chapter II

An extended logistic model of photodynamic inactivation for various levels of irradiance using the example of *Streptococcus agalactiae*

1. Summary of the publication

During the work with photodynamic inactivation, researchers need to establish an optimal balance between photosensitizer concentration, time of irradiation and light intensity. Because of possible toxicity towards eucaryotic cells, researchers usually try to minimize the concentration of the photosensitizer and try to adjust irradiation parameters. Moreover, because of the lower sensitivity of Gram negative bacteria to aPDI, often also decrease of the light intensity is required to avoid excessive increase of temperature. Therefore, the main goal is to establish minimal concentration and light parameters that allow a maximal decrease of bacterial viability.

In this work novel approach for photoinactivation studies was proposed. Series of experiments were performed to determine *Streptococcus agalactiae* viability reduction caused by the RB-mediated aPDI. Bacterial viability change was assessed in 12 time points for 4 different values of light intensity, with constant RB concentration. Collected data was used for the creation of a photoinactivation dynamic properties model. The time constant of transmittance which depends on light power was determined. Performed experiments and calculations led to obtaining a dynamic first order model in the form of transmittance with a variable time constant, depending on the chosen irradiance power.

This model allows to predict with a certain probability time of irradiation required for desired effectiveness of photoinactivation. This approach may contribute to a better understanding of the photoinactivation dynamic and faster implementation of *in vitro* results into clinical practise in the future. Further analysis of similar models based on different light sources could help researchers to compare the data of experiments performed by different research teams and shorten the time of screening analyses. In this publication pilot study to reach Aim 1. was performed and Aim 6 was reached.

2. Publication



OPEN

An extended logistic model of photodynamic inactivation for various levels of irradiance using the example of *Streptococcus agalactiae*

Michal Brasel¹✉, Michal Pieranski² & Mariusz Grinholc²✉

Irradiance is an important factor influencing the acceleration of microorganism mortality in photodynamic inactivation (PDI) processes. Experimental observations of PDI processes indicate that the greater the irradiation power is, the faster the decrease in the population size of microorganisms. However, commonly used mathematical models of PDI processes usually refer only to specific values of irradiance without taking into account the influence of change in irradiance on the dynamic properties of inactivation. The main goal of this paper is to analyze the effect of irradiance on the PDI process and attempt to mathematically model the obtained dependencies. The analysis was carried out using the example of photodynamic inactivation of the bacterium *Streptococcus agalactiae* with the adopted Logistic PDI model optimized for several selected levels of irradiance. To take into account the impact of changes in irradiation power on the PDI model, the selected parameters were made appropriately dependent on this factor. The paper presents several variants of parameter modification with an evaluation of the model fitting quality criterion. The discussion on appropriate selection of parameters to be modified was carried out as a comparative analysis of several case studies. The extended logistic PDI model obtained in the conducted research effectively describes the dynamics of microorganism mortality in the whole tested irradiation power range.

This manuscript presents the results of experimental research on the photodynamic inactivation (PDI) process using the bacterium *Streptococcus agalactiae* as an example. Group B Streptococcus (GBS) bacteria, the most common species of which is *S. agalactiae*, are Gram-positive pathogens representing one of the major causes of life-threatening bacterial infections in newborns and infants. Perinatal infections can occur in the form of early-onset disease (EOD) or late-onset disease (LOD). Early GBS infection in newborns occurs at up to 7 days of life, causing sepsis, pneumonia or meningitis, while the late form of infection occurs between the 7th and 89th days of life, causing septicemia or meningitis, as well as inflammation of the respiratory system, joints and connective tissue¹. In recent years, an alternative form of prevention of perinatal infection has been proposed. Intensive ongoing work is focused on the generation of an effective vaccine directed against polysaccharide capsular and protein surface antigens of *S. agalactiae*. Nevertheless, the occurrence of several serotypes of this bacterium and the high percentage of strains intractable to serotyping methods significantly impede the development of a universal vaccine. Therefore, the ideal solution for the prevention of perinatal GBS infections seems to be the design of a safe and fast treatment for eradication of group B streptococci, which would be administered to all pregnant women immediately before giving birth (at the beginning of the regular systolic or shortly after rupture of the fetal membranes), regardless of the outcome of the screening test. The bacterial eradication approach, which, for many years, has been the primary subject of our research using both in vitro and in vivo studies, is PDI²⁻⁵. PDI causes damage to microbial cells by generating reactive oxygen species (ROS) induced by the interaction

¹Faculty of Electrical Engineering, West Pomeranian University of Technology, 26 Kwietnia 10, 71-126 Szczecin, Poland. ²Intercollegiate Faculty of Biotechnology, Laboratory of Molecular Diagnostics, University of Gdansk and Medical University of Gdansk, Abrahamowa 58, 80-307 Gdańsk, Poland. ✉email: michal.brasel@zut.edu.pl; mariusz.grinholc@biotech.ug.edu.pl

between visible light of an appropriate wavelength and a light-sensitive chemical called a photosensitizer (PS). PDI involves the absorption of a photon of light leading to excitation of the PS to its short-lived excited singlet electronic state. This singlet-state PS can undergo an electronic transition to a much longer-lived triplet state. The longer lifetime allows the triplet PS to react with ambient (ground state) oxygen by one of two different photochemical pathways, called Type 1 and Type 2 mechanisms. Type 1 involves an electron transfer to produce superoxide radical and then hydroxyl radicals (HO[•]), while Type 2 involves energy transfer to produce excited state singlet oxygen (¹O₂). The generated ROS, such as singlet oxygen, can exert cytotoxic effects against a variety of biomolecules, e.g., proteins, lipids, cell membranes or genetic material⁶.

The PDI outcome depends on numerous factors. Irradiance is one of the most important factors influencing the acceleration of microorganism mortality in PDI processes. Experimental PDI tests are most often performed with a constant irradiance for a specified period of time^{7–12}. Therefore, commonly used mathematical models of PDI processes usually refer only to specific values of irradiance without taking into account the influence of changes in irradiance on the dynamic properties of inactivation. In photodynamic therapy (PDT), the permissible range of irradiance may be limited for various reasons; thus, the choice of specific irradiation level may be limited. This is important because various levels of irradiation power correspond to various irradiation times required to achieve the same inactivation result. Therefore, estimation of the required irradiation time for various levels of irradiation power may be very helpful. To predict the dynamic properties of the PDI process for various levels of irradiation power, a properly extended PDI model is needed. Therefore, the present study was focused on analyzing the effect of irradiance on the PDI process and attempted to mathematically model the obtained dependencies.

The manuscript presents the results of experimental research on PDI for four selected levels of irradiance: $\mu_1 = 70 \text{ mW/cm}^2$, $\mu_2 = 52.5 \text{ mW/cm}^2$, $\mu_3 = 35 \text{ mW/cm}^2$, and $\mu_4 = 17.5 \text{ mW/cm}^2$, corresponding to 100, 75, 50 and 25% of the maximal output power produced by the LED, respectively. The commonly known Logistic PDI model was used to approximate the obtained results^{13–17}. The parameters of this model were fitted to the collected experimental data by using the root mean square error (RMSE) minimization method. Based on the conducted research, it was found that the level of irradiance significantly affects the dynamic properties of the inactivation process of microorganisms. In particular, it has been observed that the greater the radiation power is, the faster the decline in bacterial population. For this reason, the parameters of the selected PDI model optimized for various irradiation levels are no longer the same. This indicates that there is a need to take into account the irradiance in the PDI model used. The main goal of this manuscript is to analyze the effect of the irradiance on the dynamics of the inactivation process using the example of the bacterium *S. agalactiae* and to propose the inclusion of this effect in the Logistic model by using a parameter variation approach. Because the logistic model has as many as three parameters, it may be a complicated task to modify these parameters appropriately. The following questions arise: should all model parameters be changed, and if not, which ones should be changed and how? A useful method in the selection of parameters that are most suitable for modification may be to examine their sensitivity to changes in the irradiance level. This approach is proposed in the manuscript. First, the effect of irradiation level on the survival curves of the Logistic model is described in the manuscript. Then, the issue of including obtained dependencies in the considered model is investigated. The main results of the experimental research on PDI are presented as several case studies for alternative variants of Logistic model modification, i.e., for the following cases: A, for all modified parameters; B, for two modified parameters; C and D, for one modified parameter; and E, for all constant parameters. The discussion on appropriate selection of parameters to be modified is described as a comparative analysis of the considered cases. The fitting quality and the degree of complexity of the proposed modified models were the most important comparative criteria utilized in this analysis. The extended Logistic PDI model obtained from these studies effectively describes the dynamics of microorganism mortality in the whole tested range of irradiance.

Materials and methods

Bacterial strains and reagents. This study was conducted with the *S. agalactiae* strain ATTC 27,956 isolated from an infected bovine udder, representing Lancefield's group B streptococci. Bacteria were grown in tryptic soy broth (TSB) (Biomerieux, France). A stock solution of rose bengal (RB) (Sigma-Aldrich, Germany) was prepared in sterile double-distilled water and kept at 4 °C. All solvents and other chemicals were of analytical grade.

Light source. The LED light source with an emission maximum at 515 nm (FWHM = 33 nm) was custom made by EMD Technology (Warsaw, Poland). The light source was precisely characterized in our previous publication¹⁸.

Inactivation experiment. *Streptococcus agalactiae* was grown overnight (16–20 h) in glass tubes containing 5 ml of TSB medium with shaking (150 RPM) at 37 °C. The culture was adjusted to an optical density of 2.4 McFarland (8×10^7 CFU/ml) units in fresh TSB medium. A 2 μM solution of RB was prepared from the stock solution and then diluted 10 \times with bacterial culture to obtain a final 0.2 μM concentration of RB. Samples were incubated in the dark for 15 min at 37 °C with shaking and then centrifuged twice and washed with PBS. Then, 100- μl bacterial cultures in PBS were transferred into 96-well plates and irradiated for 0, 1, 2, 5, 10, 15, 20, 30, 45, 60, 120, 180, 240, 300, or 360 s. Irradiated samples were serially diluted in PBS, plated onto Columbia blood agar plates and incubated at 37 °C. After 24 h of incubation, colony forming units (CFU) were counted. Experiments were performed in three independent repetitions for four selected levels of irradiance: $\mu_1 = 70 \text{ mW/cm}^2$, $\mu_2 = 52.5 \text{ mW/cm}^2$, $\mu_3 = 35 \text{ mW/cm}^2$, $\mu_4 = 17.5 \text{ mW/cm}^2$, corresponding to 100, 75, 50 and 25% of the maximal output power produced by the LED, respectively. In the course of inactivation experiment, the temperature of

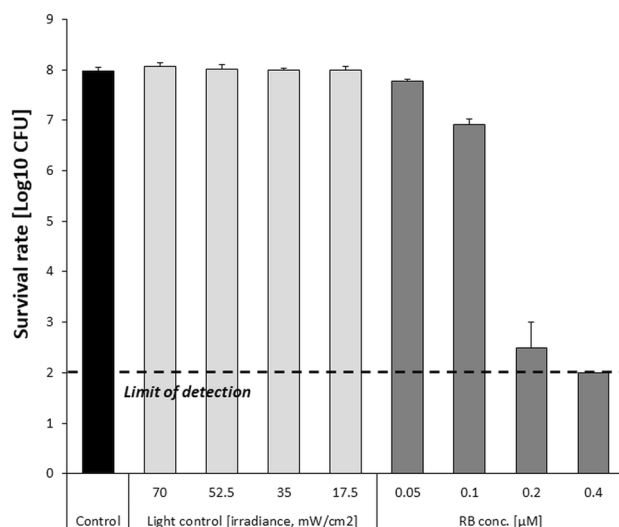


Figure 1. Dose-dependent PDI efficacy against *S. agalactiae*. Microbial overnight cultures (8×10^7 CFU/ml) were treated with up to $0.4 \mu\text{M}$ RB and exposed to a light dose of $20 \text{ J}/\text{cm}^2$ (λ_{max} 515 nm). After illumination, samples were serially diluted, streaked horizontally, and incubated at 37°C for 24 h, and then colonies were counted. Control groups included: (1) cells that were not treated with PSs or light (marked as “control”); (2) cells treated with light for 6 min with various irradiance and no PS administration (marked as “light control”). The detection limit was 100 CFU/ml. The values are the means of three separate experiments. Error bars represent standard deviations (SDs).

PDI treated bacterial culture was measured using waterproof pocket-size pH-meter CP-105 for pH, mV, redox potential and temperature measurement (range: $-5/60^\circ\text{C}$, accuracy: $\pm 0.8^\circ\text{C}$) (Elmetron, Poland).

Rose bengal uptake. Microbial OV cultures were adjusted to an optical density of 2.4 McFarland units in TSB medium. Bacterial suspensions were centrifuged and resuspended in PBS and then mixed with RB to obtain a final concentration of $0.2 \mu\text{M}$. Samples were incubated for 15 min at 37°C and immediately centrifuged at $10,000g$ for 3 min after incubation. Supernatants (1 ml) were then transferred into BRAND UV cuvettes (optical path length 1 cm), and the absorbance at 549 nm was measured by a SPECORD PLUS spectrophotometer (Analytic Jena). Additionally, each sample was serially diluted end plated for CFU enumeration. Using the molar extinction coefficient ($\epsilon = 95,000$), the number of RB particles absorbed by a single bacterial cell was calculated according to the formula below^{19,20}:

$$n = \frac{[A_0 - A_t] \times N_A}{\epsilon \times l \times N}$$

in which the variables are defined as follows: n is the number of RB molecules per bacterial cell, A_0 is the initial absorbance of bacterial supernatant administered with RB (blanked with the supernatant of bacterial culture not administered with RB), A_t is the absorbance of supernatant of bacterial culture administered with RB for 15 min (blanked with the supernatant of bacterial culture not administered with RB), N_A is Avogadro's Constant ($6.02214086 \times 10^{23}/\text{mol}$), ϵ is molar extinction coefficient (M/cm), l is optical path length (cm), N is number of bacterial cells (CFU/L).

Ethical approval. The manuscript contains no data concerning animal studies, studies involving human subjects or inclusion of identifiable human data or clinical trials; thus, no ethical approval was required.

Results

Rationale and control experiments supporting experimental conditions. To ensure adequate computational analysis, RB concentration was adjusted to result in moderate bacterial killing (not exceeding the detection limit; reduction by maximum $5 \log_{10}$ units in viable counts) when excited with visible light within few minutes. Employing higher PS concentrations reached microbial eradication regardless irradiance and prevented adequate modeling (Fig. 1). RB concentration of $0.2 \mu\text{M}$ was considered optimal as exerted the most effective bacterial killing above detection limit (Fig. 1).

Employed LED light source effectively excites studied PS by overlapping its absorption spectrum (Fig. 2a). Though negatively charged in water solutions, RB revealed substantial microbial uptake ($9.56\text{E}+05$) leading to photodynamic inactivation of *S. agalactiae* upon light treatment. The change in the absorbance spectrum of bacterial culture supernatant after 15 min incubation with RB in comparison to initial absorbance spectrum demonstrates RB uptake (Fig. 2b). The uptake of RB was calculated with the molar extinction coefficient and expressed as the number of photosensitizer molecules per bacterial cell.

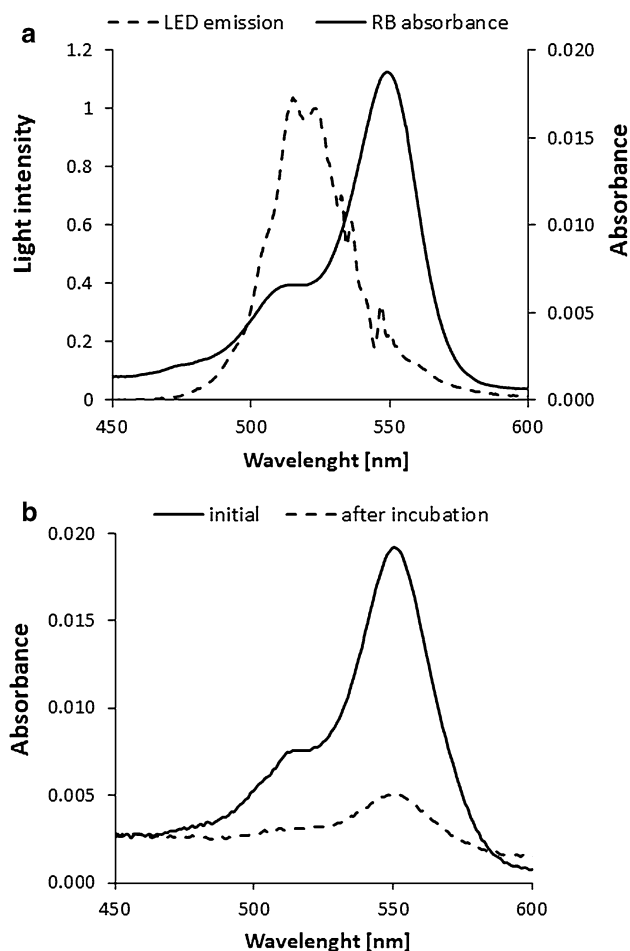


Figure 2. LED characterization and RB absorption spectra. **(a)** The emission spectrum of the LED is presented, and the maximum intensity is observed at 515 nm. A rose bengal (0.2 μM) absorption spectrum is presented in the wavelength range of interest. **(b)** The absorbance spectra of bacterial culture supernatant administered with 0.2 μM RB (termed “initial”) and supernatant of bacterial culture administered with RB for 15 min and centrifuged (termed “after incubation”) are presented.

Irradiance	Temperature ^a (°C)
$\mu_1 = 100\%$	27.3 ± 0.15
$\mu_2 = 75\%$	26.0 ± 0.11
$\mu_3 = 50\%$	24.5 ± 0.11
$\mu_4 = 25\%$	23.6 ± 0.10
Control (no light)	23.7 ± 0.10

Table 1. Temperature control upon light treatment using various levels of irradiance μ [%]. ^aTemperature measurement was performed upon light treatment for maximum time used for modeling (6 min).

Furthermore, to evidence that the observed inactivation efficacy of PDI may only be attributed to photosensitized reaction mediated by RB, the control experiments concerning light treatment with no RB administration together with temperature detection were performed. Obtained results demonstrated that light alone exerts no bactericidal activity (Fig. 1) and in the course of photodynamic treatment no substantial increase in temperature that could might affect bacterial viability was observed (Table 1).

Effect of irradiation level on the survival curves of the logistic PDI model. The PDI processes of microorganisms are most commonly modeled as microbial survival curves showing a change in the population at the time of irradiation. The population size is most often expressed as a logarithmic ratio of the current number of microorganisms (N) to the initial number (N_0) and is presented on semilogarithmic plots. One of the methods of describing the sigmoidal behavior of microbial survival curves is the Logistic model^{21–24}. There

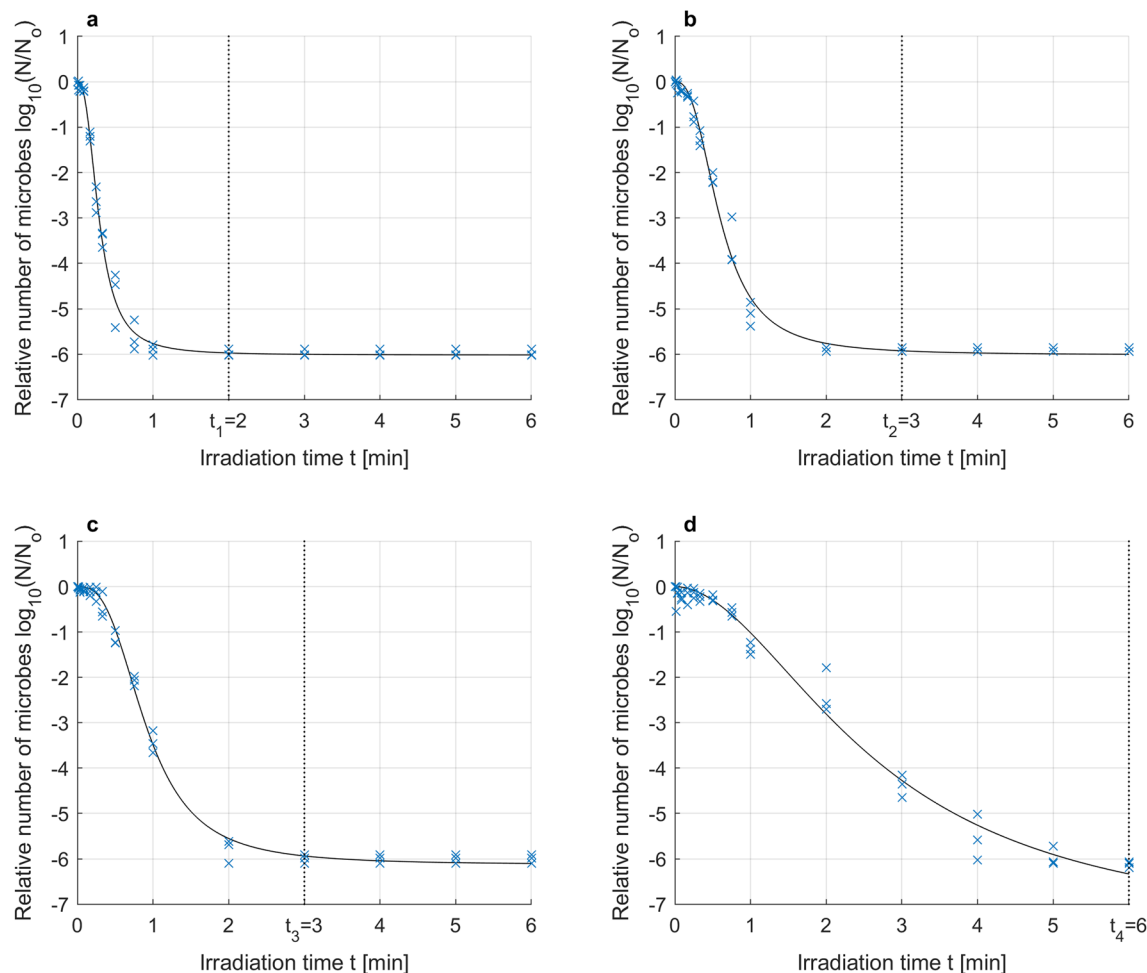


Figure 3. Photodynamic inactivation of *S. agalactiae* for irradiance $\mu_1 = 70 \text{ mW/cm}^2$ (a), $\mu_2 = 52.5 \text{ mW/cm}^2$ (b), $\mu_3 = 35 \text{ mW/cm}^2$ (c), $\mu_4 = 17.5 \text{ mW/cm}^2$ (d); experimental data (x) and microbial survival curve (-) of the Logistic PDI model optimized without data reduction.

are many variations and modifications of this model^{14,25–30}. In this manuscript, the Logistic PDI model^{13–17} was chosen to analyze the dynamic properties of the inactivation process of microorganisms.

The model under consideration is the Logistic model, expressed as follows (Eq. 1):

$$\log\left(\frac{N(t)}{N_0}\right) = N_r \left(1 - \frac{1}{1 + \left(\frac{t}{\tau}\right)^P}\right) \quad (1)$$

in which the variables are defined as follows: N is the number of microorganisms at irradiation time t , N_0 is the initial number of microorganisms at time $t=0$, N_r is parameter that describes the number of resistant microorganisms, P is parameter that describes the length of the curve shoulder, τ is parameter that describes the suddenness of the reduction in the population of microorganisms.

Based on the collected experimental data for each of the tested irradiation levels, optimal parameters in terms of RMSE (Root Mean Square Error) were determined for the Logistic model (1). Figure 3 show the collected data along with the approximate microbial survival curves for the optimized parameters.

The values of the optimized parameters of the Logistic model and the corresponding values of the RMSE quality indicators are presented in Table 2, with RMSE calculated according to the formula (Eq. 2):

$$RMSE = \sqrt{\frac{\sum_{i=1}^N (y(i) - y_m(i))^2}{N}}, \quad (2)$$

where $y(i)$ are the experimental data and $y_m(i)$ are the predicted data.

Analysis of the results presented in Fig. 3 shows that the greater the irradiation power is, the faster the increase in microbial mortality. The change in the mortality dynamics caused by the change in irradiation power leads to the mortality curves reaching the detection limit at various irradiation times. The higher the irradiation power is, the faster the detection limit is reached, which in our case is close to $\log(N/N_0) = -6$. The individual times for reaching the detection limit for a series of irradiation power levels, namely, μ_1 , μ_2 , μ_3 , and μ_4 , are $t_1 = 2$ min,

Irradiance	RMSE-optimized parameters			RMSE
	$N_{r,opt}$	τ_{opt}	P_{opt}	
$\mu_1 = 100\%$	-6.018	0.288	2.509	0.1923
$\mu_2 = 75\%$	-6.016	0.598	2.582	0.2144
$\mu_3 = 50\%$	-6.130	0.908	2.866	0.1630
$\mu_4 = 25\%$	-7.665	2.660	1.918	0.2757

Table 2. Results of parameter optimization of the Logistic PDI model without data reduction for various levels of irradiance μ [%].

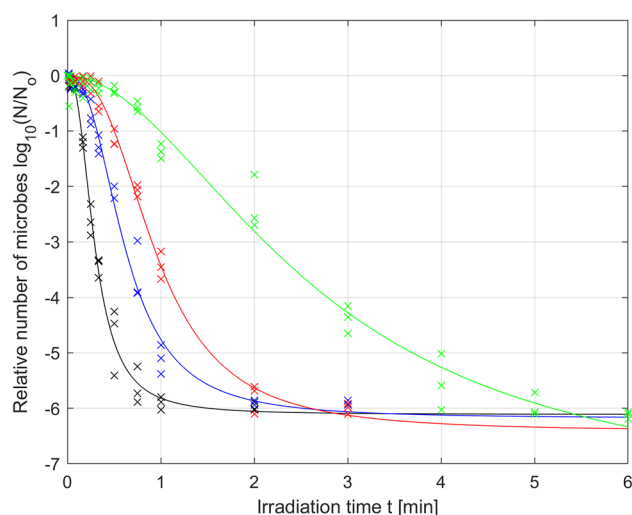


Figure 4. Photodynamic inactivation of *S. agalactiae* for various levels of irradiance: $\mu_1 = 70$ mW/cm² (black), $\mu_2 = 52.5$ mW/cm² (blue), $\mu_3 = 35$ mW/cm² (red), $\mu_4 = 17.5$ mW/cm² (green); experimental data (x) and microbial survival curves (-) of the Logistic PDI model optimized with data reduction.

$t_2 = 3$ min, $t_3 = 3$ min, $t_4 = 6$ min, respectively, as shown in Fig. 3. After these times are exceeded, we do not truly know what happens to the population number of microorganisms. We can assume that the number of microorganisms decreases further with increasing irradiation time (to the value of N_r), but we cannot experimentally verify this assumption. Therefore, it should be assumed that the collected experimental data marked in Fig. 3 for times greater than $t_1 = 2$ min, $t_2 = 3$ min, $t_3 = 3$ min, $t_4 = 6$ min, respectively, distort the reality to a certain degree. For this reason, the approach in which all the collected data are taken into account to optimize model parameters (also those for times after the detection limit has been exceeded) can be misleading and give nonoptimal results; therefore, model parameters should not be optimized based on these data. This is why further analysis reduced the experimental data used for optimization, using only the data collected for the first time the detection limit was reached by three independent samples. This reduction in the data collected was conducted for the irradiation powers μ_1 , μ_2 and μ_3 , but for the power μ_4 , this reduction was not necessary. The results of parameter optimization for the Logistic PDI model (Eq. 1) obtained based on the reduced data are shown in Fig. 4 and the corresponding Table 3.

By comparing the results from Tables 2 and 3, it can be stated that in the case of the reduced data, the fitting quality indicators for the powers μ_1 and μ_2 are slightly worse than those in the case of the unreduced data, but this is not a significant deterioration, as seen by comparing Fig. 3 with Fig. 4. For the reasons described above, the parameters optimized for the reduced data should be considered more reliable. More importantly, the data reduction results in a decrease in the optimal value of parameter N_r (parameters N_r in Table 3 are smaller than the corresponding parameters in Table 2 for all irradiances). This is consistent with expectations because the optimal value of the parameter N_r describing the number of resistant microorganisms is expected to be below the detection limit. The use of unreduced data to optimize the N_r parameter makes the value of this parameter very close to the detection level, which should be considered an abnormality.

Taking into account the effect of changes in irradiance in the Logistic PDI model. As the irradiation power changes, the dynamic properties of the photoinactivation process change, which entails changes in the optimal parameters of the identified model (Table 3). To account for these dependencies in the model, it was proposed that the parameters be changed depending on the irradiation power level. The general form of the

Irradiance	RMSE-optimized parameters			RMSE
	N_{ropt}	τ_{opt}	P_{opt}	
$\mu_1 = 100\%$	-6.112	0.293	2.426	0.2177
$\mu_2 = 75\%$	-6.182	0.615	2.478	0.2297
$\mu_3 = 50\%$	-6.418	0.950	2.645	0.1596
$\mu_4 = 25\%$	-7.665	2.660	1.918	0.2757
RMSE-weighted mean	-6.529	1.042	2.413	0.2207
Coefficient of variation	11.18%	101.75%	13.18%	-

Table 3. Results of parameter optimization of the Logistic PDI model with data reduction for various levels of irradiance μ [%].

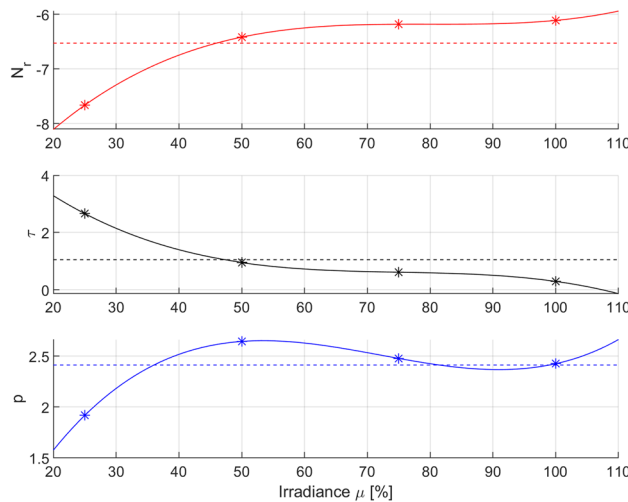


Figure 5. Optimal parameters of the Logistic PDI model (*) for various levels of irradiance μ [%] and their polynomial interpolation (-) with RMSE-weighted mean values (-). Optimization was carried out for variations in the N_r , p and τ parameters.

extended Logistic model that takes into account changes in the irradiation power can be presented as follows (Eq. 3):

$$\log \left(\frac{N(t)}{N_o} \right) = N_r(\mu) \left(1 - \frac{1}{1 + \left(\frac{t}{\tau(\mu)} \right)^{p(\mu)}} \right) \tag{3}$$

where $N_r(\mu)$, $\tau(\mu)$, and $p(\mu)$ are the parameters of the Logistic PDI model described by the appropriate irradiation power functions, and μ is the irradiation power.

The first proposed variation to take into account the effect of changes in irradiation power in the considered model is to properly vary all parameters depending on the irradiation power level (case A). However, to obtain appropriate submodels of parameter changes, it is necessary to analyze the variation in RMSE-optimized parameters depending on the change in irradiation power and approximate the collected data with appropriate parameter variation curves.

Case A: variation in all parameters of the Logistic PDI model. Based on the data presented in Table 3, it is possible to analyze the variation in optimal parameters of the Logistic model and to find appropriate functions by approximating the changes in their values in the examined range of irradiation powers. In the analyzed case, the third-order polynomial functions well enough. Figure 5 shows the optimal parameters of the Logistic for the tested irradiation powers and the curves approximating the parameters accordingly.

The obtained functions describing the variation in the parameters of the Logistic model (Eq. 3) in the domain of irradiation power can be presented in the following analytical form:

$$\begin{aligned}
 N_{rA}(\mu) &= 0.0009 \cdot 10^{-2} \mu^3 - 0.2161 \cdot 10^{-2} \mu^2 + 17.2507 \cdot 10^{-2} \mu - 1076.8000 \cdot 10^{-2} \\
 \tau_A(\mu) &= -0.0015 \cdot 10^{-2} \mu^3 + 0.3279 \cdot 10^{-2} \mu^2 - 25.0780 \cdot 10^{-2} \mu + 710.7000 \cdot 10^{-2} \\
 p_A(\mu) &= 0.0011 \cdot 10^{-2} \mu^3 - 0.2330 \cdot 10^{-2} \mu^2 + 15.6713 \cdot 10^{-2} \mu - 71.2000 \cdot 10^{-2}.
 \end{aligned} \tag{4}$$

Equations (3) and (4) constitute one of the possible versions of the extended PDI Logistic model obtained when all the parameters are varied (case A), as indicated by the index A used in the parameter subscripts. The total number of model parameters equals $n=12$ in this case, while the mean value of the RMSE quality criterion is equal to 0.2207.

The basic disadvantage of the approach in which all parameters of the identified model are modified is the increasing degree of complexity of the model with the increase in the number of modified parameters—the more parameters the model has, the more the number of submodels that describe the changes in the parameters. It is worth noting that for each varied optimal parameter, there are several coefficients, the amounts of which depend on the approximating function (in this case, on the degree of polynomials used). Moreover, this approach does not take into account differences in the sensitivity of individual parameters to changes in the irradiance or the physical significance of the parameters to be modified. However, most often, there is a situation in which individual parameters show different sensitivity to changes in irradiation power. In such cases, the variation in the less sensitive parameters may be limited or omitted without a significant deterioration in modeling quality.

An alternative approach to taking into account the changes in irradiance in the PDI model is to modify only selected parameters of the identified model. Namely, it can be assumed that only those parameters are modified that significantly react to a change in the irradiance. For this purpose, an appropriate measure of the significance of parameters of the identified model should be determined, that is, how large are their deviations from a certain characteristic value in the considered range of irradiation power. This manuscript proposes the expression of this characteristic value as a weighted mean of parameters optimized for the tested irradiation power, with weights being the inverse of the corresponding RMSE fitting quality indicators, so that optimal parameters that gave a better fit in terms of the RMSE indicator were given proportionally greater weightage for calculating the mean value. The RMSE-weighted mean values of optimal parameters calculated from the formula (Eq. 5):

$$\bar{x} = \frac{\sum_{i=1}^n \frac{1}{RMSE_i} x_i}{\sum_{i=1}^n \frac{1}{RMSE_i}} \tag{5}$$

were as follows:

$$\bar{N}_{rA} = -6.529, \quad \bar{\tau}_A = 1.042, \quad \bar{p}_A = 2.413. \tag{6}$$

These values are marked with dashed lines in Fig. 5 for each parameter. Relative deviations of the optimal parameter values from their mean values (6) within the tested irradiance in the PDI model is to modify only selected parameters of the identified model. Namely, it can be assumed that only those parameters are modified that significantly react to a change in the irradiance. For this purpose, an appropriate measure of the significance of parameters of the identified model should be determined, that is, how large are their deviations from a certain characteristic value in the considered range of irradiation power. This manuscript proposes the expression of this characteristic value as a weighted mean of parameters optimized for the tested irradiation power, with weights being the inverse of the corresponding RMSE fitting quality indicators, so that optimal parameters that gave a better fit in terms of the RMSE indicator were given proportionally greater weightage for calculating the mean value. The RMSE-weighted mean values of optimal parameters calculated from the formula (Eq. 5):

$$CV_x = \frac{\sigma_x}{|\bar{x}|} 100\%, \tag{7}$$

where σ_x is the standard deviation:

$$\sigma_x = \sqrt{\frac{\sum_{i=1}^n (x_i - \bar{x})^2}{n - 1}} \tag{8}$$

The coefficients of variation of the Logistic model parameters in case A are as follows:

$$CV_{N_{rA}} = 11.18\%, \quad CV_{\tau_A} = 101.75\%, \quad CV_{p_A} = 13.18\%. \tag{9}$$

Based on the estimated coefficients of variation, it can be concluded that parameter N_r is the least sensitive to changes in irradiation. A comparable value of variation is also shown by the p parameter, while the τ parameter is clearly more sensitive to changes in irradiation power than other parameters.

Case B: variation in parameters p and τ for constant N_r . The results of the conducted analysis of parameter variation led to the formulation of a hypothesis that in the case under study, limiting or omitting the modification of parameter N_r (and possibly p) in the Logistic model, could give similar results in terms of the RMSE optimization to the results obtained for case A. Therefore, in the next example, it was assumed that parameters p and τ in the Logistic model will be modified, while the N_r parameter will set at a constant value equal to $-6,529$, determined as (6) in case A. Of course, setting of the parameter N_r at a constant value required repeating the parameter optimization procedure for the same experimental data. The results of optimization of the p and τ parameters of the Logistic model at a constant value of the parameter N_r are shown in Fig. 6 (solid lines) and Table 4.

In contrast to Fig. 4, Fig. 6 shows that setting parameter N_r at a constant value with increasing irradiation time led to the convergence of all microbial mortality curves to the same fixed residual value, which was consistent with the physical significance of this parameter characterizing the number of resistant microorganisms.

Figure 7 presents the optimal values of parameters p and τ (with a constant value of parameter N_r) of the Logistic model for the tested irradiation powers and the corresponding approximation curves (third-degree polynomial functions).

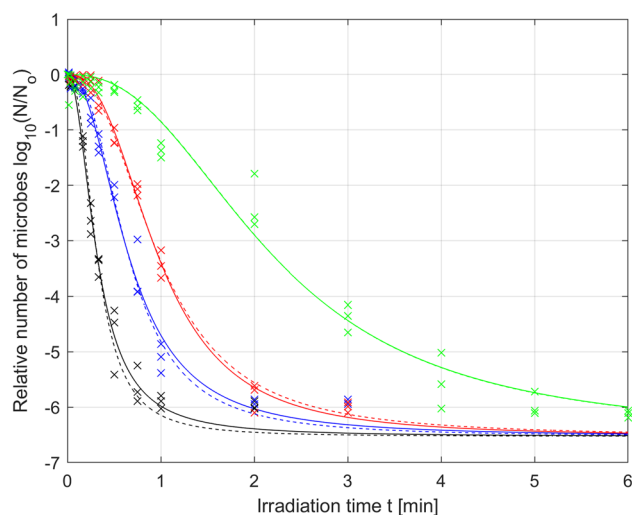


Figure 6. Photodynamic inactivation of *S. agalactiae* for various levels of irradiance: $\mu_1 = 70 \text{ mW/cm}^2$ (black), $\mu_2 = 52.5 \text{ mW/cm}^2$ (blue), $\mu_3 = 35 \text{ mW/cm}^2$ (red), $\mu_4 = 17.5 \text{ mW/cm}^2$ (green); experimental data (x) and microbial survival curves of the Logistic PDI model optimized for variation in the p and τ parameters (–) and only the τ parameter (—).

Irradiance	RMSE-optimized parameters			RMSE
	N_{ropt}	τ_{opt}	p_{opt}	
$\mu_1 = 100\%$	-6.529	0.318	2.084	0.2539
$\mu_2 = 75\%$		0.655	2.230	0.2515
$\mu_3 = 50\%$		0.969	2.555	0.1612
$\mu_4 = 25\%$		2.198	2.410	0.3072
RMSE-weighted mean	-6.529	1.045	2.421	0.2435
Coefficient of variation	0%	83.90%	8.87%	–

Table 4. Results of parameter optimization of the Logistic PDI model with a constant N_r parameter for various levels of irradiance μ [%].

The obtained functions that describe the variation in the optimal parameters p and τ of the Logistic model in the domain of irradiation power are expressed by the following formulas (Eq. 10):

$$\begin{aligned}
 N_{rB} &= -6.529 \\
 \tau_B(\mu) &= -0.0010 \times 10^{-2} \mu^3 + 0.2233 \times 10^{-2} \mu^2 - 17.2847 \times 10^{-2} \mu + 528.0000 \times 10^{-2} \\
 p_B(\mu) &= 0.0007 \times 10^{-2} \mu^3 - 0.1414 \times 10^{-2} \mu^2 + 8.1593 \times 10^{-2} \mu + 114.6000 \times 10^{-2}.
 \end{aligned} \quad (10)$$

Equations (3) and (10) constitute the next possible version of the extended Logistic PDI model obtained for the case of variation in two selected parameters (p and τ) of the Logistic model (case B), as indicated by the index B used in the parameter subscript. The total number of model parameters decreased compared to that in case A and was equal to $n=9$ in this case, while the mean value of the RMSE quality criterion increased and was equal to 0.2435. However, the increase in the mean value of the RMSE indicator to 0.2435 did not cause significant changes in the quality of fitting of the mortality curves to the experimental data, which can be seen by comparing Fig. 6 (solid lines) with Fig. 4. Thus, this result confirms the hypothesis that the N_r parameter of the Logistic model can be excluded from the need for variation without a significant reduction in the modeling quality. This is consistent with the assumptions because this parameter is responsible for the residual value of the microbial population and has little effect on the rate of decrease in the mortality curve.

However, setting the N_r parameter at a constant value requires new calculations to analyze the variation in optimal parameters of the Logistic model. Using formulas (5) and (7), new weighted mean values of the optimal parameters were calculated as follows:

$$\bar{N}_{rB} = -6.529, \quad \bar{\tau}_B = 1.045, \quad \bar{p}_B = 2.421. \quad (11)$$

In addition, the following new coefficients of variation were obtained, respectively:

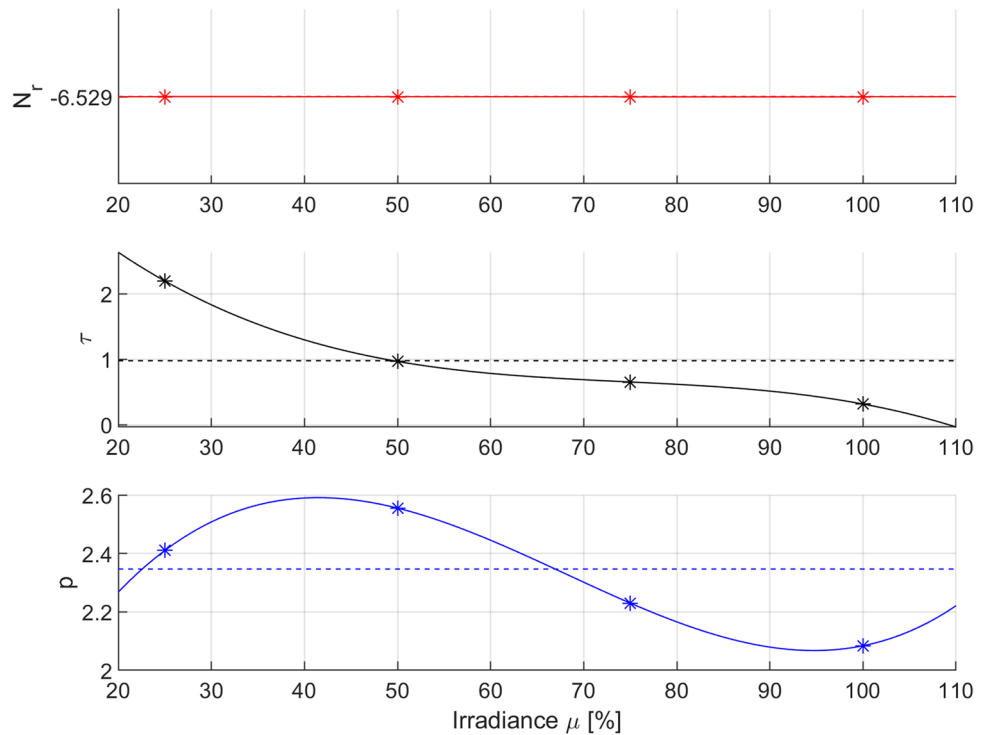


Figure 7. Optimal parameters of the Logistic PDI model (*) for various levels of irradiance μ [%] and their polynomial interpolation (-) with RMSE-weighted mean values (-). Optimization was carried out for variation in the p and τ parameters.

$$CV_{N_{rB}} = 0\%, \quad CV_{\tau B} = 83.90\%, \quad CV_{pB} = 8.87\%. \tag{12}$$

The mean values of parameters (11) are marked in Fig. 7 with dashed lines, and the coefficients of parameter variation (12) are given in Table 4. As expected, it can be seen that the coefficient of variation of parameter N_r in this case is equal to zero. It can also be seen that the coefficients of variation of parameters p and τ have slightly decreased compared with the results from case A; however, parameter τ still shows a significantly higher (approximately ten times) sensitivity to variation in irradiation power than parameter p . A similar ratio of coefficients of variation of parameters p and τ was observed in case A. However, it should be clearly noted here that this did not have to happen—in general, setting a chosen parameter to a constant value can significantly affect the mutual ratios of coefficients of variation of other parameters. Therefore, each time after the selected parameter has been varied, it is necessary to reanalyze the variation in the remaining parameters of the identified model.

Case C: variation in the τ parameter for constant N_r and p . The results of the analysis of parameter variation presented in case B led to the formulation of the hypothesis that omitting the variation in parameter p of the Logistic model may also give similar results in terms of the RMSE quality indicator to the results obtained in case A and case B. Therefore, in the next example, it was assumed that only parameter τ of the Logistic model was modified, while parameters N_r and p were set to constant values (11) determined in case B. As in the previous case, this required repeating of the parameter optimization procedure for the same experimental data. The optimization results for the τ parameter of the Logistic model with constant values for parameters N_r and p are shown in Fig. 6 (dashed lines) and Table 5.

Figure 8 presents the optimal values of parameter τ (with constant values of parameters p and N_r) of the Logistic model for the tested irradiation powers and the corresponding approximation curve (third-degree polynomial function).

The obtained function describing the variation in the optimal value of parameter τ of the Logistic model in the domain of irradiation power is expressed as follows (Eq. 13):

$$\begin{aligned} N_{rC} &= -6.529 \\ \tau_C(\mu) &= -0.0010 \times 10^{-2} \mu^3 + 0.2194 \times 10^{-2} \mu^2 - 17.0733 \times 10^{-2} \mu + 525.0000 \times 10^{-2} \\ p_C &= 2.421. \end{aligned} \tag{13}$$

Equations (3) and (13) constitute the next possible version of the extended Logistic PDI model obtained for the case of variation in only one selected parameter (τ) of the Logistic model (case C), as indicated by the index C used in the parameter subscripts. The total number of parameters of the Logistic model decreased compared to that in case B and was equal to $n=6$ in this case, while the mean value of the RMSE fitting quality criterion

Irradiance	RMSE-optimized parameters			RMSE
	$N_{r\text{opt}}$	τ_{opt}	p_{opt}	
$\mu_1 = 100\%$	-6.529	0.318	2.421	0.2853
$\mu_2 = 75\%$		0.653		0.2597
$\mu_3 = 50\%$		0.974		0.1664
$\mu_4 = 25\%$		2.200		0.3072
RMSE-weighted mean	-6.529	1.001	2.421	0.2547
Coefficient of variation	0%	82.06%	0%	-

Table 5. Results of parameter optimization of the Logistic PDI model with constant N_r and p parameters for various levels of irradiance μ [%].

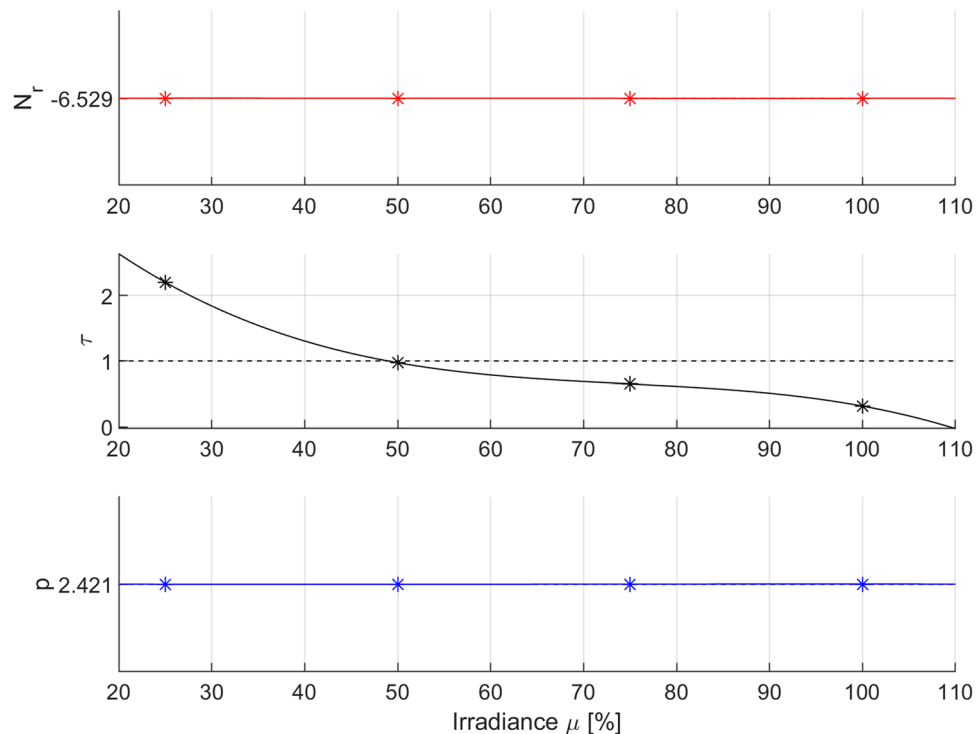


Figure 8. Optimal parameters of the Logistic PDI model (*) for various levels of irradiance μ [%] and their polynomial interpolation (-) with RMSE-weighted mean values (-). Optimization was carried out for variation in the τ parameter.

increased and was equal to 0.2547. However, as in case B, the deterioration of the RMSE fitting quality indicator was not so significant, which can be seen by comparing solid lines and dashed lines in Fig. 6. Thus, this finding confirms the hypothesis that the N_r and p parameters of the Logistic model can be excluded from the need for variation without a significant deterioration in the modeling quality.

The weighted mean values of the optimal parameters calculated from formula (Eq. 5) in this case are as follows:

$$\bar{N}_{rC} = -6.529, \quad \bar{\tau}_C = 1.001, \quad \bar{p}_C = 2.421. \tag{14}$$

The coefficients of variation calculated from formula (Eq. 7) of the individual parameters of the Logistic model are as follows:

$$CV_{N_{rC}} = 0\%, \quad CV_{\tau C} = 82.06\%, \quad CV_{pC} = 0\%. \tag{15}$$

The mean values of the parameters (14) are marked in Fig. 8 with dashed lines, and the coefficients of parameter variation (15) are given in Table 5. It can be seen that the coefficients of variation of parameters N_r and p were equal to zero, while the coefficient of variation of parameter τ maintained its value at a similar level as that in case B. The relatively high value of the coefficient of variation of parameter τ suggests that the variation in this parameter may be of key importance for maintaining the required quality of model fitting to the experimental

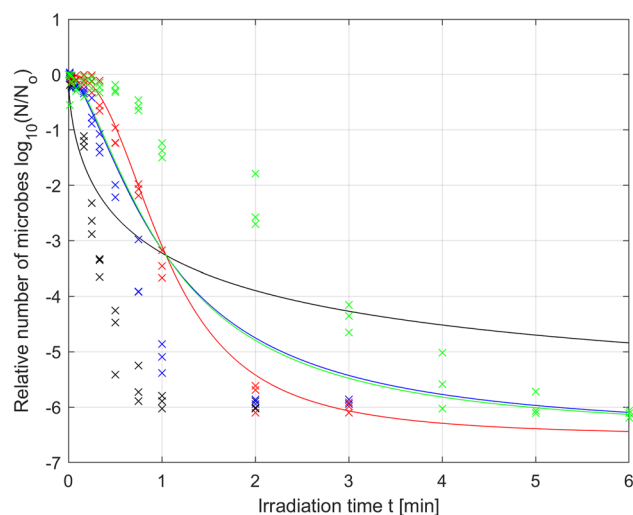


Figure 9. Photodynamic inactivation of *S. agalactiae* for various levels of irradiance: $\mu_1 = 70 \text{ mW/cm}^2$ (black), $\mu_2 = 52.5 \text{ mW/cm}^2$ (blue), $\mu_3 = 35 \text{ mW/cm}^2$ (red), $\mu_4 = 17.5 \text{ mW/cm}^2$ (green): experimental data (x) and microbial survival curves (-) of the Logistic PDI model optimized for variation in only the p parameter.

Irradiance	RMSE-optimized parameters			RMSE
	N_{ropt}	τ_{opt}	p_{opt}	
$\mu_1 = 100\%$	-6.529	1.045	0.602	1.5812
$\mu_2 = 75\%$			1.551	0.7858
$\mu_3 = 50\%$			2.439	0.2104
$\mu_4 = 25\%$			1.565	1.0631
RMSE-weighted mean	-6.529	1.045	2.029	0.9101
Coefficient of variation	0%	0%	46.31%	-

Table 6. Results of parameter optimization of the Logistic PDI model with constant N_r and τ parameters for various levels of irradiance μ [%].

data. To confirm this hypothesis, case D was analyzed, in which instead of variation in parameter τ , parameter p was varied for constant values of parameters N_r and τ .

Case D: Variation in the p parameter for constant N_r and τ . In this case, it was assumed that only parameter p of the Logistic model will be modified, while parameters N_r and τ will be set to constant values (11) determined in case B. The optimization results of the p parameter of the Logistic model for constant values of the N_r and τ parameters are shown in Fig. 9 and Table 6.

As seen in Table 6, in this case, the mean value of the RMSE fitting quality criterion is significantly higher compared to that in case C and is equal to 0.9101. It can be clearly seen in Fig. 9 that the quality of fitting the Logistic model to the experimental data obtained by changing parameter p for constant values of parameters N_r and τ does not give the expected results.

Case E: Logistic PDI model with all constant parameters: N_r , p and τ . The last considered case is the variant in which all parameters of the Logistic model are excluded from modification. In this case, it was assumed that all parameters of the Logistic model will be set to constant values (11) determined in case B. The optimization results in this case are shown in Fig. 10 and Table 7.

Of course, in this case, the quality of model fitting significantly deteriorates compared to all previous cases. This confirms the need to modify the parameters of the Logistic model.

Discussion

The problem of mathematical inclusion of the effect of changes in irradiance into the PDI models is not a trivial issue. The discussed cases show that for multiparameter PDI models, there are many variants of parameter modification that take into account the utilized irradiance. The parameter dependence on irradiation power was adopted as the method of parameter modification in this study. An appropriate dependence on irradiation power was obtained by approximation of parameter variation by third-degree polynomial functions within the tested

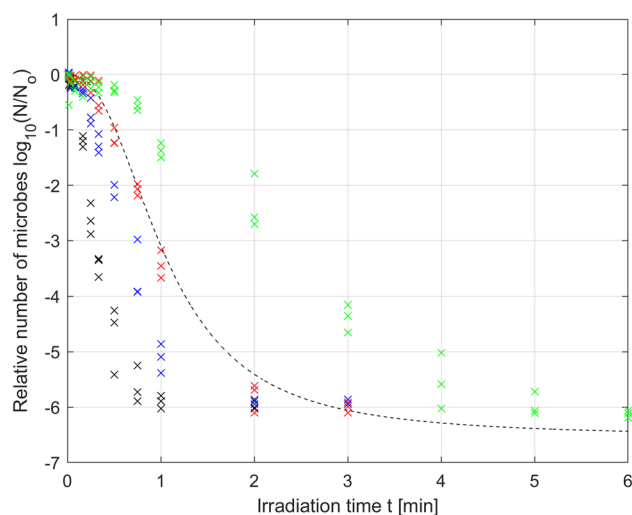


Figure 10. Photodynamic inactivation of *S. agalactiae* for various levels of irradiance: $\mu_1 = 70 \text{ mW/cm}^2$ (black), $\mu_2 = 52.5 \text{ mW/cm}^2$ (blue), $\mu_3 = 35 \text{ mW/cm}^2$ (red), $\mu_4 = 17.5 \text{ mW/cm}^2$ (green): experimental data (x) and microbial survival curve (–) of the Logistic PDI model optimized for all constant parameters.

Irradiance	RMSE-optimized parameters			RMSE
	N_{ropt}	τ_{opt}	p_{opt}	
$\mu_1 = 100\%$	– 6.529	1.045	2.421	2.1824
$\mu_2 = 75\%$				0.9013
$\mu_3 = 50\%$				0.2105
$\mu_4 = 25\%$				1.1300
RMSE-weighted mean	– 6.529	1.045	2.421	1.1060
Coefficient of variation	0%	0%	0%	–

Table 7. Results of parameter optimization of the Logistic PDI model with all constant parameters for various levels of irradiance μ [%].

irradiation power range. That choice was sufficient in each of the considered cases. The model fitting quality and the degree of complexity of the proposed parameter modification were the most important comparative criteria utilized in this analysis. However, the fulfillment of both of these criteria usually results in mutual contradiction. In general, the decrease in the number of parameters to be modified leads to deterioration in the fitting quality indicators. Deterioration of the model fitting quality may also be caused by inappropriate selection of the function that approximates the optimal parameter variations. Each of the considered cases is characterized by a different fitting quality and a different degree of model complexity related to the total number of parameters. The most important results of this study are presented in Table 8.

The purpose of this comparative analysis is to find an effective compromise between the fitting quality and the total number of parameters of the proposed extended PDI model (Eq. 3) in the whole tested irradiation power range. In case A, all parameters of the Logistic PDI model were modified. This solution provides the best fit results but has a serious drawback in terms of model complexity. In this case, the total number of parameters is equal to 12, which makes it very difficult to use such a model. In case B, where only two parameters were modified, the total number of parameters decreased compared to case A and equaled 9, but at the cost of model fitting quality. However, this difference is not significant. In case C, the number of modified parameters was reduced to 1, and the total number of extended model parameters was reduced to 6. As in case B, the model fitting quality slightly deteriorated, but this difference was still not significant. In case D, the number of modified parameters was also reduced to 1, with the total number of extended model parameters also equal to 6, but the model fitting quality deteriorated significantly. Case E, in which no parameters were modified, exhibited the worst model fitting quality.

A comparative analysis of cases C and D confirms the hypothesis in case C that the variation in the τ parameter is of key importance for maintaining a high quality of the extended Logistic model within the tested irradiation power range. This may be slightly surprising because the combination of the p and τ parameters is responsible for the shape and the rate of decrease of the microbial mortality curve in the Logistic model, so it would seem that both these parameters should be changed to maintain the required fitting quality. However, the results of the conducted analysis of parameter variation clearly show that the variation in parameter p in the

Modification case	Parameters of extended logistic PDI model	Total number of parameters	Mean RMSE
A	$N_{rA}(\mu) = 0.0009 \times 10^{-2} \mu^3 - 0.2161 \times 10^{-2} \mu^2 + 17.2507 \times 10^{-2} \mu - 1076.8000 \times 10^{-2}$ $\tau_A(\mu) = -0.0015 \times 10^{-2} \mu^3 + 0.3279 \times 10^{-2} \mu^2 - 25.0780 \times 10^{-2} \mu + 710.7000 \times 10^{-2}$ $p_A(\mu) = 0.0011 \times 10^{-2} \mu^3 - 0.2330 \times 10^{-2} \mu^2 + 15.6713 \times 10^{-2} \mu - 71.2000 \times 10^{-2}$	12	0.2207
B	$N_{rB} = -6.529$ $\tau_B(\mu) = -0.0010 \times 10^{-2} \mu^3 + 0.2233 \times 10^{-2} \mu^2 - 17.2847 \times 10^{-2} \mu + 528.0000 \times 10^{-2}$ $p_B(\mu) = 0.0007 \times 10^{-2} \mu^3 - 0.1414 \times 10^{-2} \mu^2 + 8.1593 \times 10^{-2} \mu + 114.6000 \times 10^{-2}$	9	0.2435
C	$N_{rC} = -6.529$ $\tau_C(\mu) = -0.0010 \times 10^{-2} \mu^3 + 0.2194 \times 10^{-2} \mu^2 - 17.0733 \times 10^{-2} \mu + 525.0000 \times 10^{-2}$ $p_C = 2.421$	6	0.2547
D	$N_{rD} = -6.529$ $\tau_D = 1.045$ $p_D(\mu) = 0.0018 \times 10^{-2} \mu^3 - 0.4131 \times 10^{-2} \mu^2 + 26.5420 \times 10^{-2} \mu - 277.2000 \times 10^{-2}$	6	0.9101
E	$N_{rE} = -6.529$ $\tau_E = 1.045$ $p_E = 2.421$	3	1.1060

Table 8. Comparative analysis of several case studies of parameter modification of the Logistic PDI model for various irradiances μ [%].

case under study can be omitted. Under the studied conditions, the variation in the irradiation power most likely affects such characteristics of the mortality curve for which the τ parameter of the Logistic model is decisively responsible. The only problem is finding the appropriate values of parameters N_r and p , for which the variation in parameter τ gives satisfactory results for fitting the model to the experimental data. The presented method of parameter modification describes the method for finding these values by using the coefficients of variation of the Logistic model parameters.

The conducted comparative analysis shows that the most favorable of the presented cases of parameter variation is case C. In this case, the best compromise between the total number of model parameters ($n = 6$) and the mean RMSE fitting indicator (0.2547) were obtained. The final extended Logistic PDI model that takes into account the effect of changes in the irradiance can be presented in the following form (Eq. 16):

$$\log\left(\frac{N(t)}{N_o}\right) = \bar{N}_{rC} \left(1 - \frac{1}{1 + \left(\frac{t}{a_{\tau 3} \mu^3 + a_{\tau 2} \mu^2 + a_{\tau 1} \mu + a_{\tau 0}}\right)^{\bar{p}_C}} \right) \tag{16}$$

where the parameters of this model are as follows:

$$\begin{aligned} \bar{N}_{rC} &= -6.529, \\ \bar{p}_C &= 2.421, \end{aligned} \tag{17}$$

while the τ parameter is expressed as a four-element vector of polynomial coefficients:

$$\boldsymbol{\tau} = [a_{\tau 3} \ a_{\tau 2} \ a_{\tau 1} \ a_{\tau 0}]^T = 10^{-2} \times [0.0010 \ 0.2194 \ -17.0733 \ 525.0000]^T \tag{18}$$

The extended Logistic PDI model (Eqs. 16–18) obtained in the conducted research effectively describes the dynamics of microorganism mortality in the whole tested irradiation power range μ [%]. The usefulness of this model is illustrated in Fig. 11.

The resulting extended model expressed in the form (Eqs. 16–18) can be successfully used to estimate the required irradiation time for any power level within the tested range. Assuming $x_{req} = \log(N/N_o)$ as the relative logarithmic number of microorganisms required and μ [%] as the level of irradiance used, the required irradiation time t_{req} [min] can be calculated from the following formula (Eq. 19):

$$t_{req}(x_{req}, \mu) = \left(\frac{1}{1 - \frac{x_{req}}{\bar{N}_{rC}}} - 1 \right)^{\frac{1}{\bar{p}_C}} \cdot (a_{\tau 3} \mu^3 + a_{\tau 2} \mu^2 + a_{\tau 1} \mu + a_{\tau 0}) \tag{19}$$

where all parameters are the same as in Eqs. (17, 18).

The mathematical expression presented in Eq. (19) is a model describing the dependence of the required irradiation time t_{req} [min] as a function of the required size of the microorganism population $x_{req} = \log(N/N_o)$ and used level of irradiance μ [%]. The usefulness of this model is shown in Fig. 12.

Analysis of the number of microbes as dependent of radiant exposure (light dose) can be an added value to the resulting extended model (Eq. 19). The results presented in Fig. 13 show that the greater the radiant exposure is, the smaller the population size, but for various levels of irradiance the curves have a slightly different shape

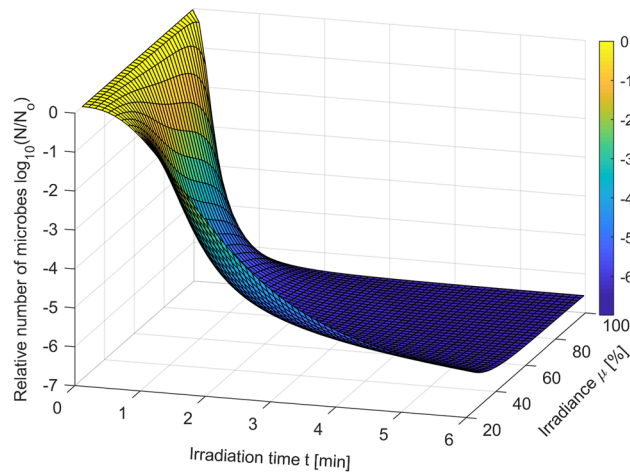


Figure 11. Extended logistic model of *S. agalactiae* photodynamic inactivation in the whole tested range of irradiance μ [%].

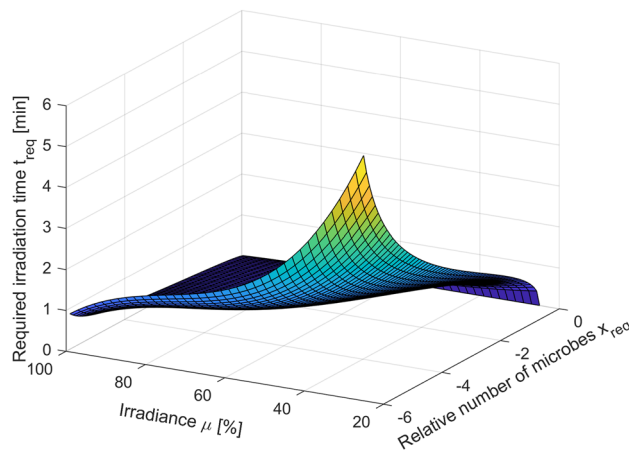


Figure 12. *S. agalactiae* PDI model estimating the required irradiation time t_{req} [min] for required size of microorganism population x_{req} and used level of irradiance μ [%].

and differ for lower radiant exposures (less than 10 J/cm²). In particular, the curve for irradiance $\mu_1 = 70$ mW/cm² is slightly deviated from the others. This information can be helpful to determine the required irradiation time in relation to level of irradiance in PDI processes. The obtained results lead to the conclusion that in case of the current study the use of higher irradiance can be beneficial to minimize the radiant exposure. Nevertheless, one must be aware that irradiance is closely related to temperature; thus, this parameter should be adjusted in such manner to avoid bacterial killing from heat.

The results of the mathematical analysis made in the current study differ significantly from the results available in the literature on the subject (in particular, in the works of the Luksiene's team)^{13–15,17}. In the studies by Luksiene's group, only the results of matching the classic 3-parameter Logistic model depending on different incubation times are shown (which, like the exposure power, is one of the factors affecting the inactivation process). However, the presented results do not formulate any mathematical sub-model, which would approximate the obtained relationships to include them in the classic model. These reports do not discuss any way to modify the parameters of the classic model to optimize its extension. There is also no analysis of the significance of individual model parameters due to the examined factor, or any other method that could be used while minimizing the number of additional model parameters that are required to model the obtained relationships. Ultimately, there are also no inverse models that allow predicting the minimum necessary exposure time depending on the factor tested. Our analysis evidence which of the parameters of the classic 3-parameter Logistic model is the most important one due to the exposure power factor. The fact that it was possible to select such a parameter of the studied model is also a remarkable achievement. In the case of multi-parameter models, this problem is not a trivial matter. In general, such unambiguous selection of a parameter responsible for specific model properties may be difficult or even impossible to obtain. Then, any possible modifications to the model would have to apply to all its parameters, which would usually cause a sudden increase in the number of additional parameters and a

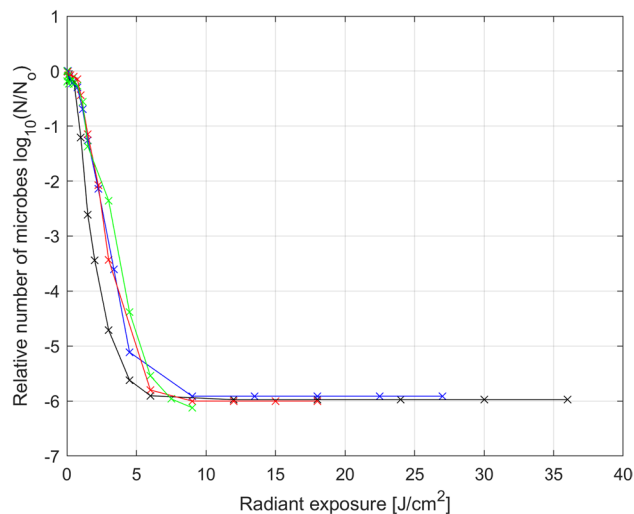


Figure 13. Photodynamic inactivation of *S. agalactiae* for various radiant exposures (light doses) and various levels of irradiance: $\mu_1 = 70$ mW/cm² (black), $\mu_2 = 52.5$ mW/cm² (blue), $\mu_3 = 35$ mW/cm² (red), $\mu_4 = 17.5$ mW/cm² (green): averaged experimental data (x) and its linear interpolation (-).

significant and disproportionate increase in modeling costs. In addition, thanks to the conducted research, it was possible to formulate an inverse model (Eq. 19, Fig. 12) that allows to predict the minimum necessary irradiation time needed to achieve the required level of population size for the adopted exposure power. Obtaining such a model could be considered the main motivation for extending the classic model.

Final conclusions

One of the methods of taking into account the effect of irradiance in the identified PDI model may be to make its parameter appropriately dependent on that factor. Unfortunately, for multiparameter PDI models, an appropriate variation in all model parameters can lead to excessive complications and an increase in the number of parameters. Therefore, striving to simplify the modifications included in the model is warranted. Determining which model parameters need to be varied and which do not is not a trivial matter in general. As shown in the manuscript, by properly conducting an analysis of model parameter variation, it is possible to effectively limit the total number of parameters of the examined model without worsening the model fitting quality to the collected experimental data. The main result of the manuscript is the extended Logistic PDI model that takes into account the irradiance by varying the appropriately selected parameters of this model with functions depending on the used irradiation power. Furthermore, the developed extended Logistic PDI model can be successfully used to estimate the required irradiation time for any power level within the tested range.

Data availability

The datasets generated during and/or analysed during the current study are available from the corresponding author on reasonable request.

Received: 5 February 2020; Accepted: 7 August 2020

Published online: 25 August 2020

References

1. Heath, P. T. & Schuchat, A. Perinatal group B streptococcal disease. *Best Pract. Res. Clin. Obstet. Gynaecol.* **21**, 411–424. <https://doi.org/10.1016/j.bpobgyn.2007.01.003> (2007).
2. Fila, G., Kawiak, A. & Grinholc, M. S. Blue light treatment of *Pseudomonas aeruginosa*: Strong bactericidal activity, synergism with antibiotics and inactivation of virulence factors. *Virulence* **8**, 938–958. <https://doi.org/10.1080/21505594.2016.1250995> (2017).
3. Fila, G., Krychowiak, M., Rychlowski, M., Bielawski, K. P. & Grinholc, M. Antimicrobial blue light photoinactivation of *Pseudomonas aeruginosa*: Quorum sensing signaling molecules, biofilm formation and pathogenicity. *J Biophoton.* <https://doi.org/10.1002/jbio.201800079> (2018).
4. Wozniak, A., Rapacka-Zdanczyk, A., Mutters, N. T. & Grinholc, M. Antimicrobials are a photodynamic inactivation adjuvant for the eradication of extensively drug-resistant *Acinetobacter baumannii*. *Front. Microbiol.* **10**, 229. <https://doi.org/10.3389/fmicb.2019.00229> (2019).
5. Rapacka-Zdanczyk, A. *et al.* Development of *Staphylococcus aureus* tolerance to antimicrobial photodynamic inactivation and antimicrobial blue light upon sub-lethal treatment. *Sci. Rep.* **9**, 9423. <https://doi.org/10.1038/s41598-019-45962-x> (2019).
6. Tanielian, C., Mechin, R., Seghrouchni, R. & Schweitzer, C. Mechanistic and kinetic aspects of photosensitization in the presence of oxygen. *Photochem. Photobiol.* **71**, 12–19. [https://doi.org/10.1562/0031-8655\(2000\)071%3c0012:makaop%3e2.0.co;2](https://doi.org/10.1562/0031-8655(2000)071%3c0012:makaop%3e2.0.co;2) (2000).
7. Wang, Y. *et al.* Photoinactivation of *Neisseria gonorrhoeae*: A paradigm-changing approach for combating antibiotic-resistant gonococcal infection. *J. Infect. Dis.* **220**, 873–881. <https://doi.org/10.1093/infdis/jiz018> (2019).
8. Vollmer, A. *et al.* Antimicrobial photoinactivation using visible light plus water-filtered infrared-A (VIS + wIRA) and hypericum perforatum modifies in situ oral biofilms. *Sci. Rep.* **9**, 20325. <https://doi.org/10.1038/s41598-019-56925-7> (2019).

9. Aroso, R. T. *et al.* Photoinactivation of microorganisms with sub-micromolar concentrations of imidazolium metallophthalocyanine salts. *Eur. J. Med. Chem.* **184**, 111740. <https://doi.org/10.1016/j.ejmech.2019.111740> (2019).
10. Muehler, D. *et al.* Light-activated phenalen-1-one bactericides: Efficacy, toxicity and mechanism compared with benzalkonium chloride. *Future Microbiol.* **12**, 1297–1310. <https://doi.org/10.2217/fmb-2016-0229> (2017).
11. Wen, X. *et al.* Potassium iodide potentiates antimicrobial photodynamic inactivation mediated by rose bengal in vitro and in vivo studies. *Antimicrob. Agents Chemother.* <https://doi.org/10.1128/AAC.00467-17> (2017).
12. Nakonieczna, J. *et al.* Rose Bengal-mediated photoinactivation of multidrug resistant *Pseudomonas aeruginosa* is enhanced in the presence of antimicrobial peptides. *Front. Microbiol.* **9**, 1949. <https://doi.org/10.3389/fmicb.2018.01949> (2018).
13. Buchovec, I., Vaitonis, Z. & Luksiene, Z. Novel approach to control *Salmonella enterica* by modern biophotonic technology: photosensitization. *J. Appl. Microbiol.* **106**, 748–754. <https://doi.org/10.1111/j.1365-2672.2008.03993.x> (2009).
14. Dementavicius, D., Lukseviciute, V., Gomez-Lopez, V. M. & Luksiene, Z. Application of mathematical models for bacterial inactivation curves using Hypericin-based photosensitization. *J. Appl. Microbiol.* **120**, 1492–1500. <https://doi.org/10.1111/jam.13127> (2016).
15. Vaitonis, Z. & Luksiene, Z. LED-based light sources for decontamination of food: Modelling photosensitization-based inactivation of pathogenic bacteria. *Lith. J. Phys.* **505080**, 141–145. <https://doi.org/10.3952/lithjphys.50102> (2010).
16. Aponiene, K., Paskeviciute, E., Reklaitis, I. & Luksiene, Z. Reduction of microbial contamination of fruits and vegetables by hypericin-based photosensitization: Comparison with other emerging antimicrobial treatments. *J. Food Eng.* **144**, 29–35. <https://doi.org/10.1016/j.jfoodeng.2014.07.012> (2015).
17. Luksiene, Z. K. & Katauskis, P. Novel approach to effective and uniform inactivation of gram-positive *Listeria monocytogenes* and gram-negative *Salmonella enterica* by photosensitization. *Food Technol. Biotechnol.* **51**, 338–344 (2013).
18. Ogonowska, P. W. *et al.* Application and characterization of light-emitting diodes for photodynamic inactivation of bacteria. *Light. Res. Technol.* **51**, 612–624. <https://doi.org/10.1177/1477153518781478> (2019).
19. Werts, M. H. *et al.* Quantitative full-colour transmitted light microscopy and dyes for concentration mapping and measurement of diffusion coefficients in microfluidic architectures. *Lab. Chip* **12**, 808–820. <https://doi.org/10.1039/c2lc20889j> (2012).
20. Ludvikova, L. *et al.* Photochemistry of rose bengal in water and acetonitrile: a comprehensive kinetic analysis. *Phys. Chem. Chem. Phys.* **18**, 16266–16273. <https://doi.org/10.1039/c6cp01710j> (2016).
21. Kamau, D. N., Doores, S. & Pruitt, K. M. Enhanced thermal destruction of *Listeria monocytogenes* and *Staphylococcus aureus* by the lactoperoxidase system. *Appl. Environ. Microbiol.* **56**, 2711–2716 (1990).
22. Gibson, A. M., Bratchell, N. & Roberts, T. A. Predicting microbial growth: growth responses of salmonellae in a laboratory medium as affected by pH, sodium chloride and storage temperature. *Int. J. Food Microbiol.* **6**, 155–178. [https://doi.org/10.1016/0168-1605\(88\)90051-7](https://doi.org/10.1016/0168-1605(88)90051-7) (1988).
23. Li, H. X. & Edmondson, A. Evolution and limitations of primary models in predictive microbiology. *Br. Food J.* **109**, 608–626 (2007).
24. Smelt, J. P. & Brul, S. Thermal inactivation of microorganisms. *Crit. Rev. Food Sci. Nutr.* **54**, 1371–1385. <https://doi.org/10.1080/10408398.2011.637645> (2014).
25. Talkington, A. I., Holmes, L. & Wei, G. An extension of a logistic model for microbial kinetics. *Adv. Syst. Sci. Appl.* **13**, 80–99 (2013).
26. Wolf, K. H. V. J. Description of the delayed microbial growth by an extended logistic equation. *Acta Biotechnol.* **12**, 405–410. <https://doi.org/10.1002/abio.370120509> (1992).
27. Whiting, R. C. A classification of models for predictive microbiology. *Food Microbiol.* **10**, 175–177 (1993).
28. Fujikawa, H. K. & Morozumi, S. A new logistic model for *Escherichia coli* growth at constant and dynamic temperatures. *Food Microbiol.* **21**, 501–509. <https://doi.org/10.1016/j.fm.2004.01.007> (2004).
29. Fakruddin, M. M. & Mannan, S. Predictive microbiology: Modeling microbial responses in food. *Ceylon J. Sci.* **40**, 121–131. <https://doi.org/10.4038/cjsbs.v40i2.3928> (2011).
30. Jin, W., McCue, S. W. & Simpson, M. J. Extended logistic growth model for heterogeneous populations. *J. Theor. Biol.* **445**, 51–61. <https://doi.org/10.1016/j.jtbi.2018.02.027> (2018).

Acknowledgements

Work was supported by Grant no. NCN 2016/23/B/NZ7/03236 (M.G.).

Author contributions

M.B. performed computational modeling, participated in the data interpretation and wrote the manuscript. M.P. did the experimental work and participated in conception of the study. M.G. has been involved in the coordination, conception, and design of the study, participated in the writing the manuscript. All of the authors have read and approved the final manuscript.

Competing interests

The authors declare no competing interests.

Additional information

Correspondence and requests for materials should be addressed to M.B. or M.G.

Reprints and permissions information is available at www.nature.com/reprints.

Publisher's note Springer Nature remains neutral with regard to jurisdictional claims in published maps and institutional affiliations.



Open Access This article is licensed under a Creative Commons Attribution 4.0 International License, which permits use, sharing, adaptation, distribution and reproduction in any medium or format, as long as you give appropriate credit to the original author(s) and the source, provide a link to the Creative Commons licence, and indicate if changes were made. The images or other third party material in this article are included in the article's Creative Commons licence, unless indicated otherwise in a credit line to the material. If material is not included in the article's Creative Commons licence and your intended use is not permitted by statutory regulation or exceeds the permitted use, you will need to obtain permission directly from the copyright holder. To view a copy of this licence, visit <http://creativecommons.org/licenses/by/4.0/>.

© The Author(s) 2020

Chapter III

Increased photoinactivation stress tolerance of *Streptococcus agalactiae* upon consecutive sublethal phototreatments

1. Summary of the publication

In a complex environment such as a skin wound or vaginal mucosa, no one can exclude the possibility, that some bacteria will be given only a suboptimal dose of illumination and will survive. If a situation like this will be repeated many times, bacteria may adapt in a similar manner as to the antibiotics.

As the phenomenon of aPDI tolerance was shown for the first time for *S. aureus* [36], this study has extended this research and was first to show that this phenomenon applies also to other bacterial families. Three strains of *S. agalactiae* were treated with consecutive cycles of sub-lethal doses of aPDI. It led to the development of tolerance, which stability was further confirmed. There were observed genetic alterations induced with sub-lethal aPDI treatment and also significant changes in the expression levels of oxidative stress-related genes. The response of tolerant strain to different oxidants like superoxide, hydrogen peroxide, hypochlorite and singlet oxygen was also examined. Moreover, phenotypic changes were observed, as well as reduced RB uptake when compared to that of the wild-type strain.

Nevertheless, it is important to highlight that obtained significant aPDI tolerance development cannot be considered as resistance to phototreatment. The employment of more rigorous experimental conditions (increased RB concentrations or longer time of illumination) may still result in bacterial eradication of the aPDI-tolerant phenotype. The most important take-home message that comes from this study is the responsibility of researchers during the implementation of new approaches to the clinic. In this publication research concerning Aim 1. was extended and Aim 3. was reached.

2. Publication



Original article

Increased photoinactivation stress tolerance of *Streptococcus agalactiae* upon consecutive sublethal phototreatmentsMichal Pieranski^a, Izabela Sitkiewicz^b, Mariusz Grinholc^{a,*}^a Intercollegiate Faculty of Biotechnology, Laboratory of Molecular Diagnostics, University of Gdansk and Medical University of Gdansk, Abrahama 58, 80-307, Gdansk, Poland^b Department of Drug Biotechnology and Bioinformatics, National Medicines Institute, Chelmska 30/34, 00-725, Warszawa, Poland

ARTICLE INFO

Keywords:

Oxidative stress
 Photodynamic inactivation
 Photoinactivation
Streptococcus agalactiae
 Stress tolerance

ABSTRACT

Streptococcus agalactiae (Group B Streptococcus, GBS) is a common commensal bacterium in adults but remains a leading source of invasive infections in newborns, pregnant women, and the elderly, and more recently, causes an increased incidence of invasive disease in nonpregnant adults. Reduced penicillin susceptibility and emerging resistance to non- β -lactams pose challenges for the development and implementation of novel, nonantimicrobial strategies to reduce the burden of GBS infections. Antimicrobial photodynamic inactivation (aPDI) via the production of singlet oxygen or other reactive oxygen species leads to the successful eradication of pathogenic bacteria, affecting numerous cellular targets of microbial pathogens and indicating a low risk of resistance development. Nevertheless, we have previously reported possible aPDI tolerance development upon repeated sublethal aPDI applications; thus, the current work was aimed at investigating whether aPDI tolerance could be observed for GBS and what mechanisms could cause it. To address this problem, 10 cycles of sublethal aPDI treatments employing rose bengal as a photosensitizer, were applied to the *S. agalactiae* ATCC 27956 reference strain and two clinical isolates (2306/02 and 2974/07, serotypes III and V, respectively). We demonstrated aPDI tolerance development and stability after 5 cycles of subculturing with no aPDI exposure. Though the treatment resulted in a stable phenotype, no increases in mutation rate or accumulated genetic alterations were observed (employing a RIF-, CIP-, STR-resistant mutant selection assay and *cyl* sequencing, respectively). qRT-PCR analysis demonstrated that 10 sublethal aPDI exposures led to increased expression of all tested major oxidative stress response elements; changes in *sodA*, *ahpC*, *npv*, *cylE*, *tpx* and *recA* expression indicate possible mechanisms of developed tolerance. Increased expression upon sublethal aPDI treatment was reported for all but two genes, namely, *ahpC* and *cylE*. aPDI targeting *cylE* was further supported by colony morphology changes induced with 10 cycles of aPDI (increased SCV population, increased hemolysis, increased numbers of dark- and unpigmented colonies). In oxidant killing assays, aPDI-tolerant strains demonstrated no increased tolerance to hypochlorite, superoxide (paraquat), singlet oxygen (new methylene blue) or oxidative stress induced by aPDI employing a structurally different photosensitizer, i.e., zinc phthalocyanine, indicating a lack of cross resistance. The results indicate that *S. agalactiae* may develop stable aPDI tolerance but not resistance when subjected to multiple sublethal phototreatments, and this risk should be considered significant when defining efficient *anti-S. agalactiae* aPDI protocols.

1. Introduction

Streptococcus agalactiae (Group B Streptococcus, GBS) is a β -hemolytic Gram-positive bacterium that asymptotically colonizes the lower gastrointestinal and genitourinary tract of approximately 10–30% of human adults [1,2]. It is the leading cause of invasive bacterial infections in newborns (neonatal sepsis and meningitis) but has also recently been recognized as a pathogen in adult populations,

including pregnant women, the elderly, immune-compromised patients, and adults with underlying diseases such as diabetes and cancer [3–6]. *S. agalactiae* is traditionally considered a pathogen affecting infants and pregnant women; however, the incidence of GBS infection is increasing among nonpregnant adults [6]. Invasive infection due to GBS results in a wide spectrum of clinical diseases, such as bacteremia, sepsis, pneumonia, urinary tract infections (including cystitis, pyelonephritis, and asymptomatic bacteriuria), acute and chronic osteomyelitis, soft tissue

* Corresponding author.

E-mail address: mariusz.grinholc@biotech.ug.edu.pl (M. Grinholc).<https://doi.org/10.1016/j.freeradbiomed.2020.09.003>

Received 3 June 2020; Received in revised form 24 August 2020; Accepted 2 September 2020

Available online 08 September 2020

0891-5849/© 2020 The Author(s). Published by Elsevier Inc. This is an open access article under the CC BY-NC-ND license

<http://creativecommons.org/licenses/by-nc-nd/4.0/>.

and skin infections (manifesting as cellulitis, abscesses, foot infections, or decubitus ulcers), and thus is an increasing source of morbidity and mortality [7–14]. Moreover, *S. agalactiae* is an etiological factor causing the majority of cases of meningitis in neonates and is responsible for up to 7.4% of all community-acquired meningitis in adults with substantial mortality [15–17]. Furthermore, GBS infection continues to increase, and it remains a significant pathogen among both infants and adults [18]. β -Lactams (penicillin G, ampicillin, cephalosporins, and carbapenems) are first-line antimicrobial agents for both intrapartum prophylaxis and the treatment of GBS infections [19]. However, clinical isolates with reduced penicillin susceptibility, exhibiting often additional and increasing nonsusceptibility or resistance to other classes of antibiotics such as fluoroquinolones, glycopeptides and macrolides [20–25]; thus, the development and implementation of novel strategies leading to prevention and treatment of invasive GBS disease and the reductions in the burden of *S. agalactiae* infections are essential.

Antimicrobial photodynamic inactivation (aPDI) has gained increasing importance as a novel, nonantibiotic method targeting a wide variety of both Gram-positive and Gram-negative microbes [26–30]. In principle, the photochemical mechanism of aPDI is based on interactions of a photosensitizer (PS), light and molecular oxygen, which leads to the production of singlet oxygen as the most important cytotoxic and highly reactive molecule that can oxidize lipids, proteins, and nucleic acids, causing cell death [31]. In addition to singlet oxygen, other reactive oxygen species (ROS) were also confirmed to be involved in the bactericidal activity of aPDI. These ROS include hydroxyl radicals, hydrogen peroxide, and the superoxide anion [32]. The most important advantage of aPDI is that the bactericidal efficacy appears not to be affected by the antibiotic resistance status of the targeted microorganisms [33–35]. The risk of resistance post aPDI is still an open topic, as it was proven impossible to artificially generate aPDI-resistant microorganisms due to repeated application of sublethal photoinactivation and subsequent bacterial recovery [36–38]. Despite the above-mentioned advantages and most likely the fact that no resistance to aPDI was found under optimal photoinactivation conditions, we are aware that when treating the heterogeneous environment of infection sites, aPDI may reach the target site at sublethal doses, resulting in microorganisms being exposed to sublethal doses of oxidative stress that would not result in total cell death. We have previously demonstrated that such sublethal inactivation results in a substantial increase in mutational events, leading to selection for the survival of more aPDI-tolerant *S. aureus* strains [39]. Moreover, under sublethal treatment, a tolerant phenotype expressing enhanced SOS response and DNA mutagenicity was not only detected but a stable phenotype transferred to subsequent generations with no selective pressure [39].

Though previous studies seem to disregard and underestimate the significance of the possible development of aPDI tolerance, we consider the risk of tolerance development a significant factor that should be included when designing phototreatment protocols for clinical settings. Here, we ask the question of whether aPDI tolerance occurs in *S. agalactiae* and what molecular mechanisms may explain this phenomenon. We provide evidence that both reference and clinical GBS isolates, when administered sublethal killing amounts of aPDI, may develop a stable aPDI-tolerant phenotype. Moreover, the obtained data indicate that the increased basal and aPDI-induced expression of genes coding for key elements of oxidative stress defense and increased population of nonhemolytic small colony variants (SCVs) reported upon repeated administration of sublethal photoinactivation may explain decreased *S. agalactiae* susceptibility to aPDI.

2. Materials and methods

Experimental workflow. The experimental design included the two following: i) control samples (three biologically independent *S. agalactiae* cultures passaged through 10 cycles with no treatment to demonstrate whether genetic alterations gained with no selective

pressure may induce a detectable level of aPDI tolerance), and ii) aPDI-treated samples (three biologically independent *S. agalactiae* cultures treated with rose bengal (RB) and 515 nm light that resulted in sublethal inactivation of the microbial population to assess the risk of the development of tolerance to aPDI). For the proper implementation of this study, all of the *S. agalactiae* cultures described above (regrown from the 0, 5th and 10th cycle glycerol stocks) were tested to demonstrate i) a treatment-induced changes in the susceptibility to H_2O_2 , superoxide, hypochlorite, and singlet oxygen; ii) whether developed tolerance is limited to the selection treatment or translates into other phototreatments (the *S. agalactiae* susceptibility to aPDI employing PSs with different structures – new methylene blue (NMB) and zinc phthalocyanine (ZnPc)); iii) the phenotypic stability of the developed tolerance (with *S. agalactiae* cultures passaged for 5 cycles without selective pressure); iv) a treatment-induced change in the hemolysis and granadaene content; v) treatment-induced change in the RB uptake; and vi) whether sublethal aPDI leads to change in the expression levels of genes involved in oxidative stress response (to support the probable mechanism of tolerance development). All experiments were performed in three independent replicates.

Strains and culture conditions. This study was conducted with the *S. agalactiae* strain ATTC 27956, which was isolated from an infected bovine udder and represents Lancefield's group B streptococci, and two clinical strains, no. 2306/06 and 2974/07, which represent serotypes III and V, respectively. Bacteria were grown in tryptic soy broth (TSB) (Biomérieux, France). Overnight (OV) cultures were prepared by inoculating single colony into 5 mL of TSB medium and incubating at 37 °C for 16–20 h with shaking at 150 RPM. Log-phase culture was prepared by transferring 1.5 mL of OV culture into 30 mL of fresh TSB medium and incubating for approx. 3.5 h under the abovementioned conditions, which corresponds with the mid-log phase of growth (LOG).

Light source. LED light sources with emission maxima at 515 nm and 632 nm were custom made by EMD Technology (Warsaw, Poland). The light sources were precisely characterized in our previous publication [40]. For all experiments, maximal power settings were used. A 515 nm lamp was used for RB, and a 632 nm lamp was used for NMB and ZnPc.

Determination of the aPDI lethal and sublethal conditions. Microbial OV cultures were adjusted to optical density of 2.4 McFarland units (8×10^7 CFU/ml) in TSB, and aliquots of 200 μ l were transferred to Eppendorf tubes. PS was added to the bacterial suspensions at a final concentration of up to 1 μ M (RB and ZnPc) or 150 μ M (NMB). The aPDI samples treated with RB, ZnPc or NMB were incubated in the dark for 15 min at 37 °C. The samples were centrifuged at 10,000 g for 3 min and washed 2 times with phosphate-buffered saline (PBS). Then, 100 μ l of samples in 96 well microtiter plates was exposed to different light doses (up to 40 J/cm² at λ_{max} 515 nm for RB or 50 J/cm² at λ_{max} 632 nm for ZnPc and NMB). After illumination, 10 μ l aliquots were serially diluted tenfold in PBS to generate dilutions of 10^{-1} to 10^{-4} and streaked horizontally on Columbia blood agar plates (Biomérieux, France). The blood agar plates were incubated at 37 °C for 16–20 h, and then colonies were counted to estimate the survival rate. Control groups included cells that were not treated with PSs or light. Each experiment was performed in triplicate. For the purpose of this study, lethal doses of aPDI were defined as those that resulted in an approximately ≥ 3 log₁₀ reduction in CFU, and sublethal doses were defined as a ≤ 2 log₁₀ reduction in CFU/ml.

Determination of tolerance development following repeated sublethal exposures to aPDI. Microbial OV culture was adjusted to an optical density of 2.4 McFarland units in TSB and then incubated with 0.1 μ M RB (Sigma) in the dark for 15 min at 37 °C. The sample was centrifuged at 10,000 g for 3 min and washed 2 times with PBS. Then, 100 μ l of the sample was illuminated with 20 J/cm². After illumination 50 μ l of the sample was transferred into 5 ml of fresh TSB medium and cultured overnight. The cycle of exposure – regrowth – exposure was repeated for 10 days. From the regrown cultures 20% glycerol stocks

were prepared and stored at -80°C . Analogous passages without incubation with RB or illumination were performed to obtain control samples.

aPDI tolerance examination. Microbial OV cultures were prepared from glycerol stocks. Samples were adjusted to an optical density of 2.4 McFarland units in TSB and then incubated with $0.2\ \mu\text{M}$ RB in the dark for 15 min at 37°C . The samples were centrifuged and washed 2 times with PBS. Then, $100\ \mu\text{l}$ of the samples were illuminated at 0, 8, 14, 20, 30 or $40\ \text{J}/\text{cm}^2$. Illuminated samples were then serially diluted in PBS, plated on Columbia blood agar plates (Biomérieux), and incubated for 24 h at 37°C for CFU/ml enumeration.

Stability of the acquired tolerance to aPDI. The samples from the 10th consecutive cycle of aPDI treatment were transferred to 5 mL of fresh TSB medium and cultured at 37°C for 16–20 h. Aliquots of $50\ \mu\text{l}$ of the OV cultures were transferred to another tube containing TSB medium. The cycle of transfer - regrowth - transfer was repeated 5 times. On the 5th day, the cultures were treated with the same conditions as for aPDI tolerance examination. The resulting reductions in CFU/ml were compared with those of initial samples from the 10th consecutive cycle and with the CFU/ml values from untreated controls.

Toxicity assays of different oxidative stressors. Responses to different oxidative stressors were examined by incubation of OV cultures adjusted to 2.4 McFarland units in TSB with 320 mM paraquat dichloride (Sigma) for 24 h, 0.03% sodium hypochlorite for 45 min, and 0.03% hydrogen peroxide for 2 h. Incubation was performed at 37°C . Samples were then serially diluted in PBS and plated for CFU/ml enumeration. Additionally, the responses for samples with $25\ \mu\text{M}$ NMB illuminated at $15\ \text{J}/\text{cm}^2$ and with $0.1\ \mu\text{M}$ ZnPc illuminated at $20\ \text{J}/\text{cm}^2$ were examined with the protocol described for aPDI tolerance examination.

Detection of reactive oxygen species production. Detection of ROS was performed in accordance with a previously published protocol [41]. Briefly, for the detection of reactive oxygen species production by aPDI with RB, ZnPc or NMB, commercial ROS indicators were used (Invitrogen™). 3'-p-(Aminophenyl) fluorescein (APF) was used for singlet oxygen and hydroxyl radical detection, and singlet oxygen sensor green (SOSG) was used for singlet oxygen detection. APF ($10\ \mu\text{M}$) was mixed with a PS in PBS for 1O_2 and $\cdot\text{OH}$ detection or in DMSO for 1O_2 detection only. Samples were illuminated in black microtiter plates with a $20\ \text{J}/\text{cm}^2$ light dose, and then 515 nm fluorescence was immediately measured with an EnVision® Multilabel Reader (PerkinElmer). SOSG ($5\ \mu\text{M}$) was mixed with a PS in PBS for 1O_2 detection. Then, samples were illuminated in black microtiter plates with a $20\ \text{J}/\text{cm}^2$ light dose, and 525 nm fluorescence was immediately measured. RB, ZnPc and NMB were used at concentrations of $0.1\ \mu\text{M}$, $1\ \mu\text{M}$ and $50\ \mu\text{M}$, respectively. For each set of conditions, two controls were also performed: indicator in a solvent alone and indicator with PS without illumination.

Hydrogen peroxide detection. Working reagent (WR) used in Pierce™ quantitative peroxide assay reagent was prepared in accordance to manufacturer's recommendation (Thermo Fisher Scientific, USA). OV cultures of *S. agalactiae* 2974/07 strain were adjusted to optical density 2.4 McFarland units, then the photosensitizer (RB) was added followed with 15 min incubation at 37°C , and afterwards, illuminated with sublethal aPDI. Next, $10\ \mu\text{l}$ of WR were added to $100\ \mu\text{l}$ of irradiated samples and the spectrophotometric measurement was performed at the wavelength of 570 nm (Wallac 1420 Victor, PerkinElmer). Additionally, the same experiment was performed for cells treated with aPDI (without photosensitizer) and cells treated with RB (without light). For estimation of the H_2O_2 concentration in tested samples, the standard curve was prepared.

Hemolysis and granae production. Microbial OV cultures from glycerol stocks were diluted 100,000-fold in PBS, and $100\ \mu\text{l}$ of the samples was plated with a spreader on Columbia blood agar and Granada plates (Biomérieux). Plates were incubated for 24 h at 37°C for CFU/ml enumeration and determination of colony morphology. On

blood plates, colonies with regular hemolysis, increased hemolysis and SCVs were distinguished by sight. On Granada plates, white/gray colonies with undetectable granae content, yellow colonies with regular granae content and orange colonies with increased granae content were distinguished.

Rose bengal uptake. Microbial OV cultures were adjusted to an optical density of 2.4 McFarland units in TSB medium. Bacterial suspensions were centrifuged and resuspended in PBS and then mixed with RB to obtain a final concentration of $0.2\ \mu\text{M}$. Samples were incubated for 5 or 15 min at 37°C and immediately centrifuged at 10,000 g for 3 min after incubation. Supernatants were then transferred into BRAND® UV cuvettes, and the absorbance at 549 nm was measured by a SPECORD® PLUS spectrophotometer (Analytic Jena). Additionally, each sample was serially diluted and plated for CFU enumeration. Using the molar extinction coefficient ($\epsilon = 95,000$), the number of RB particles absorbed by a single bacterial cell was calculated [42,43].

Determination of the minimum inhibitory concentrations (MICs) of antibacterial agents by broth microdilution. MIC values of streptomycin (STR), ciprofloxacin (CIP) and rifampicin (RIF) were tested by the microbroth dilution method according to the European Committee for Antimicrobial Susceptibility Testing (EUCAST) guidelines [44].

Determination of the spontaneous mutation frequencies associated with antibiotic resistance following repeated sublethal exposures to aPDI. To assess increases in the mutation rate, samples were examined after 1, 5 and 10 cycles. One hundred microliters of OV cultures was spread onto TBS plates containing $256\ \mu\text{g}/\text{ml}$ STR ($2\times$ MIC), $1\ \mu\text{g}/\text{ml}$ CIP ($1\times$ MIC) or $0.5\ \mu\text{g}/\text{ml}$ RIF ($2\times$ MIC). The plates were incubated at 37°C for 48 h. The same cultures were serially diluted and streaked horizontally on plain TSB plates for CFU/ml enumeration. After colonies grown on plates with antibiotics were counted, mutation rates were calculated according to a previously published protocol [45].

Assessment of mutagenic potential associated with single nucleotide changes in intragenic DNA fragments. Preparation of control groups. For assessment of mutagenic potential, a control passage with CIP was prepared. Microbial OV cultures were adjusted to an optical density of 2.4 McFarland units in TSB with $\frac{1}{2}\times$ MIC CIP ($0.5\ \mu\text{g}/\text{ml}$) and incubated for 16–20 h at 37°C , and the next day $50\ \mu\text{l}$ of the 2.4 McFarland OV culture was transferred to a new tube with TSB and $\frac{1}{2}\times$ MIC CIP. The cycle of growth with CIP-transfer to a new tube-growth with CIP was repeated for the following 10 days. After 10 days of treatment with CIP, samples were plated into blood agar plates. Samples of bacteria from day 0, day 10 (control) and day 10 (treated with aPDI) were plated as well. **DNA isolation.** Five single colonies from each group above were transferred into tubes with 5 ml of TSB and incubated overnight at 37°C . An aliquot of 1.5 mL of each OV culture was centrifuged, and the pellet was suspended in $100\ \mu\text{l}$ of lysis buffer (20 mM Tris-HCl pH 8.0; 2 mM EDTA pH 8.0; 1.2% Triton X-100) with the addition of 35 U of mutanolysin (A&A Biotechnology). Samples were incubated at 37°C for 30 min. Then, DNA isolation was continued according to the manufacturer's manual for 'Kit for genomic DNA isolation from bacteria' (EXTRACTME®; Blirt S.A., Poland). DNA was eluted from the kit minicolumn membrane with water and stored at -20°C . **PCR analysis.** For the polymerase chain reaction (PCR), a 1525 bp fragment of the DNA upstream of the *cytE* gene was chosen. The oligonucleotide primer sequences were as follows: 5' CTTGTACGGTTTATCTAAATCACAAGTACG 3' (forward) and 5' TTATAACATGTA TTCCGGGCATCTTTTCATTTTAACTTTTAAATAAAAATG 3' (reverse). PCR was carried out with Taq polymerase according to the manufacturer's protocol (Thermo Scientific™) with 10 cycles of 15 s at 94°C , 40 s at 45°C and 1 min at 72°C followed by 30 cycles of 15 s at 94°C , 30 s at 55°C and 2 min at 72°C . Amplification products were then purified using the Syngen PCR Mini Kit (Syngen) and sequenced by IBB PAN (Oligo.pl, Warsaw). Forward and reverse sequences were assembled and compared between the groups with Geneious Prime

software. Finally, for each group, i.e., no treatment, CIP treatment, passaged with no selective pressure and aPDI treatment, we received 5 DNA fragment sequences that were further analyzed with respect to the reference genome sequence (GenBank accession no. LR134512), and the number of changed nucleotides was calculated.

RNA isolation. A 0.6 mL aliquot of log-phase culture was incubated for 15 min at 37 °C with 0.08 μM RB (aPDI) or alone (control). Then, the cells were washed with PBS, transferred into a 24-well plate and illuminated at 20 J/cm² or incubated at RT. After illumination, all samples were incubated for 15 min at 37 °C, and 0.5 mL of each sample was mixed with 1 ml of RNA Later™ (Sigma Aldrich). After 5 min of incubation, the samples were centrifuged for 10 min at 5000 × g, and the precipitate was lysed the same way as for DNA isolation. RNA was isolated with a Syngen Blood/Cell RNA Mini Kit (Syngen) according to manufacturer's manual with an extra step of DNA degradation (RNase-Free DNase Set, Qiagen). Samples were stored at –80 °C. The next day, RNA was purified with a second step of DNA degradation using the same kit as for isolation. The concentration of the RNA was measured with a NanoDrop™ spectrophotometer.

cDNA synthesis and quantitative real-time PCR conditions. Immediately after measurement of the RNA concentration, 1 ng of RNA was used for cDNA synthesis with the TranScriba Kit (A&A Biotechnology) according to manufacturer's manual. As a control to test for DNA contamination, samples were processed without reverse transcriptase. Real-time PCR was performed with SG qPCR Master Mix (EURx) and 0.05 μM gene-specific primers (Table 1). Duplicate samples were routinely used in a total volume of 10 μl. The amplification and detection of specific products were performed using a Light Cycler 480 II (Roche) under the following conditions: 1 step of 3 min at 95 °C and 39 cycles of 95 °C for 10 s and 60 °C for 30 s, which were followed with a melting curve. The relative fold change in gene expression was calculated using the Pfaffl model. *gyrA* was used as the internal control and for normalization of expression relative to basal levels of expression (without aPDI treatment).

Statistical analysis. Statistical analysis was performed in Statistica 12.0 (StatSoft, Tulsa, USA). Data were expressed as mean values. To assess differences between groups, one-way or two-way ANOVA was applied. P values less than 0.05 were considered statistically significant.

3. Results

3.1. Sublethal aPDI leads to tolerance development

The adequate assessment of tolerance development requires the application of sublethal treatment conditions that result in cell viability reductions of 1–3 log₁₀ units. To meet this requirement, within the current study, aPDI treatment conditions leading to an approximately 1 log₁₀ unit reduction were considered sublethal and selected for the tolerance development study. These conditions were 0.08 μM RB activated with green light with a fluence of 20 J/cm² (Fig. 1).

The application of 10 cycles of sublethal aPDI resulted in significant tolerance development for all tested *S. agalactiae* strains, including both the reference strain (ATCC 27956) and clinical isolates (strains no. 2306/06 and 2974/07). Developed tolerance decreased aPDI efficacy

Table 1
Oligonucleotide primers used for RT-PCR.

Gene	Forward primer (5' to 3')	Reverse primer (5' to 3')
<i>tpx</i>	GCATTTGTTAACGCGTGCAG	CAGCATTAAATCGCCGCTTCG
<i>ahpC</i>	GCGGATGTATTGAGCAGCAC	GATCCAGACGGTGTATCCCA
<i>npX</i>	GACCGCCTCCCTGATTCAT	TAGCAGTTGTTGGGGCAGG
<i>gyrA</i>	CGGGACACGTACAGGCTACT	CGATACGAGAAGTCCCACA
<i>recA</i>	ATTACGGCGCAGTTGATTTAGTT	TCAATCTCAGCACGAGGAACA
<i>sodA</i>	AACCACGCTCTTTCTGGGA	CCTGTTGCTGCTGCTGTGAA
<i>cylE</i>	GGAAGTTACCGATTGAGCA	TGCCAGGAGGAGAATAGGAA

up to 3 log₁₀ units in viable counts (Fig. 2). Furthermore, to assess the phenotypic stability of the developed tolerance, *S. agalactiae* cultures expressing significant aPDI tolerance and originating from the 10th consecutive cycle were passaged for the next five cycles with no selection pressure. Afterwards, the susceptibility of the passaged *S. agalactiae* cultures to aPDI was determined. No loss of the developed aPDI tolerance was reported, and the obtained results indicated increased tolerance after passaging that reduced the aPDI efficacy by 5 logs (Fig. 2). The obtained results support the assumption that developed tolerance results from genetic alterations and may be transferred to subsequent generations with no selective pressure.

3.2. No genetic alterations in *S. agalactiae* were detected

The demonstrated phenotypic stability indicates that the application of consecutive cycles of sublethal aPDI results in the accumulation of genetic alterations within the genome of *S. agalactiae*. To support this assumption, we investigated whether sublethal aPDI leads to an increased mutation rate in *S. agalactiae* no. 2974/07 exhibiting the most pronounced aPDI tolerance development. As resistance to RIF, CIP, and STR may result from a single spontaneous mutation, a RIF-, CIP-, and STR-resistant mutant selection assay was considered an adequate methodology for mutation rate analysis. Though expected, no significantly increased mutation rate was reported for any of the studied antimicrobials (Fig. 3).

Though the accumulation of genetic alterations with the employment of antibiotic-resistant mutant detection was expected but not evidenced, we furthermore made an effort to investigate the genetic alterations induced with sublethal aPDI treatment by sequencing 1525 bp upstream DNA fragments of one of the GBS genes, i.e., *cylE*, which plays a key role in the oxidative stress response within *S. agalactiae*. Current work shows that the functionality of the *cyl* operon, determining cell pigmentation and hemolytic properties, changes significantly over the course of sublethal aPDI treatment; thus, changes in the sequence of *cylE* (one of the prominent *cyl* operon components) were expected to emerge upon consecutive aPDI cycles in the case of aPDI-tolerant strains. The obtained results demonstrated that both CIP treatment (as a positive control) and 10 cycles of aPDI treatment resulted in the greatest increase in single mutation events calculated as the percentage of changed nucleotides from the reference sequence (Table 2), indicating that sublethal aPDI may indeed result in genetic alterations.

3.3. aPDI tolerance confers no resistance to killing by reactive oxygen species

The aPDI killing mechanism relies on the formation and activity of various ROS induced upon photoactivation of the sensitizer; thus, one may expect that the developed aPDI tolerance could be easily translated into tolerance/resistance to other oxygen species. To substantiate this hypothesis, we exposed aPDI-tolerant *S. agalactiae* (strain no. 2974/07, developed upon 10 cycles of sublethal aPDI) to five oxidants: superoxide (paraquat), hydrogen peroxide (H₂O₂), hypochlorite, singlet oxygen (NMB), and ROS induced with aPDI employing a structurally different PS (i.e., ZnPc) (Fig. 4). We found that aPDI-tolerant *S. agalactiae* exhibited no change in susceptibility to death via oxidants (Fig. 4ACD), with the exception of slightly increased tolerance to hydrogen peroxide (Fig. 4B).

Furthermore, the obtained results indicate no cross resistance, as 10 consecutive cycles of sublethal aPDI did not induce *S. agalactiae* tolerance to phototreatments employing other photosensitizing compounds, i.e., NMB and ZnPc. Interestingly, RB-aPDI-treated *S. agalactiae* exhibited even higher susceptibility to NMB-mediated aPDI, resulting in an approximately 4 log₁₀ increase in NMB-aPDI antimicrobial efficacy (Fig. 4E).

The slightly increased tolerance to H₂O₂ of aPDI-tolerant *S.*

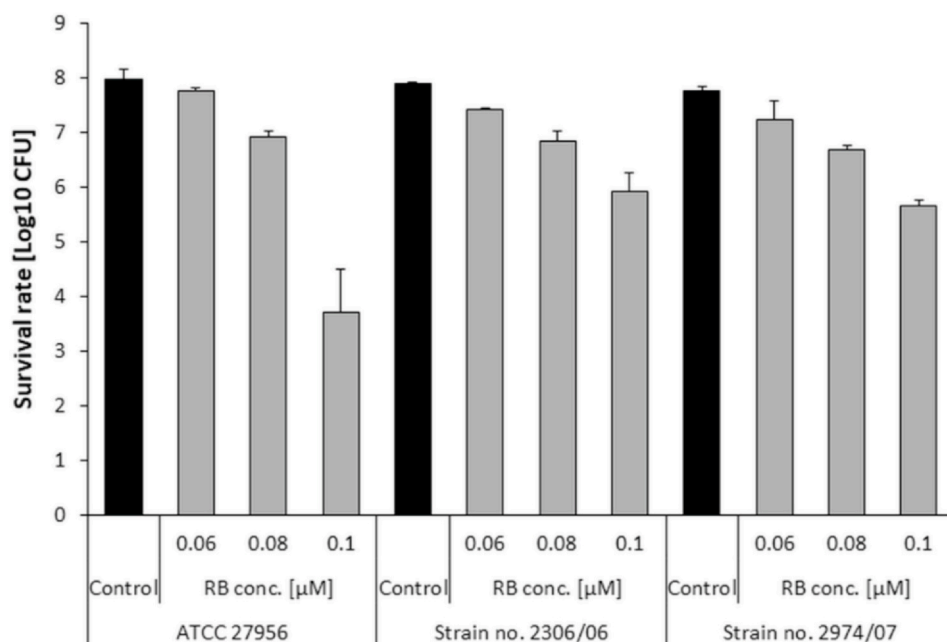


Fig. 1. Influence of aPDI on *S. agalactiae* strains. Microbial overnight cultures (8×10^7 CFU/ml) were treated with up to 0.1 μ M RB and exposed to a light dose of 20 J/cm² (λ_{\max} 515 nm). After illumination, samples were serially diluted, streaked horizontally, and incubated at 37 °C for 24 h, and then colonies were counted. Control groups included cells that were not treated with PSs or light. For the purpose of this study, sub-lethal doses were defined as those resulting in a 1 log₁₀ reduction in CFU. The detection limit was 100 CFU/ml. The values are the means of three separate experiments. Error bars represent standard deviations (SDs).

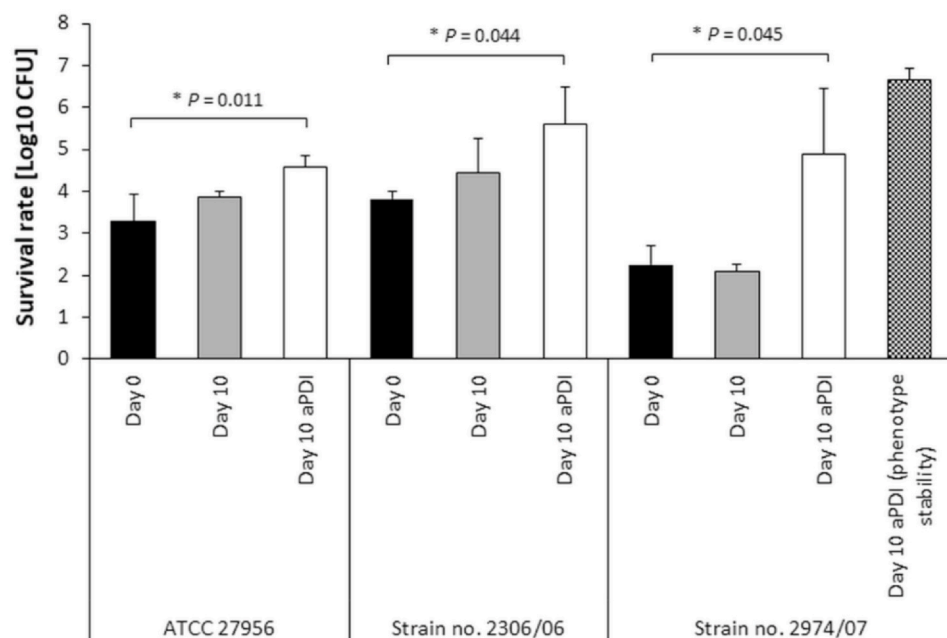


Fig. 2. aPDI tolerance development upon sub-lethal treatment. Overnight *S. agalactiae* cultures (5×10^7 CFU/ml) were incubated with 0.08 μ M RB and illuminated with 515 nm light at a dose of 20 J/cm². Following exposure, the sample was centrifuged and washed with PBS. Fifty microliters of the sample was transferred into fresh TSB medium (5 mL) to regrow overnight. The next day, the treatment was repeated under the same conditions. The cycle of exposure - regrowth - exposure was repeated 10 times. Afterwards, the susceptibility of *S. agalactiae* to aPDI was investigated for 0.1 μ M RB illuminated with 515 nm light at a dose of 40 J/cm². The detection limit was 100 CFU/ml. The values are the means of three separate experiments. Error bars represent the standard deviation (SD).

agalactiae may indicate hydrogen peroxide involvement in the RB-aPDI mechanism of action. To support this thesis, the amount of H₂O₂ produced upon sublethal RB-aPDI treatment was measured using the Pierce™ quantitative peroxide assay. The obtained results indicate that hydrogen peroxide is generated upon aPDI treatment; however, only barely measurable amounts of H₂O₂ are formed (Table 3).

To investigate the lack of cross resistance in more detail, ROS production was evaluated for all studied phototreatment conditions, i.e., RB, NMB, and ZnPc aPDI. These PSs are structurally different chemicals and are considered model sensitizers for singlet oxygen and hydroxyl radical formation (RB and NMB for the former and ZnPc for the latter). Our data indicate that RB and NMB, though representing different chemical classes, demonstrate mainly singlet oxygen formation upon light activation (Fig. 5), and ZnPc may produce hydroxyl radicals and barely measurable amounts of singlet oxygen when photoactivated (Fig. 5).

The obtained results indicate that the developed aPDI tolerance is strictly limited to the selection treatment and is not translated into tolerance to aPDI involving other PSs with either both similar or quite different mechanisms of photoactivity.

3.4. Increased expression of oxidative stress response genes may be a possible mechanism for developing tolerance

The crucial element of aPDI that conditions for microbial killing is oxidative stress evoked with ROS and/or singlet oxygen generation; thus, one could hypothesize that increased expression of genes consisting of key elements of microbial oxidative stress defense may be the most obvious mechanism of aPDI tolerance development. To verify this thesis, we investigated whether aPDI affects the expression levels of oxidative stress-related genes, i.e., *sodA*, *ahpC*, *npx*, *cylE*, *tpx*, and *recA* (coding for superoxide dismutase, alkylhydroperoxide reductase, NADH

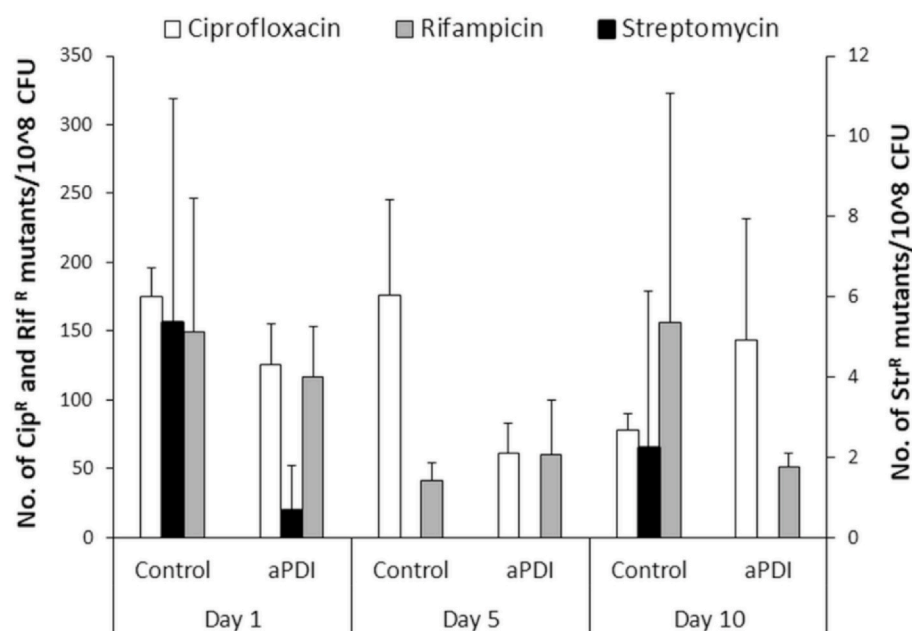


Fig. 3. Effect of sublethal phototreatment on the mutation rate. Potential increases in the mutation rate were examined after the 1st, 5th and 10th consecutive cycles of aPDI. One hundred microliter aliquots of the overnight *S. agalactiae* (2974/07) cultures from the 1st, 5th, and 10th cycles were spread on TSB agar plates containing CIP (1 µg/mL, 1 × MIC), RIF (0.5 µg/mL, 2 × MIC), and STR (256 µg/mL, 2 × MIC) and incubated at 37 °C. After 24 h of incubation, CFUs were counted, and the mutation frequency was defined as the ratio of resistant colonies in relation to the total number of bacteria (CFU). The bars represent the mean values of three biological replicates ± standard deviations (SDs).

Table 2
Percentage of changed nucleotides.

Conditions	Percentage of changed nucleotides ^a [%] (± SD)	P value (vs. no treatment)
No treatment	0.17 (0.08)	
CIP treatment	0.33 (0.05)	0.016
Passaged with no selective pressure	0.25 (0.06)	0.019
aPDI treatment	0.53 (0.15)	0.016

^a) With respect to the GenBank reference sequence under the accession no. LR134512.

peroxidase, granadaene (β-hemolysin/cytolysin and carotenoid pigment), thiol peroxidase, and recombinase A (SOS response element, respectively). The obtained results demonstrate that directly upon sublethal treatment, aPDI leads to increased expression of *sodA*, *tpx*, or *recA* and decreased expression of *ahpC* and *cylE* (Fig. 6, white bars). No significant change in *npx* expression was reported. Interestingly, when gene expression was investigated for strains treated with 10 cycles of sublethal aPDI, expression with no aPDI treatment was significantly increased for all tested genes (including *ahpC* and *cylE*), indicating that undergoing multiple phototreatment cycles promotes *S. agalactiae* increasing expression of all oxidative stress-related genes (Fig. 6, black bars). In addition, when the aPDI-tolerant strain was treated with sublethal aPDI, the expression of *sodA*, *npx*, *tpx*, and *recA* was further significantly increased (Fig. 6, black bars). These phenomena were inconclusive for strains subjected to 10 cycles of passaging with no

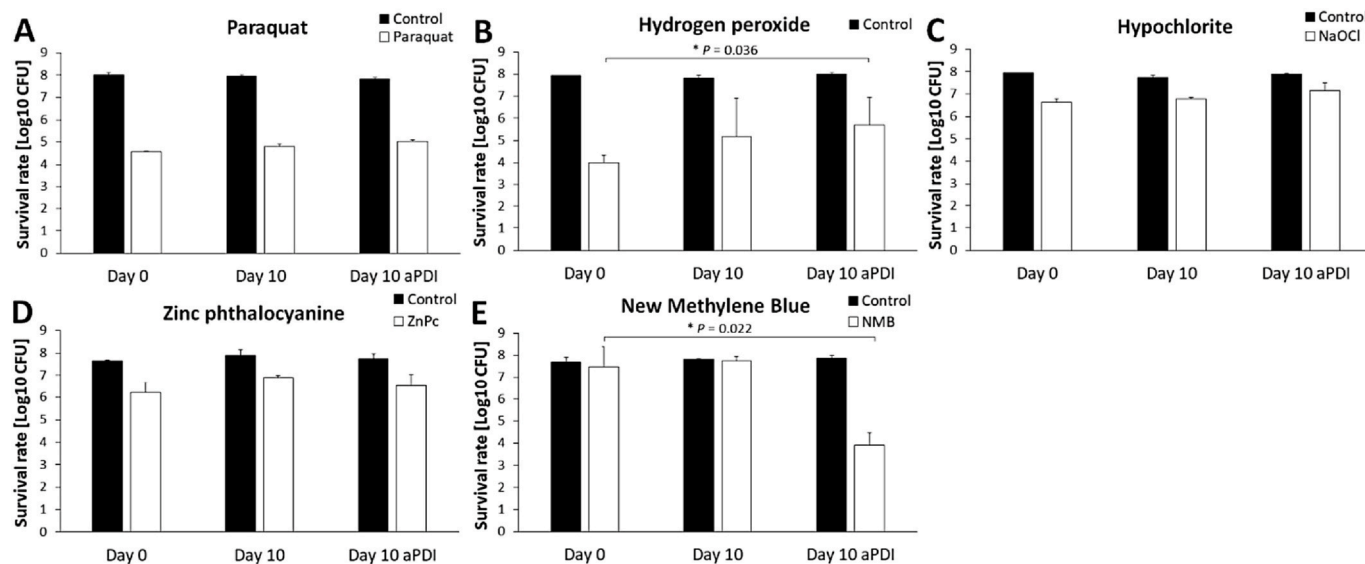


Fig. 4. *S. agalactiae* tolerance to reactive oxygen species. Overnight *S. agalactiae* 2974/07 cultures originating from day 0 (wild-type strain), day 10 (with no selective pressure), and day 10 aPDI (aPDI tolerant) (5×10^7 CFU/ml) samples were exposed to (A) superoxide (320 mM paraquat for 24 h), (B) hydrogen peroxide (0.03% for 2 h), (C) hypochlorite (0.3% for 45 min), (D) oxidative stress induced with ZnPc-aPDI (zinc phthalocyanine at 0.1 µM, 20 J/cm² at λ_{max} 632 nm), or (E) singlet oxygen (new methylene blue 25 µM, 15 J/cm² at λ_{max} 632 nm). The detection limit was 100 CFU/ml. The values are the means of three separate experiments. Error bars represent the standard deviations (SDs).

Table 3
Hydrogen peroxide measurement.

Conditions	H ₂ O ₂ [$\mu\text{mol/L}$] (+/- SD)	P value (vs. aPDI)
aPDI	21.3 (0.37)	
Control (Light)	18.3 (1.33)	0.09
Control (RB dark)	16.9 (1.25)	0.03

selective pressure (Fig. 6, gray bars).

The obtained results indicate that all studied oxidative stress response elements provide defense machinery against the oxidative burst induced by aPDI, and their increased expression may explain the mechanism underlying the observed aPDI tolerance development.

3.5. aPDI-tolerant strains exhibit colony morphology differences

The gene expression analysis made it necessary to further test the

indication of *cylE* involvement in aPDI tolerance development; thus, not only its expression but also its functionality as expressed through colony pigmentation and hemolytic activity were evaluated, as *cylE* contributes to the production of β -hemolysin and carotenoid pigment [46]. The obtained results show that in the course of aPDI tolerance development, changes in *S. agalactiae* colony morphology occurred, indicating an impact of aPDI on *cylE* functionality and/or expression. Compared to the wild-type strain, the aPDI-tolerant strain exhibited different proportions of dark- and unpigmented colonies (Fig. 7, gray and white bars). The same was true for colonies exhibiting highly hemolytic properties; the proportions of these colonies was significantly increased for the aPDI-tolerant strain vs. the wild-type strain (Fig. 7, black line).

The data presented here demonstrated that different aPDI treatments led to changes in *cylE* expression and/or functionality that result in different compositions of the *S. agalactiae* cell population in regard to hemolytic properties and pigment content (i.e., morphological traits

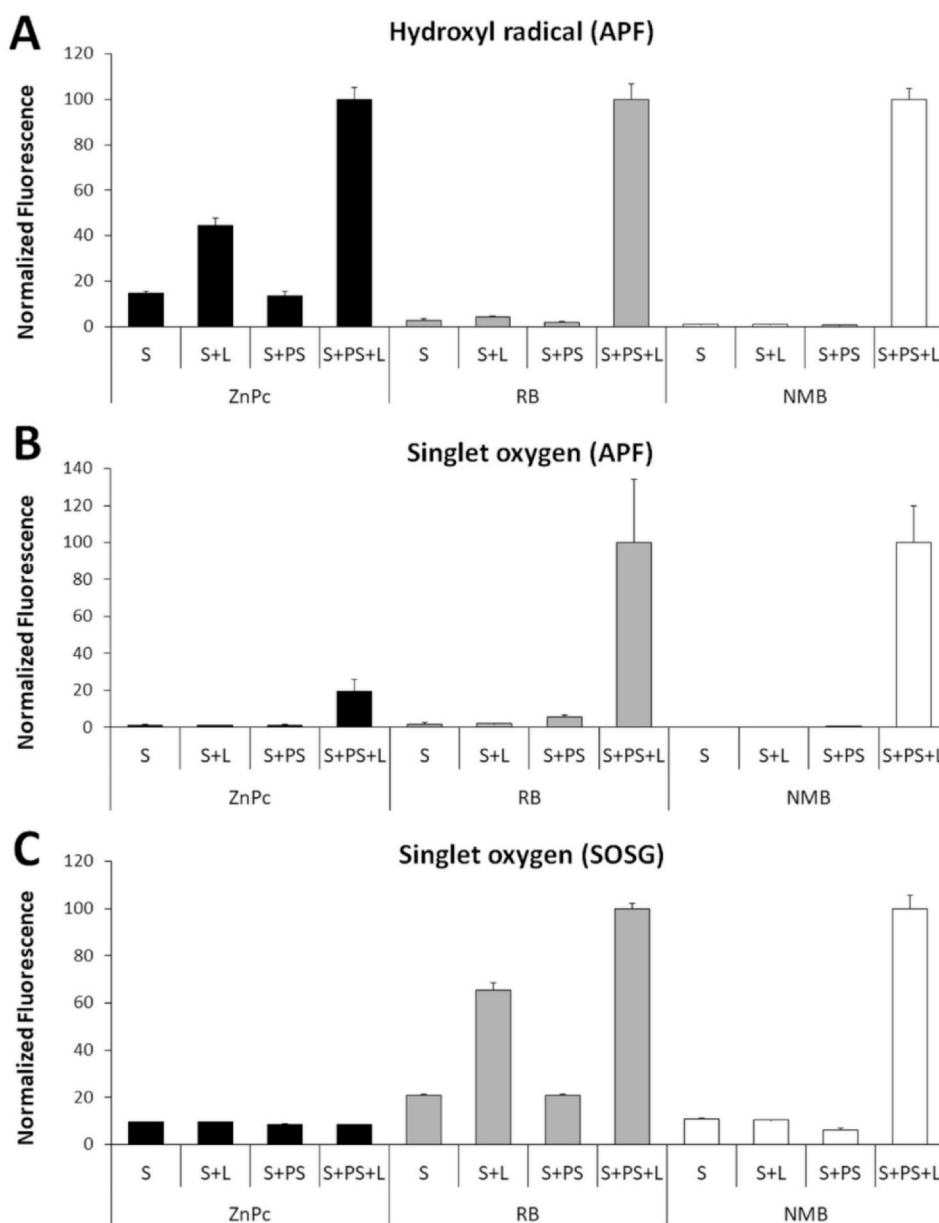


Fig. 5. ROS detection. ROS detection was performed for three photosensitizers (zinc phthalocyanine, ZnPc; rose Bengal, RB; and new methylene blue, NMB). Cell-free suspensions of PSs were incubated with ROS-detecting fluorescent probes to detect hydroxyl radicals ($\cdot\text{OH}$) (panel A) and singlet oxygen (panels B and C) upon irradiation. The values are the means of three separate experiments. Abbreviations: S, sensor (probe); L, light; PS, photosensitizer.

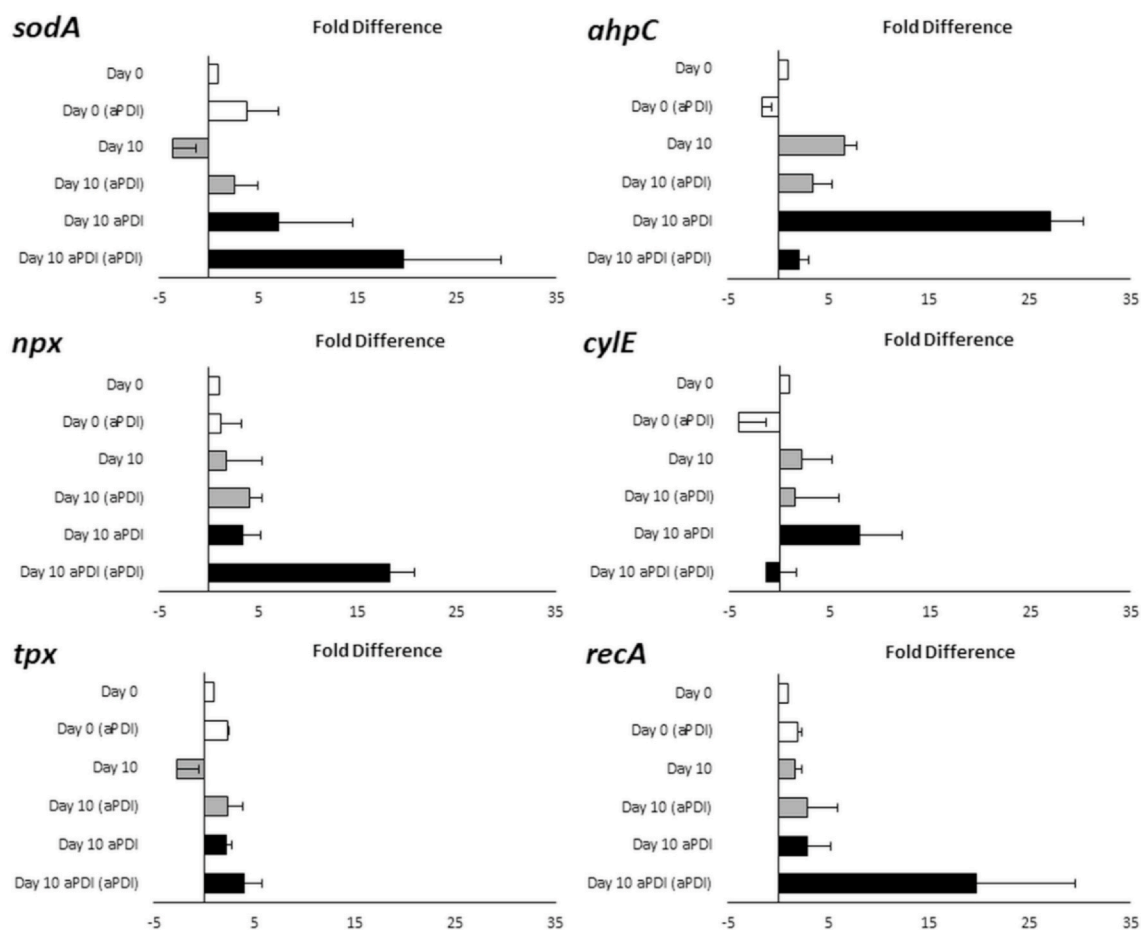


Fig. 6. Effect of sublethal aPDI and multiple aPDI treatments on *S. agalactiae* gene expression. *S. agalactiae* was grown to exponential phase before RNA sampling. The relative expression of genes related to *gyrA* was assessed by qRT-PCR. Each graph represents the mean fold difference in transcript levels for *S. agalactiae* subjected to no multiple aPDI treatments (Day 0, white bars); *S. agalactiae* subjected to 10 cycles of passing with no selective pressure (Day 10, gray bars); and *S. agalactiae* subjected to 10 cycles of aPDI (Day 10, black bars). For each experimental condition, both the basal and aPDI-induced expression of genes was investigated (marked as “aPDI”). Bars represent the mean values of at least three biological replicates \pm standard deviations (SDs).

under the control of the *cyl* operon). The data may further uncover a possible strategy leading to increased aPDI tolerance, as carotenoid pigments may confer significant protection against oxidative burst.

In addition to aPDI-induced changes in *cyl*-dependent phenotypes, an increased share of SCVs was reported for the aPDI-tolerant strain vs. wild-type strain (Fig. 7, gray line). As changes in SCVs, including atypical colony morphology, slow growth rates, a lack of pigmentation and reduced hemolytic activity, demonstrate a well-known strategy for oxidative stress adaptation, the increased proportion of SCVs in aPDI-tolerant strains may provide the next possible explanation for reduced *S. agalactiae* susceptibility to photoinactivation.

3.6. aPDI tolerance may result from decreased RB uptake

The obvious microbial strategy for increased aPDI tolerance may be decreasing PS uptake to reduce oxidative burst and the killing efficacy of photoinactivation. To support this thesis, we evaluated the RB uptake of wild-type and aPDI-tolerant *S. agalactiae* variants. The obtained results indeed showed that the aPDI-tolerant strain significantly reduced RB uptake when compared to that of the wild-type strain, both for 5 and 15 min of *S. agalactiae* incubation in the presence of PS (Fig. 8).

Decreased RB uptake was not observed for *S. agalactiae* passaged for 10 cycles with no selective pressure.

3.7. Developed aPDI tolerance may not be considered resistance

The presented results demonstrate significant aPDI tolerance development; however, one could not consider this phenomenon resistance to phototreatment. The employment of more rigorous experimental conditions, i.e., increased PS concentrations and/or higher light doses, may still result in bacterial eradication of the aPDI-tolerant phenotype. The aPDI-tolerant *S. agalactiae* susceptibility to aPDI was evaluated with an increased RB concentration of 0.4 μ M (Fig. 9).

4. Discussion

Antimicrobial photodynamic inactivation is an attractive and highly effective antimicrobial approach that eradicates numerous pathogens, including the most threatening human pathogens despite their drug resistance profiles. Though numerous *in vitro* and *in vivo* studies concerning human microbial pathogens were most recently reviewed by Nakonieczna et al. (2019) [27], there is only one single report by Sellera et al. (2016) demonstrating the efficacy of MB aPDI in the inactivation of pathogens associated with bovine mastitis (*S. aureus*, *Streptococcus agalactiae*, *S. dysgalactiae*, *Corynebacterium bovis*, and the alga *Prototheca zopfii*), indicating that aPDI could be an interesting tool for inactivating *S. agalactiae* as a source of veterinary infections [47]. Thus, it is important to emphasize that the current study could be considered the first report of aPDI antimicrobial efficacy toward *S. agalactiae*, an important etiological agent of human infectious diseases.

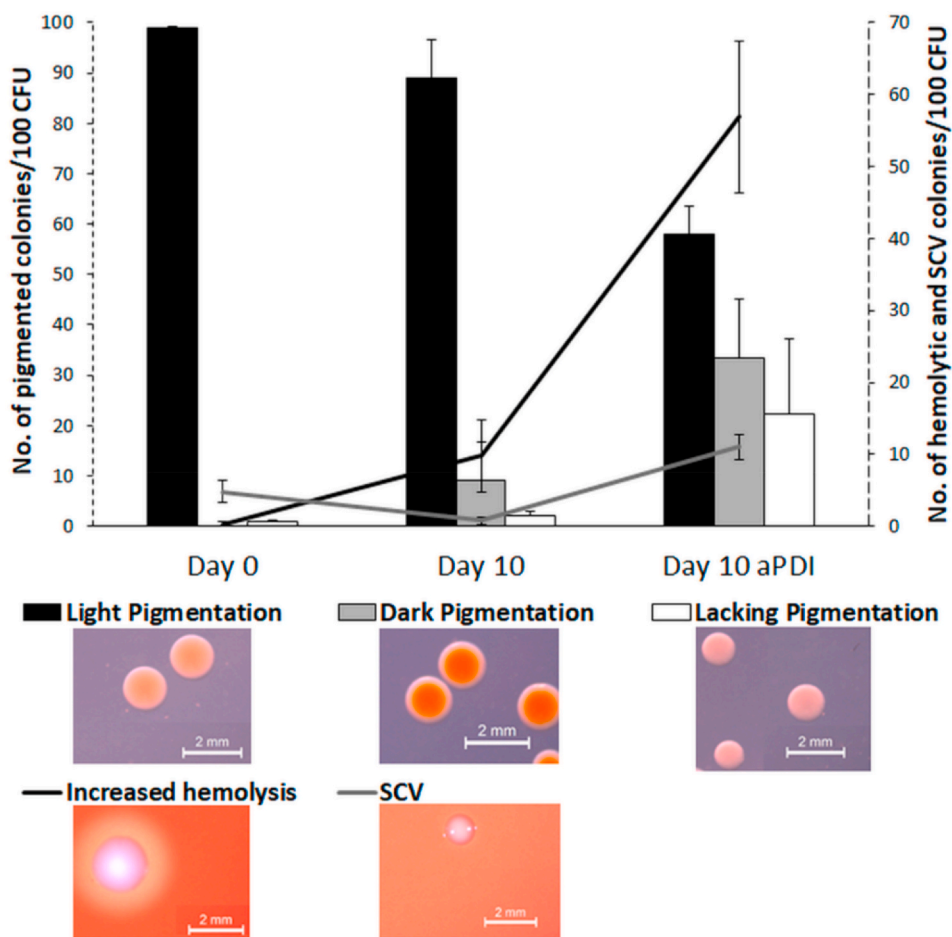


Fig. 7. Phenotypes of wild-type, 10 passaged and aPDI-tolerant *S. agalactiae*. Microbial OV cultures were diluted 100,000-fold in PBS, and 100 µl of the samples was plated on Columbia blood agar and Granada plates. Plates were incubated for 24 h at 37 °C for CFU/ml enumeration and determination of colony morphology. Hemolytic (black line) and SCV (gray line) phenotypes were detected on Columbia blood agar; light- (black bars), dark- (gray bars), and unpigmented (white bars) phenotypes were reported on Granada agar.

In a previous report, we demonstrated that sublethal aPDI leads to a significant oxidative burst in targeted microbes, substantial DNA damage, increased SOS response and aPDI tolerance development in *S. aureus* [39,48]. Those studies were the foundation for the hypothesis

stated within the current work that photoinactivation may lead to tolerance development in *S. agalactiae*, and that key elements of its oxidative stress response may underlie the acquired tolerance. As those studies were performed with the administration of RB as the

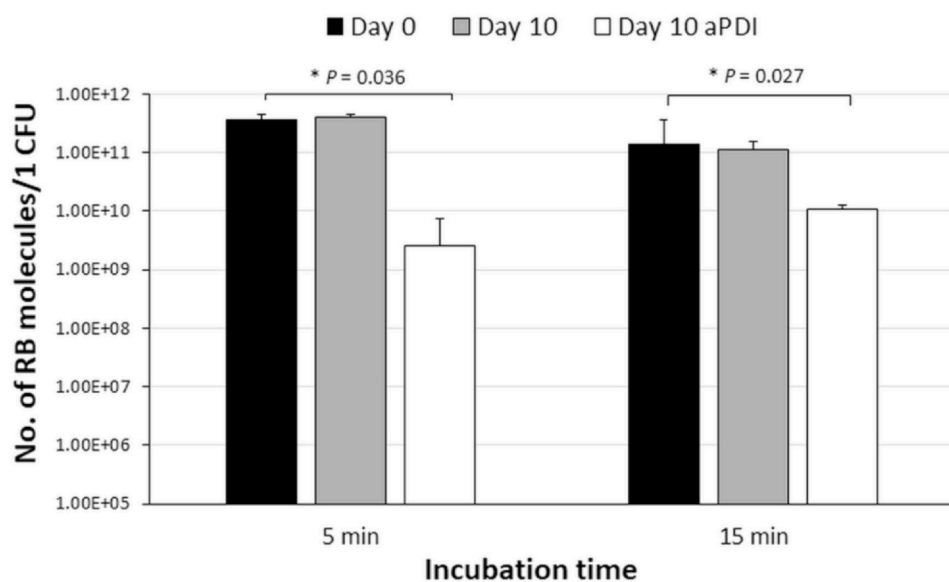


Fig. 8. Uptake of photosensitizer molecules in bacterial cells. Microbial OV cultures were adjusted to an optical density of 2.4 McFarland units, centrifuged, resuspended in PBS and mixed with RB to obtain a final concentration of 0.2 µM. Samples were incubated for 5 or 15 min at 37 °C and centrifuged. Supernatants were transferred into cuvettes, and the absorbance at 549 nm was measured. Additionally, each sample was serially diluted and plated for CFU enumeration. The uptake of RB was calculated with the molar extinction coefficient and expressed as the number of photosensitizer molecules per bacterial cell.

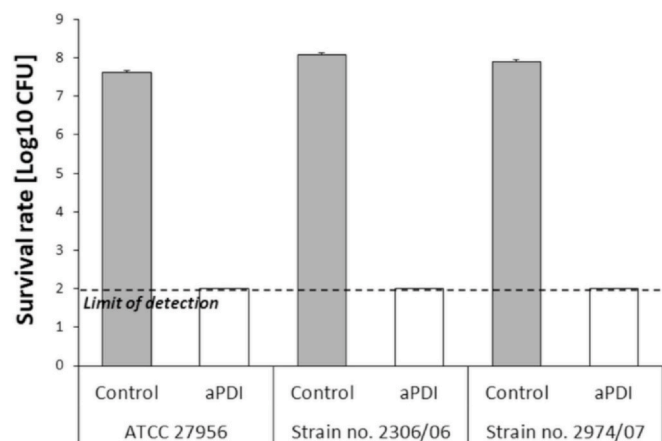


Fig. 9. Stronger aPDI treatment conditions exert bactericidal effects on *S. agalactiae* phototolerant strains. aPDI treatment of *S. agalactiae* reference strain and clinical isolates expressing aPDI tolerance due to multiple sublethal aPDI treatments. The experimental conditions were as follows: light dose of 20 J/cm² (λ 515 nm) and 0.4 μ M rose bengal. The detection limit was 100 CFU/ml. The values are the means of three separate experiments. Error bars represent the standard deviations (SDs).

photosensitizer, the same PS was employed within the current work. RB is a xanthene dye, which has been widely applied as a photosensitizer in photodynamic treatment [35,49–54]. Among xanthenes dyes which are potent PSs generating reactive oxygen species such as singlet oxygen [55], RB is one of the most efficient and widely used sources of ¹O₂ in polar solvents such as water [56]. Moreover, it is considered a molecule with high biocompatibility (a necessary criteria for therapeutic agent) and low level of cytotoxicity even at higher concentrations [35,51]. The aforementioned characteristics of RB let us to consider this molecule a model PS for the aPDI tolerance investigations.

ROS, including superoxide anions, hydrogen peroxide, and hydroxyl radicals, exert many deleterious effects on living organisms, leading to severe damage to DNA, RNA, proteins, and lipids [57]. ROS are important aspects of the highly microbicidal environment that *S. agalactiae* meets inside the macrophages [57] but may also be produced as byproducts during microbial metabolism. They are also involved in the killing mechanisms of numerous antimicrobial approaches, including antimicrobial and photodynamic inactivation; thus, numerous human pathogens have developed strategies to inactivate or detoxify ROS [58]. *S. agalactiae*, despite lacking catalase, was shown to survive exposure to high levels of ROS, indicating the presence of other enzymes that GBS uses to defend against ROS [59], including superoxide dismutase (SOD), NADH peroxidase, thiol peroxidase, and alkylhydroperoxide reductase [59]. SODs constitute one of the major defense mechanisms against oxidative stress, converting superoxide anions to molecular oxygen and hydrogen peroxide, which are further metabolized by peroxidases, and play a crucial role in the pathogenesis of numerous bacteria, e.g., *Salmonella enterica*, *Neisseria meningitidis*, *Haemophilus influenzae*, and *Streptococcus pneumoniae* [60–62]. Superoxide dismutase with Mn cofactor (SodA), which was the crucial element of the current study, is also considered the most important agent against oxidative stress in *S. agalactiae* [59]. The next important element for GBS oxidative burst protection, which was also studied within the current work, is NADH peroxidase (Npx), which detoxifies H₂O₂ [63,64]. The GBS genome also encodes two other peroxidases, thiol peroxidase (*tpx*) and alkylhydroperoxide reductase (*ahpC*), which contribute to ROS detoxification; thus, the role of these two genes in aPDI-induced ROS defense was also investigated in the current study [65]. Next, the oxidative stress defense elements in GBS are linked to carotenoid pigment production; this link is attributed to the ability of carotenoids to shield GBS from oxidative damage by scavenging free radicals [46,66]. It has been recently shown that both GBS β -hemolysin and this pigment

correspond to a unique molecule called granadaene which may be synthesized by genes of the *cyl* operon [2,67]. One of the final steps of granadaene synthesis is catalyzed by the CylE protein encoded by the *cylE* gene; thus, its contribution to oxidative stress defense induced by aPDI was evaluated within the current study as a key component of oxidative burst protection. Next, a potent microbial strategy that may lead to increased viability in the presence of a ROS-rich environment is phenotype switching, which results in the formation of SCVs [68]. Since their first description, SCVs have been described for numerous bacterial species, including *S. aureus*, *Pseudomonas aeruginosa*, and *Escherichia coli* [68–70]. SCVs are also found in various coccus genera and species, e.g., enterococci, *S. pneumoniae*, *S. tigurinus*, and, most importantly, *S. agalactiae* [71–74]. Atypical colony morphologies characterized by low growth rate, lack of pigmentation, and reduced hemolytic activity exhibit elevated antibiotic and environmental (including oxidative) stress tolerance; thus, their possible role in the adaptation and tolerance to aPDI-induced oxidative burst was examined within the current study [75,76].

As expected, the application of an adequate experimental protocol characterized previously by Rapacka-Zdonczyk et al. (2019) [39] demonstrated that multiple sublethal aPDI treatments led to significant and phenotypically stable tolerance development in *S. agalactiae*, which reduced the aPDI efficacy by 2–3.5 logs (Fig. 2). As aPDI tolerance was developed for both reference and clinical isolates that were the representatives of the most common GBS serotypes, e.g., serotypes III and V, we are convinced that the observed phenomenon is important. Most aPDI studies agree that the risk of aPDI resistance and/or tolerance is questionable, as bacterial recovery was reported following suboptimal treatments using inappropriate sensitizer or light doses, and even after 10 generations of aPDI treatments, microbes remained susceptible to aPDI at the same level [38,77,78]. We are convinced that one must not exclude suboptimal treatment even though the optimal protocol was designed. It is commonly known that despite optimal conditions, due to the heterogeneous environment of the infection site, it is extremely likely that microorganisms would be exposed to sublethal treatment, and it is questionable whether the damage is sufficient to cause microbial cell death in all treated cells and whether the remaining cells may recover and form more tolerant phenotypes. The presented data demonstrated that, indeed, bacterial recovery occurs post sublethal aPDI, and moreover, the surviving bacteria do not exhibit the same level of aPDI susceptibility but significant aPDI tolerance. Hopefully, in contrast to the action of standard antimicrobials, the observed phenomenon may not be considered resistance, as recovered microbes may still be successfully eradicated with the employment of more rigorous aPDI treatment conditions (Fig. 9), indicating that photoinactivation is a very promising alternative that may reduce antimicrobial use and slow the rate of resistance rise.

The obtained results demonstrated that aPDI tolerance is transferred to subsequent generations, indicating possible genetic alterations that occurred upon sublethal aPDI. Our previous studies demonstrated such genetic changes for *S. aureus*, demonstrating increased mutation rates and specific SOS response-related gene expression [39,48]. Within the current study, we were not able to demonstrate an increased mutation rate in *S. agalactiae*, though employment of adequate analysis and antibiotics that are the most suitable for mutation rate evaluation, i.e., aminoglycoside (STR), a quinolone (CIP), and rifampin (RIF) were used (Fig. 3), as resistance arises as a result of point mutations [79]. We consider this lack of evidence for an increased mutation rate the most important limitation of the present study, as spontaneous mutations are one of the main mechanisms for resistance/tolerance acquisition. Nevertheless, when an effort was made to detect spontaneous mutational events by sequencing the 1525 bp of DNA upstream of *cylE*, an increased percentage of nucleotide changes upon sublethal aPDI was reported (Table 2). Moreover, the application of qRT-PCR for gene expression analysis followed by colony morphology studies evidenced the existence of genetic alterations upon multiple sublethal aPDI

treatments, as both changed gene expression and different morphology resulting from the affected *cyl* operon were found.

Numerous strategies are possible to improve aPDI and reduce the risk of tolerance development; thus, it is significant to explain the possible mechanism underlying developed tolerance. The most conceivable mechanism for aPDI tolerance could be the development of GBS phenotypes expressing enhanced molecular defenses against oxidative burst; thus, the expression of genes that are key elements of the oxidative stress response was evaluated with respect to proper analysis and selection of reference genes [80]. The obtained results were supportive of this assumed mechanism, as increased expression both directly post sublethal aPDI and upon 10 passages of aPDI treatment was reported for *sodA*, *npx*, *tpx*, and *recA* (Fig. 6). In the cases of *ahpC* and *cylE*, the sublethal aPDI seemed to reduce their expression; however, the basic expression level in the aPDI-tolerant strain was evidenced to be significantly increased when compared to that in the nonpassed strain (Fig. 6). The presented data indicate that the increased expression of genes involved in oxidative stress protection may explain the developed tolerance. Increased *sodA* expression supports the previously published study by Poyart et al. (2001) and indicates that SodA expression constitutes the major defense mechanism against oxidative stress in GBS. In that study, a *sodA* mutant was extremely susceptible to oxidative stress, in particular to hydrogen peroxide; thus, one could make an assumption that its increased expression should result in increased tolerance to oxidation [59]. Accordingly, our results do indeed show that an aPDI-tolerant strain expresses increased tolerance to oxidative stress induced by phototreatment and, moreover, increased tolerance to H₂O₂ (Fig. 4). Next, the most recent study by Korir et al. (2018) showed that Npx plays an important role in defending against oxidative stress and reducing ROS production inside macrophages; thus, the increased *npx* expression detected in the current study could contribute to the development of aPDI tolerance (Fig. 6). The presumed function of NADH peroxidase was detoxifying H₂O₂ upon aPDI (H₂O₂ was demonstrated to be produced in the course of phototreatment, Table 3) and increasing microbial viability. In addition to Npx, GBS was revealed to encode two other peroxidases, i.e., thiol peroxidase (*tpx*) and alkylhydroperoxide reductase (*ahpC*), both of which contribute to ROS detoxification [65]. The obtained results demonstrated that, indeed, aPDI-tolerant *S. agalactiae* expresses increased *tpx* and *ahpC* expression when passaged with 10 cycles of sublethal phototreatment, and furthermore, *tpx* expression is increased again directly post aPDI application (Fig. 6). The last studied element of the oxidative stress defense was *cylE*, which was representative of genes in the *cyl* operon responsible for the synthesis of the 676-Da ornithine rhamno-polyene called granadaene. This carotenoid pigment, despite being a free radical scavenger giving protection against oxidative stress, is linked to the β -hemolytic activity of GBS; thus, both the gene expression assay and evaluation of pigmentation and hemolysis may indicate changes induced within the *cyl* operon [81]. A study by Liu et al. (2004) provided evidence that the *cylE* product contributes to survival in neutrophils and macrophages not only due to its toxic and β -hemolytic properties but also due to the linked carotenoid pigment protection against oxidative burst [46]. This pigment confers the ability to resist the antimicrobial effects of ROS and can protect membrane lipids against peroxidation [66,82]; thus, its contribution to the development of aPDI tolerance is highly expected. In a study by Liu et al. (2004), a *cylE* mutant was more susceptible to killing with four oxidants, i.e., hydrogen peroxide, hypochlorite, superoxide, and singlet oxygen [46]. In the current study, increased *cylE* expression was reported for the aPDI-tolerant strain as a result of 10 consecutive aPDI treatments, although, its expression directly post aPDI application was reduced (Fig. 6). Moreover, substantial changes in colony morphology, i.e., pigmentation and hemolysis, were supportive of the assumed changes in expression and/or functionality of *cyl* (Fig. 7). Finally, in accordance with the study by Liu et al. (2004), the aPDI-tolerant strain exhibited increased tolerance to oxidative killing by H₂O₂ (Fig. 4). These results support our

hypothesis that aPDI affects the expression and/or functionality of *cyl*, namely, carotenoid pigmentation, which contributes to developed tolerance. The next possible mechanism leading to adaptation and/or tolerance to oxidative stress is phenotype switching that results in the formation of SCVs, which has already been described for the *S. aureus* strategy. These slow-growing subpopulations of bacteria emerge in response to diverse environmental pressures. A study by Painter et al. (2015) [68] demonstrated that exposure of *S. aureus* to sublethal concentrations of H₂O₂ leads to a specific, dose-dependent increase in the population frequency of SCVs and that SCVs were significantly more resistant to the toxic effects of H₂O₂ than the wild-type strain [68]. The production of SCVs expressing elevated resistance to various stresses, including oxidative burst, may be the next possible explanation for aPDI tolerance development, as the more susceptible parent strain could be eradicated, leaving behind a population of SCVs that can undergo reversion, which results in a recovery of bacterial growth. Finally, the current study provides data indicating that due to the course of multiple aPDI treatments, bacteria may evolve cell envelope-related modifications, as PS uptake was substantially decreased for aPDI-tolerant microbes (Fig. 8). Lower PS availability within the cell proximity results in decreased aPDI efficacy. These cell envelope changes may include various events, i.e., decreased permeability, changes in cell wall thickness and membrane fluidity and potential [83,84].

Despite evidenced aPDI tolerance development, the crucial issue of the presented results is the lack of cross resistance between RB aPDI and aPDI mediated by other PSs, i.e., NMB and ZnPc (Fig. 4). RB and NMB, though representing different chemical classes, are considered model PSs for singlet oxygen production via aPDI; on the other hand, ZnPc exemplifies PSs that act mainly through hydroxyl radical generation (Fig. 5). Thus, the lack of cross resistance justifies drawing the general conclusion that the developed aPDI tolerance is strictly limited to the selection treatment and does not translate into tolerance to aPDI involving other PSs expressing both similar or quite different mechanisms of photoactivity. Unfortunately, we are not able to identify the reason for the observed phenomenon. We speculate that multiple factors may be involved in the observed lack of cross resistance, i.e., different cellular localizations or various specificities for microbial targets. Though the explanation remains unknown, the lack of cross resistance should be considered an extremely valuable and promising result regarding the clinical application of phototreatment.

As described above, *S. agalactiae* demonstrates the entire range of possible strategies that could lead to enhanced defense against oxidative stress induced with phototreatment and that could explain the reported development of aPDI tolerance. This phenomenon may not be caused by a single mechanism, as various ROS protective elements were activated upon multiple aPDI treatments, i.e., increased expression of genes coding for ROS-detoxifying enzymes and free radical scavengers (a carotenoid pigment), increased frequency of more tolerant SCV subpopulations, and reduced PS uptake. Performing all these processes results in significant aPDI tolerance.

When evaluating the risk of resistance development, one must differentiate the two terms tolerance and resistance. With respect to the Scientific Committee on Consumer Safety (SCCS) [85]: “the practical meaning of antibiotic resistance is to describe situations where (i) a strain is not killed or inhibited by a concentration attained *in vivo*, (ii) a strain is not killed or inhibited by a concentration to which the majority of strains of that organism are susceptible or (iii) bacterial cells that are not killed or inhibited by a concentration acting upon the majority of cells in that culture,” and tolerance denotes a reduced susceptibility to an antimicrobial approach. The *S. agalactiae* aPDI tolerance in this study is in accordance with the SCCS report, demonstrating reduced microbial susceptibility to the treatment. Thus, the emergence of aPDI-tolerant phenotypes does not prevent the successful application of phototreatments in the clinic but rather indicates the possible limitations that could be overcome with responsible treatment policies.

Author contributions

MP performed the experimental work and participated in conception of the study. IS participated in conception of the study and critical review of the manuscript. MG was involved in the coordination, conception, and design of the study and wrote the manuscript.

All of the authors have read and approved the final manuscript.

Data availability

The datasets generated during and/or analyzed during the current study are available from the corresponding author on reasonable request.

Ethical approval

The manuscript contains no data concerning animal studies, studies involving human subjects or inclusion of identifiable human data or clinical trials; thus, no ethical approval was required.

Declaration of competing interest

The authors declare no competing interests.

Acknowledgements and funding

Work was supported by grant no. NCN 2016/23/B/NZ7/03236 (M.G.)

References

- [1] E.J. Saad, D.F. Baenas, C.S. Boisseau, M.J. Garcia, S.A. Nunez, P.E. Sanchez, et al., Streptococcus agalactiae bacteremia in non-pregnant adult patients at two teaching hospitals, *Rev. Argent. Microbiol.* 50 (3) (2018) 280–284.
- [2] M. Rosa-Fraile, S. Dramsi, B. Spellerberg, Group B streptococcal haemolysin and pigment, a tale of twins, *FEMS Microbiol. Rev.* 38 (5) (2014) 932–946.
- [3] N.J. Kothari, C.A. Morin, A. Glennen, D. Jackson, J. Harper, S.J. Schrag, et al., Invasive group B streptococcal disease in the elderly, Minnesota, USA, 2003–2007, *Emerg. Infect. Dis.* 15 (8) (2009) 1279–1281.
- [4] M.M. Farley, Group B streptococcal disease in nonpregnant adults, *Clin. Infect. Dis.* 33 (4) (2001) 556–561.
- [5] A. Tazi, P.C. Morand, H. Reglier-Poupet, N. Dmytruk, A. Billoet, D. Antona, et al., Invasive group B streptococcal infections in adults, France (2007–2010), *Clin. Microbiol. Infect.* 17 (10) (2011) 1587–1589.
- [6] T.H. Skoff, M.M. Farley, S. Petit, A.S. Craig, W. Schaffner, K. Gershman, et al., Increasing burden of invasive group B streptococcal disease in nonpregnant adults, 1990–2007, *Clin. Infect. Dis.* 49 (1) (2009) 85–92.
- [7] W. Louthrenoo, N. Kasitanon, S. Wangkaew, S. Hongsongkiat, W. Sukitawat, R. Wichainun, Streptococcus agalactiae: an emerging cause of septic arthritis, *J. Clin. Rheumatol.* 20 (2) (2014) 74–78.
- [8] P. Sendi, L. Johansson, A. Norrby-Teglund, Invasive group B Streptococcal disease in non-pregnant adults: a review with emphasis on skin and soft-tissue infections, *Infection* 36 (2) (2008) 100–111.
- [9] S. Amico, L. Calvo, S. Corrao, An "aubergine" in the heart: huge native mitral valve endocarditis caused by Streptococcus agalactiae, *Intern Emerg Med* 13 (1) (2018) 137–138.
- [10] A. Verghese, S.L. Berk, L.J. Boelen, J.K. Smith, Group b Streptococcal pneumonia in the elderly, *Arch. Intern. Med.* 142 (9) (1982) 1642–1645.
- [11] S.Y. Leclercq, M.J. Sullivan, D.S. Ipe, J.P. Smith, A.W. Cripps, G.C. Ulett, Pathogenesis of Streptococcus urinary tract infection depends on bacterial strain and beta-hemolysin/cytolysin that mediates cytotoxicity, cytokine synthesis, inflammation and virulence, *Sci. Rep.* 6 (2016) 29000.
- [12] J. Solis-Garcia del Pozo, E. Martinez-Alfaro, L. Abad, J. Solera, Vertebral osteomyelitis caused by Streptococcus agalactiae, *J. Infect.* 41 (1) (2000) 84–90.
- [13] C. Ruppen, J. Notter, C. Strahm, B. Sonderegger, P. Sendi, Osteoarticular and skin and soft-tissue infections caused by Streptococcus agalactiae in elderly patients are frequently associated with bacteremia, *Diagn. Microbiol. Infect. Dis.* 90 (1) (2018) 55–57.
- [14] K.B. Ulett, W.H. Benjamin Jr., F. Zhuo, M. Xiao, F. Kong, G.L. Gilbert, et al., Diversity of group B streptococcus serotypes causing urinary tract infection in adults, *J. Clin. Microbiol.* 47 (7) (2009) 2055–2060.
- [15] M. Kohli-Lynch, N.J. Russell, A.C. Seale, Z. Dangor, C.J. Tann, C.J. Baker, et al., Neurodevelopmental impairment in children after group B streptococcal disease worldwide: systematic review and meta-analyses, *Clin. Infect. Dis.* 65 (suppl_2) (2017) S190–S199.
- [16] M.W. Bijlsma, M.C. Brouwer, E.S. Kananmoolib, A.T. Kloek, M.J. Lucas, M.W. Tanck, et al., Community-acquired bacterial meningitis in adults in The Netherlands, 2006–14: a prospective cohort study, *Lancet Infect. Dis.* 16 (3) (2016) 339–347.
- [17] E. Wilder-Smith, K.M. Chow, R. Kay, M. Ip, N. Tee, Group B streptococcal meningitis in adults: recent increase in Southeast Asia, *Aust. N. Z. J. Med.* 30 (4) (2000) 462–465.
- [18] V.N. Raabe, A.L. Shane, Group B Streptococcus (Streptococcus agalactiae), *Microbiol. Spectr.* 7 (2) (2019).
- [19] S. Schrag, R. Gorwitz, K. Fultz-Butts, A. Schuchat, Prevention of perinatal group B streptococcal disease. Revised guidelines from CDC, *MMWR Recomm. Rep. (Morb. Mortal. Wkly. Rep.)* 51 (RR-11) (2002) 1–22.
- [20] K. Kimura, N. Nagano, Y. Nagano, S. Suzuki, J. Wachino, K. Shibayama, et al., High frequency of fluoroquinolone- and macrolide-resistant streptococci among clinically isolated group B streptococci with reduced penicillin susceptibility, *J. Antimicrob. Chemother.* 68 (3) (2013) 539–542.
- [21] T. Seki, K. Kimura, M.E. Reid, A. Miyazaki, H. Banno, W. Jin, et al., High isolation rate of MDR group B streptococci with reduced penicillin susceptibility in Japan, *J. Antimicrob. Chemother.* 70 (10) (2015) 2725–2728.
- [22] P.A. Hawkins, C.S. Law, B.J. Metcalf, S. Chochua, D.M. Jackson, L.F. Westblade, et al., Cross-resistance to lincosamides, streptogramins A and pleuromutilins in Streptococcus agalactiae isolates from the USA, *J. Antimicrob. Chemother.* 72 (7) (2017) 1886–1892.
- [23] W. Wehbeh, R. Rojas-Diaz, X. Li, N. Mariano, L. Grenner, S. Segal-Maurer, et al., Fluoroquinolone-resistant Streptococcus agalactiae: epidemiology and mechanism of resistance, *Antimicrob. Agents Chemother.* 49 (6) (2005) 2495–2497.
- [24] C. Hays, M. Louis, C. Plainvert, N. Dmytruk, G. Touak, P. Trieu-Cuot, et al., Changing epidemiology of group B Streptococcus susceptibility to fluoroquinolones and aminoglycosides in France, *Antimicrob. Agents Chemother.* 60 (12) (2016) 7424–7430.
- [25] G. Piccinelli, F. Gargiulo, S. Corbellini, G. Ravizzola, C. Bonfanti, A. Caruso, et al., Emergence of the first levofloxacin-resistant strains of Streptococcus agalactiae isolated in Italy, *Antimicrob. Agents Chemother.* 59 (4) (2015) 2466–2469.
- [26] Y. Wang, Y. Wang, Y. Wang, C.K. Murray, M.R. Hamblin, D.C. Hooper, et al., Antimicrobial blue light inactivation of pathogenic microbes: state of the art, *Drug Resist. Updates* 33–35 (2017) 1–22.
- [27] J. Nakonieczna, A. Wozniak, M. Pieranski, A. Rapacka-Zdonczyk, P. Ogonowska, M. Grinholc, Photoinactivation of ESKAPE pathogens: overview of novel therapeutic strategy, *Future Med. Chem.* 11 (5) (2019) 443–461.
- [28] T.G. St Denis, T. Dai, L. Izikson, C. Astrakas, R.R. Anderson, M.R. Hamblin, et al., All you need is light: antimicrobial photoinactivation as an evolving and emerging discovery strategy against infectious disease, *Virulence* 2 (6) (2011) 509–520.
- [29] G.B. Kharkwal, S.K. Sharma, Y.Y. Huang, T. Dai, M.R. Hamblin, Photodynamic therapy for infections: clinical applications, *Laser Surg. Med.* 43 (7) (2011) 755–767.
- [30] M. Wainwright, T. Maisch, S. Nonell, K. Plaetzer, A. Almeida, G.P. Tegos, et al., Photoantimicrobials—are we afraid of the light? *Lancet Infect. Dis.* 17 (2) (2017) e49–e55.
- [31] M. Wainwright, Photodynamic antimicrobial chemotherapy (PACT), *J. Antimicrob. Chemother.* 42 (1) (1998) 13–28.
- [32] M.S. Baptista, J. Cadet, P. Di Mascio, A.A. Ghogare, A. Greer, M.R. Hamblin, et al., Type I and type II photosensitized oxidation reactions: guidelines and mechanistic pathways, *Photochem. Photobiol.* 93 (4) (2017) 912–919.
- [33] M. Grinholc, A. Rapacka-Zdonczyk, B. Rybak, F. Szabados, K.P. Bielawski, Multiresistant strains are as susceptible to photodynamic inactivation as their naive counterparts: protoporphyrin IX-mediated photoinactivation reveals differences between methicillin-resistant and methicillin-sensitive Staphylococcus aureus strains, *Photomed Laser Surg* 32 (3) (2014) 121–129.
- [34] G. Fila, A. Kawiak, M.S. Grinholc, Blue light treatment of Pseudomonas aeruginosa: strong bactericidal activity, synergism with antibiotics and inactivation of virulence factors, *Virulence* 8 (6) (2017) 938–958.
- [35] J. Nakonieczna, K. Wolnikowska, P. Ogonowska, D. Neubauer, A. Bernat, W. Kamysz, Rose bengal-mediated photoinactivation of multidrug resistant Pseudomonas aeruginosa is enhanced in the presence of antimicrobial peptides, *Front. Microbiol.* 9 (2018) 1949.
- [36] R.M. Amin, B. Bhayana, M.R. Hamblin, T. Dai, Antimicrobial blue light inactivation of Pseudomonas aeruginosa by photo-excitation of endogenous porphyrins: in vitro and in vivo studies, *Laser Surg. Med.* 48 (5) (2016 Jul) 562–568.
- [37] F. Giuliani, M. Martinelli, A. Cocchi, D. Arbia, L. Fantetti, G. Roncucci, In vitro resistance selection studies of RLP068/Cl, a new Zn(II) phthalocyanine suitable for antimicrobial photodynamic therapy, *Antimicrob. Agents Chemother.* 54 (2) (2010) 637–642.
- [38] N. Kashef, M. Akbarizadeh, S.K. Kamrava, Effect of sub-lethal photodynamic inactivation on the antibiotic susceptibility and biofilm formation of clinical Staphylococcus aureus isolates, *Photodiagnosis Photodyn. Ther.* 10 (4) (2013) 368–373.
- [39] A. Rapacka-Zdonczyk, A. Wozniak, M. Pieranski, A. Woziwodzka, K.P. Bielawski, M. Grinholc, Development of Staphylococcus aureus tolerance to antimicrobial photodynamic inactivation and antimicrobial blue light upon sub-lethal treatment, *Sci. Rep.* 9 (1) (2019) 9423.
- [40] A. Ogonowska Pw, M. Pieranski, T. Wasylew, P. Kwiek, M. Brasel, M. Grinholc, J. Nakonieczna, Application and characterization of light-emitting diodes for photodynamic inactivation of bacteria, *Light. Res. Technol.* 51 (4) (2019) 612–624.
- [41] M. Price, J.J. Reiners, A.M. Santiago, D. Kessel, Monitoring singlet oxygen and hydroxyl radical formation with fluorescent probes during photodynamic therapy, *Photochem. Photobiol.* 85 (5) (2009) 1177–1181.
- [42] M.H. Werts, V. Raimbault, R. Texier-Picard, R. Poizat, O. Francais, L. Griscom,

- et al., Quantitative full-colour transmitted light microscopy and dyes for concentration mapping and measurement of diffusion coefficients in microfluidic architectures, *Lab Chip* 12 (4) (2012) 808–820.
- [43] L. Ludvikova, P. Fris, D. Heger, P. Sebej, J. Wirz, P. Klan, Photochemistry of rose bengal in water and acetonitrile: a comprehensive kinetic analysis, *Phys. Chem. Chem. Phys.* 18 (24) (2016) 16266–16273.
- [44] (Ecsmid) ECfAST/EotESoCmaId, Determination of minimum inhibitory concentrations (MICs) of antibacterial agents by broth dilution, *Clin. Microbiol. Infect.* 9 (8) (2003) ix–xv.
- [45] W. Schroder, C. Goerke, C. Wolz, Opposing effects of aminocoumarins and fluoroquinolones on the SOS response and adaptability in *Staphylococcus aureus*, *J. Antimicrob. Chemother.* 68 (3) (2013) 529–538.
- [46] G.Y. Liu, K.S. Doran, T. Lawrence, N. Turkson, M. Puliti, L. Tissi, et al., Sword and shield: linked group B streptococcal beta-hemolysin/cytolysin and carotenoid pigment function to subvert host phagocyte defense, *Proc. Natl. Acad. Sci. U. S. A.* 101 (40) (2004) 14491–14496.
- [47] F.P. Sellera, C.P. Sabino, M.S. Ribeiro, R.G. Gargano, N.R. Benites, P.A. Melville, et al., In vitro photoinactivation of bovine mastitis related pathogens, *Photodiagnosis Photodyn. Ther.* 13 (2016) 276–281.
- [48] M. Grinholc, A. Rodziewicz, K. Forsys, A. Rapacka-Zdonczyk, A. Kawiak, A. Domachowska, et al., Fine-tuning recA expression in *Staphylococcus aureus* for antimicrobial photoinactivation: importance of photo-induced DNA damage in the photoinactivation mechanism, *Appl. Microbiol. Biotechnol.* 99 (21) (2015) 9161–9176.
- [49] L. Sabbahi Sba, M. Jemli, *Staphylococcus aureus* photodynamic inactivation mechanisms by rose bengal: use of antioxidants and spectroscopic study, *Appl Water Science* 8 (56) (2018) 1–9.
- [50] A.F. Silva, A. Borges, C.F. Freitas, N. Hioka, J.M.G. Mikcha, M. Simoes, Antimicrobial photodynamic inactivation mediated by rose bengal and erythrosine is effective in the control of food-related bacteria in planktonic and biofilm states, *Molecules* 23 (9) (2018).
- [51] T. Dubey, N.V. Gorantla, K.T. Chandrashekhara, S. Chinnathambi, Photodynamic exposure of Rose-Bengal inhibits Tau aggregation and modulates cytoskeletal network in neuronal cells, *Sci. Rep.* 10 (1) (2020) 12380.
- [52] B. Wang, J.H. Wang, Q. Liu, H. Huang, M. Chen, K. Li, et al., Rose-bengal-conjugated gold nanorods for in vivo photodynamic and photothermal oral cancer therapies, *Biomaterials* 35 (6) (2014) 1954–1966.
- [53] E. Panzarini, V. Inguscio, G.M. Fimia, L. Dini, Rose Bengal acetate photodynamic therapy (RBAC-PDT) induces exposure and release of Damage-Associated Molecular Patterns (DAMPs) in human HeLa cells, *PLoS One* 9 (8) (2014) e105778.
- [54] G. Amescua, A. Arboleda, N. Nikpoor, H. Durkee, N. Relhan, M.C. Aguilar, et al., Rose bengal photodynamic antimicrobial therapy: a novel treatment for resistant *Fusarium keratitis*, *Cornea* 36 (9) (2017) 1141–1144.
- [55] H. Kato, K. Komagoe, Y. Nakanishi, T. Inoue, T. Katsu, Xanthene dyes induce membrane permeabilization of bacteria and erythrocytes by photoinactivation, *Photochem. Photobiol.* 88 (2) (2012) 423–431.
- [56] E. Alarcon, A.M. Edwards, A. Aspee, C.D. Borsarelli, E.A. Lissi, Photophysics and photochemistry of rose bengal bound to human serum albumin, *Photochem. Photobiol. Sci.* 8 (7) (2009) 933–943.
- [57] R.A. Miller, B.E. Britigan, Role of oxidants in microbial pathophysiology, *Clin. Microbiol. Rev.* 10 (1) (1997) 1–18.
- [58] E. Cabisco, J. Tamarit, J. Ros, Oxidative stress in bacteria and protein damage by reactive oxygen species, *Int. Microbiol.* 3 (1) (2000) 3–8.
- [59] C. Poyart, E. Pellegrini, O. Gaillot, C. Boumaila, M. Baptista, P. Trieu-Cuot, Contribution of Mn-cofactored superoxide dismutase (SodA) to the virulence of *Streptococcus agalactiae*, *Infect. Immun.* 69 (8) (2001) 5098–5106.
- [60] R.M. Tsois, A.J. Baumber, F. Heffron, Role of *Salmonella typhimurium* Mn-superoxide dismutase (SodA) in protection against early killing by J774 macrophages, *Infect. Immun.* 63 (5) (1995) 1739–1744.
- [61] K.E. Wilks, K.L. Dunn, J.L. Farrant, K.M. Reddin, A.R. Gorringe, P.R. Langford, et al., Periplasmic superoxide dismutase in meningococcal pathogenicity, *Infect. Immun.* 66 (1) (1998) 213–217.
- [62] H. Yesilkaya, A. Kadioglu, N. Gingles, J.E. Alexander, T.J. Mitchell, P.W. Andrew, Role of manganese-containing superoxide dismutase in oxidative stress and virulence of *Streptococcus pneumoniae*, *Infect. Immun.* 68 (5) (2000) 2819–2826.
- [63] M.L. Korir, R.A. Flaherty, L.M. Rogers, J.A. Gaddy, D.M. Aronoff, S.D. Manning, Investigation of the role that NADH peroxidase plays in oxidative stress survival in group B *Streptococcus*, *Front. Microbiol.* 9 (2018) 2786.
- [64] S. La Carbona, N. Sauvageot, J.C. Giard, A. Benachour, B. Posteraro, Y. Auffray, et al., Comparative study of the physiological roles of three peroxidases (NADH peroxidase, Alkyl hydroperoxide reductase and Thiol peroxidase) in oxidative stress response, survival inside macrophages and virulence of *Enterococcus faecalis*, *Mol. Microbiol.* 66 (5) (2007) 1148–1163.
- [65] P. Glaser, C. Rusniok, C. Buchrieser, F. Chevalier, L. Frangetul, T. Msadek, et al., Genome sequence of *Streptococcus agalactiae*, a pathogen causing invasive neonatal disease, *Mol. Microbiol.* 45 (6) (2002) 1499–1513.
- [66] N.I. Krinsky, K.J. Yeum, Carotenoid-radical interactions, *Biochem. Biophys. Res. Commun.* 305 (3) (2003) 754–760.
- [67] C.A. Pritzlaff, J.C. Chang, S.P. Kuo, G.S. Tamura, C.E. Rubens, V. Nizet, Genetic basis for the beta-haemolytic/cytolytic activity of group B *Streptococcus*, *Mol. Microbiol.* 39 (2) (2001) 236–247.
- [68] K.L. Painter, E. Strange, J. Parkhill, K.B. Bamford, D. Armstrong-James, A.M. Edwards, *Staphylococcus aureus* adapts to oxidative stress by producing H2O2-resistant small-colony variants via the SOS response, *Infect. Immun.* 83 (5) (2015) 1830–1844.
- [69] L.E. Bryan, S. Kwan, Aminoglycoside-resistant mutants of *Pseudomonas aeruginosa* deficient in cytochrome d, nitrite reductase, and aerobic transport, *Antimicrob. Agents Chemother.* 19 (6) (1981) 958–964.
- [70] C.A. Colwell, Small colony variants of *Escherichia coli*, *J. Bacteriol.* 52 (4) (1946) 417–422.
- [71] N. Wellinghausen, I. Chatterjee, A. Berger, A. Niederfuehr, R.A. Proctor, B.C. Kahl, Characterization of clinical *Enterococcus faecalis* small-colony variants, *J. Clin. Microbiol.* 47 (9) (2009) 2802–2811.
- [72] M. Allegrucci, K. Sauer, Formation of *Streptococcus pneumoniae* non-phase-variable colony variants is due to increased mutation frequency present under biofilm growth conditions, *J. Bacteriol.* 190 (19) (2008) 6330–6339.
- [73] A. Zbinden, C. Quiblier, D. Hernandez, K. Herzog, P. Bodler, M.M. Senn, et al., Characterization of *Streptococcus tigurinus* small-colony variants causing prosthetic joint infection by comparative whole-genome analyses, *J. Clin. Microbiol.* 52 (2) (2014) 467–474.
- [74] H. Banno, K. Kimura, Y. Tanaka, T. Sekizuka, M. Kuroda, W. Jin, et al., Analysis of multidrug resistant group B streptococci with reduced penicillin susceptibility forming small, less hemolytic colonies, *PLoS One* 12 (8) (2017) e0183453.
- [75] R.A. Proctor, C. von Eiff, B.C. Kahl, K. Becker, P. McNamara, M. Herrmann, et al., Small colony variants: a pathogenic form of bacteria that facilitates persistent and recurrent infections, *Nat. Rev. Microbiol.* 4 (4) (2006) 295–305.
- [76] B.E. Johns, K.J. Purdy, N.P. Tucker, S.E. Maddocks, Phenotypic and genotypic characteristics of small colony variants and their role in chronic infection, *Microbiol. Insights* 8 (2015) 15–23.
- [77] A. Tavares, C.M. Carvalho, M.A. Faustino, M.G. Neves, J.P. Tome, A.C. Tome, et al., Antimicrobial photodynamic therapy: study of bacterial recovery viability and potential development of resistance after treatment, *Mar. Drugs* 8 (1) (2010) 91–105.
- [78] N. Iluz, Y. Maor, N. Keller, Z. Malik, The synergistic effect of PDT and oxacillin on clinical isolates of *Staphylococcus aureus*, *Laser Surg. Med.* 50 (5) (2018) 535–551.
- [79] C.F. Pope, D.M. O'Sullivan, T.D. McHugh, S.H. Gillespie, A practical guide to measuring mutation rates in antibiotic resistance, *Antimicrob. Agents Chemother.* 52 (4) (2008) 1209–1214.
- [80] C. Florindo, R. Ferreira, V. Borges, B. Spellerberg, J.P. Gomes, M.J. Borrego, Selection of reference genes for real-time expression studies in *Streptococcus agalactiae*, *J. Microbiol. Methods* 90 (3) (2012) 220–227.
- [81] A. Six, A. Firon, C. Plainvert, C. Caplain, A. Bouaboud, G. Touak, et al., Molecular characterization of nonhemolytic and nonpigmented group B streptococci responsible for human invasive infections, *J. Clin. Microbiol.* 54 (1) (2016) 75–82.
- [82] G.Y. Liu, V. Nizet, Extracellular virulence factors of group B *Streptococci*, *Front. Biosci.* 9 (2004) 1794–1802.
- [83] M. Kossakowska-Zwierucho, R. Kazmierkiewicz, K.P. Bielawski, J. Nakonieczna, Factors determining *Staphylococcus aureus* susceptibility to photoantimicrobial chemotherapy: RsbU activity, staphyloxanthin level, and membrane fluidity, *Front. Microbiol.* 7 (2016) 1141.
- [84] U.O. Hasdemir, J. Chevalier, P. Nordmann, J.M. Pages, Detection and prevalence of active drug efflux mechanism in various multidrug-resistant *Klebsiella pneumoniae* strains from Turkey, *J. Clin. Microbiol.* 42 (6) (2004) 2701–2706.
- [85] Safety SCoC, Opinion on Triclosan Antimicrobial Resistance European Commission, (2010).

Chapter IV

Optimization of *Streptococcus agalactiae* Biofilm Culture in a Continuous Flow System for Photoinactivation Studies

1. Summary of the publication

As the bacteria in planktonic culture are much more susceptible to any antimicrobial agent, to truly assess the effectiveness of the new therapy, examination of its effectiveness against biofilm culture is of high importance. The selection of the proper experimental model has a tremendous impact on the results of the experiments. Researchers always need to maneuver between model complexity and its similarity to the actual environmental conditions.

In this publication, two models of *S. agalactiae* biofilm were evaluated. While biofilm culture on microtiter plates is very easy to obtain, there are some concerns about its maturity and similarity to real-life situations. Another obstacle is the selection of the proper medium. The richness of the nutrients in the medium can almost completely inhibit biofilm formation for Gram-negative bacteria. Besides the use of different growth media by different research groups makes their results very hard to compare. In this publication influence of the medium on the biofilm growth of four *S. agalactiae* strains was evaluated. The next step was to optimize a more complicated biofilm model – continuous flow system biofilm culture, which because of longer time of culture, change in medium concentration during the growth and shear forces caused by medium flow, induce growth of more resistant and mature biofilm. Both biofilm models were then implemented in aPDI effectiveness evaluation. It was the very first report of *S. agalactiae* biofilm culture treatment with aPDI. To ensure that increased concentrations of RB, required for successful biofilm eradication, would not be harmless for human tissue, an MTT assay with human keratinocytes was performed. Hence, in this publication Aim 1. was extended from planktonic culture to biofilm culture evaluation and the first attempt for the fulfilment of Aim 4. was made.

2. Publication

Article

Optimization of *Streptococcus agalactiae* Biofilm Culture in a Continuous Flow System for Photoinactivation Studies

Michał K. Pieranski ^{1,*} , Michał Rychłowski ² and Mariusz Grinholc ¹ 

¹ Laboratory of Photobiology and Molecular Diagnostics, Intercollegiate Faculty of Biotechnology University of Gdansk and Medical University of Gdansk, 80-307 Gdansk, Poland; mariusz.grinholc@biotech.ug.edu.pl

² Laboratory of Virus Molecular Biology, Intercollegiate Faculty of Biotechnology University of Gdansk and Medical University of Gdansk, 80-307 Gdansk, Poland; michal.rychlowski@biotech.ug.edu.pl

* Correspondence: michal.pieranski@phdstud.ug.edu.pl

Abstract: *Streptococcus agalactiae* is a relevant cause of neonatal mortality. It can be transferred to infants via the vaginal tract and cause meningitis, pneumonia, arthritis, or sepsis, among other diseases. The cause of therapy ineffectiveness and infection recurrence is the growth of bacteria as biofilms. To date, several research teams have attempted to find a suitable medium for the cultivation of *S. agalactiae* biofilms. Among others, simulated vaginal fluid has been used; however, biofilm production in this medium has been found to be lower than that in tryptic soy broth. We have previously shown that *S. agalactiae* can be successfully eradicated by photoinactivation in planktonic culture, but there have been no studies on biofilms. The aim of this study was to optimize *S. agalactiae* biofilm culture conditions to be used in photoinactivation studies. We compared biofilm production by four strains representing the most common serotypes in four different broth media with crystal violet staining. Then, we evaluated stationary biofilm culture in microtiter plates and biofilm growth in a CDC Biofilm Reactor[®] (BioSurface Technologies, Bozeman, MT, USA) under continuous flow conditions. Subsequently, we applied Rose Bengal-mediated photoinactivation to both biofilm models. We have shown that photoinactivation is efficient in biofilm eradication and is not cyto-/phototoxic to human keratinocytes. We found conditions allowing for stable and repetitive *S. agalactiae* biofilm growth in continuous flow conditions, which can be successfully utilized in photoinactivation assays and potentially in all other antibacterial studies.

Keywords: *S. agalactiae*; Group B *Streptococcus* (GBS); biofilm; continuous flow; Center for Disease Control and Prevention (CDC) Biofilm Reactor; photoinactivation; Rose Bengal



Citation: Pieranski, M.K.; Rychłowski, M.; Grinholc, M. Optimization of *Streptococcus agalactiae* Biofilm Culture in a Continuous Flow System for Photoinactivation Studies. *Pathogens* **2021**, *10*, 1212. <https://doi.org/10.3390/pathogens10091212>

Academic Editors: Kirsty Le Doare and Konstantinos Karampatsas

Received: 30 August 2021

Accepted: 14 September 2021

Published: 18 September 2021

Publisher's Note: MDPI stays neutral with regard to jurisdictional claims in published maps and institutional affiliations.



Copyright: © 2021 by the authors. Licensee MDPI, Basel, Switzerland. This article is an open access article distributed under the terms and conditions of the Creative Commons Attribution (CC BY) license (<https://creativecommons.org/licenses/by/4.0/>).

1. Introduction

Streptococcus agalactiae, the most common representative of Group B *Streptococcus* (GBS), is a relevant cause of neonatal mortality. Approximately 10–30% of women carry *S. agalactiae* in their vaginal tract, from which it can be transferred to infants during labor and cause meningitis, pneumonia, arthritis, or sepsis, among other diseases. Prenatal antibiotic prophylaxis has significantly decreased the incidence of newborn infections in the Western Hemisphere, but there are still parts of the world where this procedure is not routine [1]. Worrying issues are the increasing incidence of antibiotic resistance among GBS, such as to penicillin G or macrolides, which are first-line therapies. In our study, we chose the most frequently represented capsular serotypes in Poland, which are IA, III, and V [2]. These serotypes are also the most common cause of urinary tract infections among adults [3]. Apart from antibiotic resistance, a significant cause of persistence and recurrence of infections such as bacterial vaginosis is biofilm production [4]. Additionally, bacteria grown as biofilms are significantly less susceptible to antibiotics than bacteria grown in planktonic culture. The minimum biofilm eradication concentration (MBEC) of penicillin G against *S. agalactiae* is approximately 500 times higher than the minimum inhibitory concentration (MIC) effective against planktonic culture [5]. As the physiological

vaginal pH is below 4.5 and *S. agalactiae* serotypes III and V form strong biofilms under acidic conditions, it is important to evaluate the effectiveness of the proposed therapies in a biofilm model [6].

To date, several research groups have attempted to find a suitable medium for the cultivation of *Streptococcus* biofilms. Among others, simulated vaginal fluid has been used. However, in the case of *S. agalactiae*, biofilm production in simulated vaginal fluid has been found to be lower than that in tryptic soy broth (TSB) [7]. Biofilm formation has also been found to be greater in TSB than in Todd Hewitt broth (THB), Luria Bertani broth (LB), or brain–heart infusion broth (BHI) [8]. For these reasons, we decided to evaluate *S. agalactiae* biofilm formation in other broths used for the cultivation of vaginal physiological flora or vaginal pathogens. New York City III (NYC) broth has been used in the culture of *Trichomonas vaginalis* and biofilms of *Gardnerella sp.*, *Atopobium vaginae*, *Lactobacillus iners*, *Mobiluncus curtisii*, *Peptostreptococcus anaerobius*, and *Prevotella bivia* [9,10]. Schaedler broth has been used in biofilm cultures of *Gardnerella vaginalis* [11]. De Mann, Rogosa, and Sharpe broth (MRS) has been used in biofilm cultures of *Lactobacillus plantarum*, *Lactobacillus crispatus*, *G. vaginalis*, and *P. bivia* [12–14].

With increasing antibiotic resistance, there is a tremendous demand for alternative antibacterial therapy development. In our research, we propose antimicrobial photodynamic inactivation (aPDI). aPDI requires the simultaneous presence of photosensitizing molecules, light, and oxygen. During the aPDI process, reactive oxygen species (ROS) are created inside or in close proximity to the bacterial cell. This phenomenon leads to damage to proteins, nucleic acids, and lipids and ultimately to bacterial death [15]. Rose Bengal (RB) is a photosensitizing dye efficient in inactivation of both planktonic and biofilm cultures of, i.e., *Staphylococcus aureus*, *Listeria innocua*, *Enterococcus hirae* and *Escherichia coli* [16,17]. It is characterized by the most efficient single oxygen generation of xanthene dyes and high water solubility [18]. Moreover, it is considered a molecule with a low level of cytotoxicity and high biocompatibility [19]. We have already shown that *S. agalactiae* can be successfully eradicated with RB-mediated aPDI in planktonic culture, but there have been no studies about the photoinactivation of *S. agalactiae* biofilms [20]. Therefore, the aim of this study was to optimize *S. agalactiae* biofilm culture conditions so that an assay system can be used in photoinactivation studies and potentially in all other antibacterial treatment tests.

2. Results

2.1. Microtiter Plate Biofilm Culture and Crystal Violet Staining Revealed Differences in Biofilm Production among the Studied Strains

The first stage of biofilm culture optimization was to screen for strong biofilm producers among the studied *S. agalactiae* strains using the most commonly applied microtiter plate method and crystal violet (CV) staining. A comparison of biofilm growth in four chosen broths was performed. For each broth, the biofilm was cultured in 96-well plates with full-strength or 2-fold diluted broth. After 24 h of growth, CV staining was performed. In all investigated broths, serotype V (s. V) strain produced a weak biofilm. Strains expressing serotypes IA and III (s. IA, s. III) as well as strain ATCC 27956 were characterized as moderate and strong biofilm producers according to particular broths. For both TSB and MRS broths, biofilm growth was stronger in diluted broth than in full-strength broth. A similar effect was also observed for the s. IA strain in NYC broth, and in Schaedler broth, growth intensity did not depend on broth concentration. For the s. III and ATCC 27956 strains, biofilm growth was strong at both concentrations of the NYC and Schaedler broths (Table 1). Therefore, these two strains, i.e., s. III and ATCC 27956, were used for further investigation.

Table 1. Results of *S. agalactiae* biofilm production assessed with crystal violet staining.

<i>S. agalactiae</i> strain	Medium Type							
	TSB		MRS		NYC		Schaedler	
	0.5×	1×	0.5×	1×	0.5×	1×	0.5×	1×
ATCC 27956	++	+	++	+	++	++	++	++
s. IA	++	+	++	+	++	+	+	+
s. III	+/-	+/-	++	+	++	++	++	++
s. V	+/-	+/-	+/-	+/-	-	+/-	+/-	+/-

Legend: (-) nonadherent; (+/-) weakly adherent; (+) moderately adherent; (++) strongly adherent.

To investigate biofilm production in a more detailed manner, enumeration of bacterial burden within the biofilms was performed. For all four full-strength broths, biofilm cultures in 96-well plates were prepared. After 24 h of incubation, wells were washed with PBS, and biofilms were dispersed for CFU enumeration. For both strains, the biofilm growth estimated on the basis of bacterial cell count was the lowest in MRS broth, medium in TSB and the highest in NYC (ATCC 27956) or Schaedler broth (s. III) (Figure 1). Thus, these two broths, i.e., NYC and Schaedler broth, were chosen for further investigation focusing on the clinical strain of *S. agalactiae* (s. III).

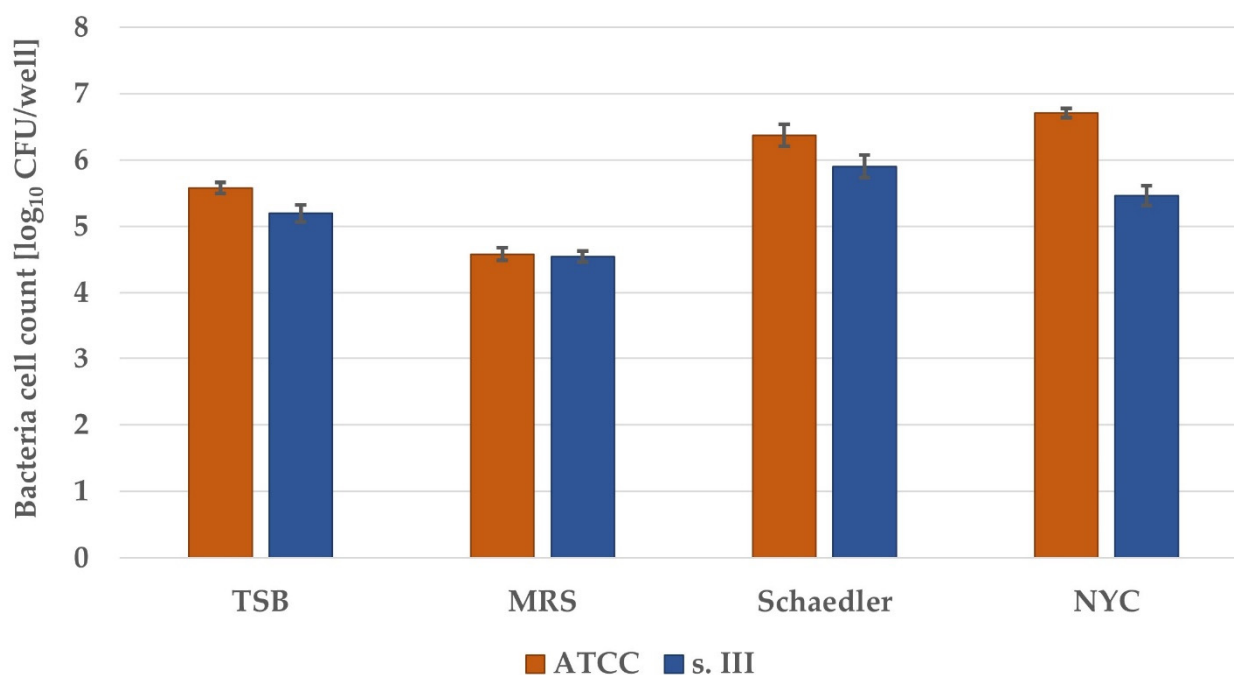


Figure 1. Growth of *S. agalactiae* biofilm cultures on microtiter plates. Overnight cultures were diluted in appropriate medium and incubated for 4 h. Then, the broth was changed, and incubation continued for 20 h. Dispersed biofilms were plated, and colonies were enumerated. The detection limit was 1 log₁₀ CFU/well. The values are the means of three separate experiments. Error bars represent the standard errors. All differences were significant vs. control broth (TSB) ($p < 0.05$).

2.2. CDC Biofilm Reactor System Biofilm Culture

Further optimization of GBS biofilm culture required in vitro studies utilizing microtiter plates to be translated into continuous flow system culturing to mimic physiological conditions. The first step of optimization of biofilm culture under continuous flow conditions was to detect the best coupon material used as a surface for biofilm formation. Four different adherent materials were investigated, i.e., glass, polypropylene, polycarbonate, and porous polycarbonate coupons. In accordance with the results obtained for microtiter plate biofilm culture, in continuous flow biofilm culture, biofilm growth was higher in Schaedler than in NYC broth (Figure 2). In both broths, biofilm growth was

the highest on polypropylene coupons. In Schaedler broth, biofilm growth was similar on polypropylene and glass coupons, lower on porous polycarbonate, and the lowest on polycarbonate coupons. In NYC broth, the highest biofilm growth was on polypropylene coupons, then lower on glass and polycarbonate coupons and the lowest on porous polycarbonate coupons.

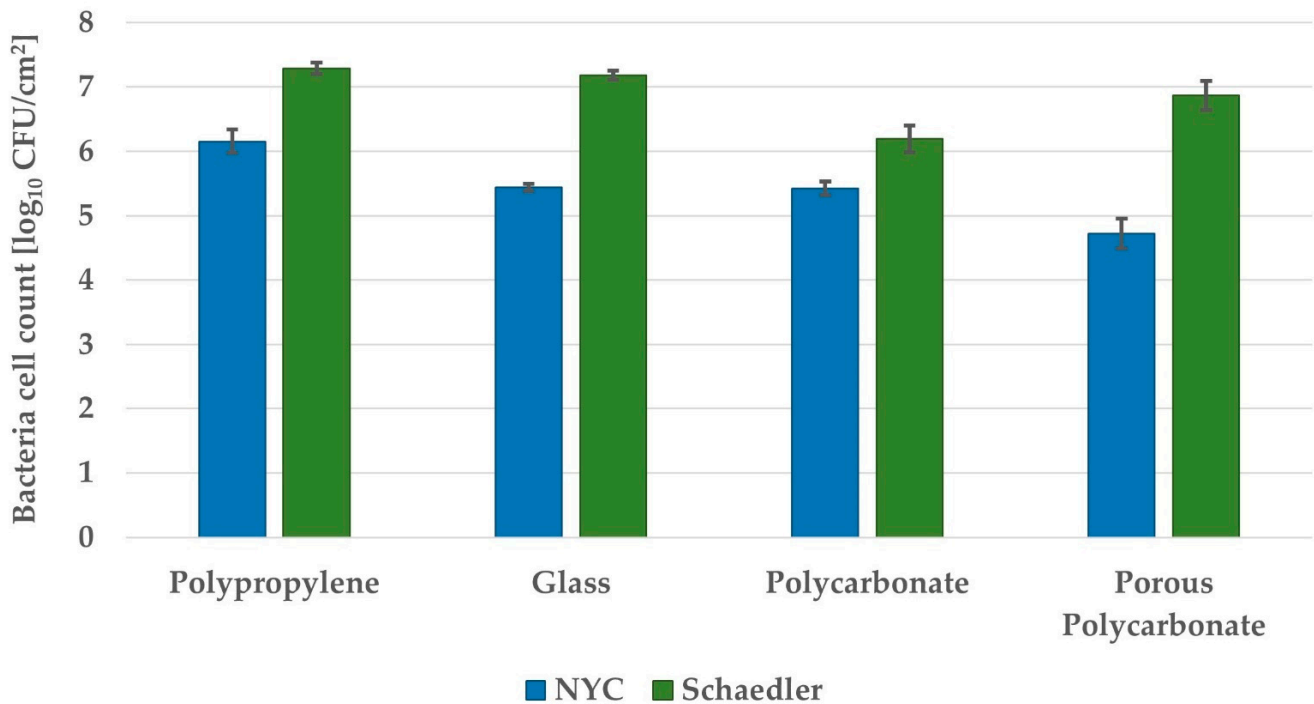


Figure 2. Growth of *S. agalactiae* s. III biofilm culture on coupons made from different materials in the CDC Biofilm Reactor System. The reactor with full-strength broth was inoculated with overnight culture. After 24 h of incubation with mixing, a flow of 5x-diluted broth was started and continued for 24 h. Coupons were removed and sonicated. Bacteria were plated, and colonies were enumerated. The detection limit was 2.59 log₁₀ CFU/cm². The values are the means of three separate experiments. Error bars represent the standard errors.

2.3. Biofilm Visualization

To decide which coupons should be used for further investigation, visualization of biofilm structures using confocal microscopy was performed. Biofilm growth was visualized with SYBR Green staining. This stain intercalates into double-stranded DNA both inside and outside of the bacterial cell. For all four coupon materials, we observed mushroom-shaped microcolonies, which indicates maturity of the biofilm (Figure 3). The size and arrangement of biofilm structures are similar on all coupon materials, so this technique did not help us choose the best material; nevertheless, it was supportive to confirm mature biofilm culturing. Finally, polypropylene coupons were chosen to be the best adherent surface for use for GBS biofilm culture.

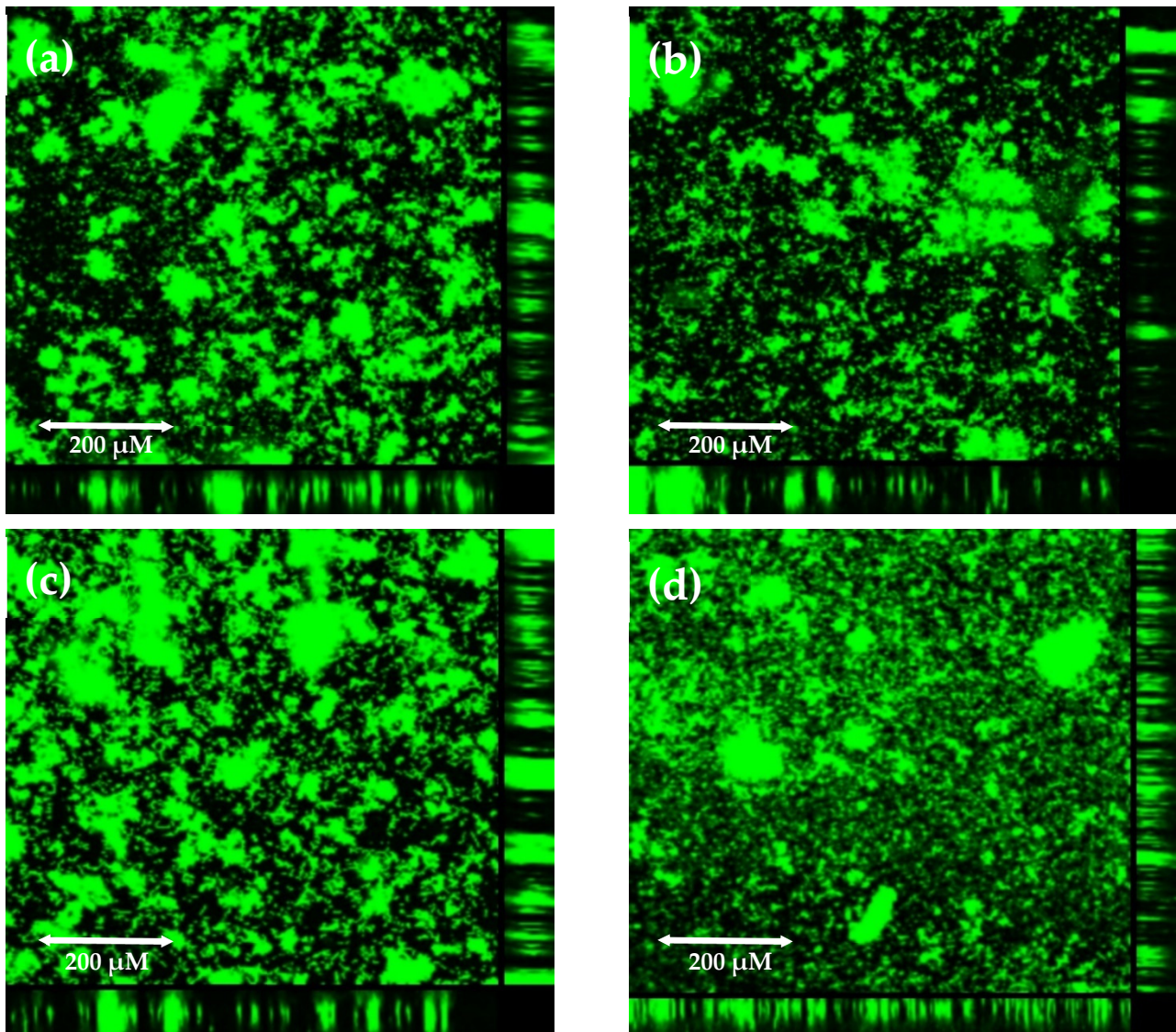


Figure 3. Growth of *S. agalactiae* s. III biofilm culture on coupons made from different materials in the CDC Biofilm Reactor System visualized with SYBR Green staining using confocal microscopy: (a) glass coupon; (b) polypropylene coupon; (c) polycarbonate coupon; (d) porous polycarbonate coupon. The reactor with full-strength broth was inoculated with overnight culture. After 24 h of incubation with mixing, a flow of 5 \times -diluted broth was started and continued for 24 h. Coupons were transferred to a glass-bottom plate, stained with SYBR Green, and viewed under a confocal laser scanning microscope.

2.4. Evaluation of Optimized GBS Biofilm Culture with Antibacterial Treatment, i.e., aPDI

2.4.1. Photodynamic Inactivation of Planktonic Cultures and Keratinocyte Safety Assays Indicate Control Conditions

S. agalactiae grown in a planktonic culture is highly susceptible to RB-mediated aPDI. The concentration of 0.3 μ M RB with 6 min of illumination causes ca. 6 log₁₀ unit reduction in bacterial viability. Since 2 log₁₀ unit CFU/mL is our limit of detection, this treatment exhibits complete eradication of all 3 clinical strains and almost complete eradication of the ATCC 27956 strain (Figure 4). Moreover, the bactericidal effectiveness was exclusively connected with the aPDI process: treatment with light only or RB in the dark did not cause a relevant reduction in bacterial viability.

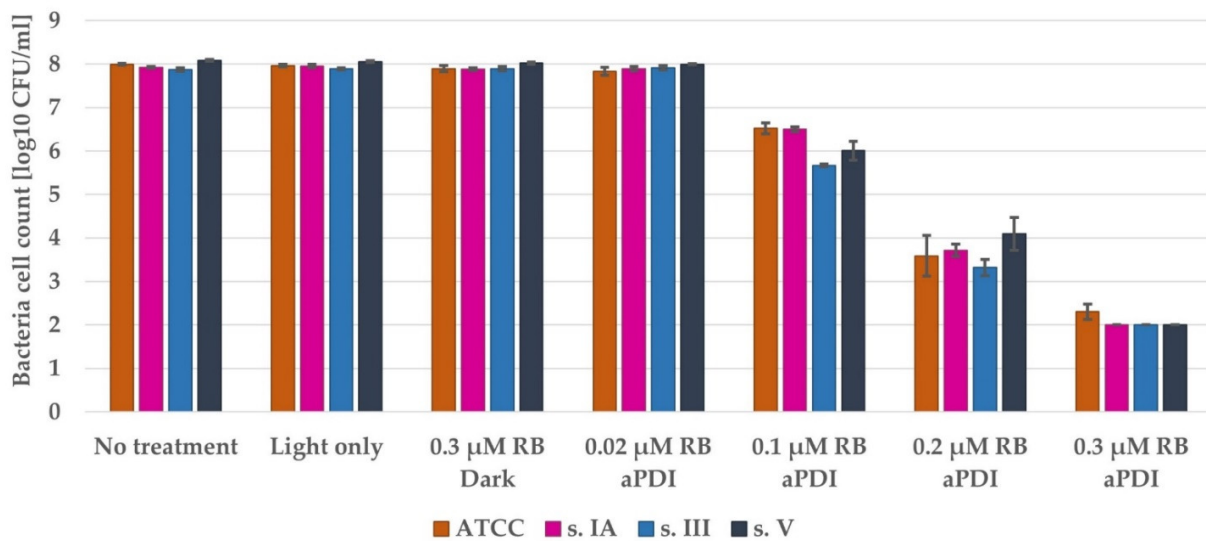


Figure 4. The antimicrobial effectiveness of aPDI with Rose Bengal on planktonic culture of *S. agalactiae*. An overnight culture was diluted in fresh TSB and incubated with the appropriate concentration of RB. Then, the bacteria were washed, suspended in PBS, and illuminated with a 522 nm LED lamp. After that, the bacteria were plated, and colonies were enumerated. The detection limit was $2 \log_{10}$ CFU/mL. The values are the means of three separate experiments. Error bars represent the standard errors.

To indicate whether the treatment conditions could exert bactericidal effects with limited harmful activity toward human keratinocytes, the cytotoxicity and phototoxicity of the treatment conditions were assayed using the MTT test. Rose Bengal manifested no cytotoxic activity against HaCaT cells at concentrations up to $10 \mu\text{M}$ (Figure 5). Moreover, aPDI under the evaluated illumination conditions was safe for HaCaT cells across the whole analyzed RB concentration spectrum.

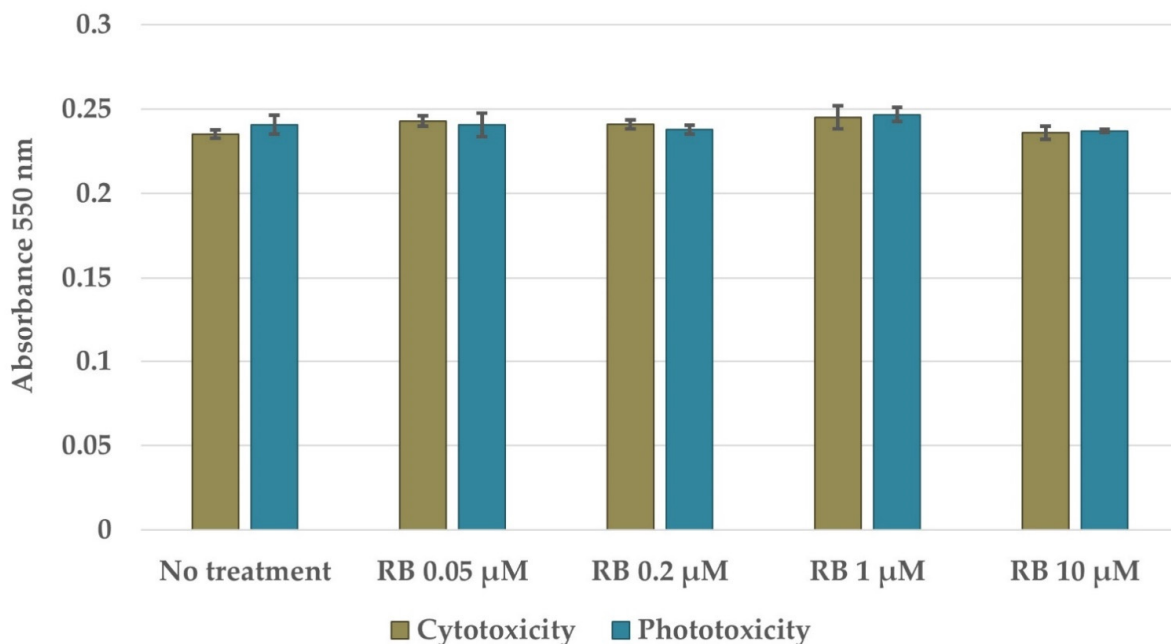


Figure 5. Viability of human keratinocytes (HaCaT cells) subjected to incubation with RB in the dark (cytotoxicity) or subjected to RB-mediated aPDI (phototoxicity). HaCaT cells were seeded into a 96-well plate. The next day, the cells were incubated in dark with RB or incubated in dark with RB and then illuminated. The following day, the cells were incubated with MTT compound and lysed with DMSO for absorbance measurement. The values are the means of three separate experiments. Error bars represent the standard deviations.

2.4.2. Photodynamic Inactivation of Microtiter Plate Biofilm Cultures

It is commonly known that microorganisms living in biofilms are more tolerant to various antibacterial treatments. The same could be observed for aPDI treatment. Therefore, to detect the most effective aPDI conditions, we screened multiple photosensitizer concentrations starting with the highest concentration used for planktonic studies. For NYC broth, a reduction in bacterial viability reaching the limit of detection was observed when RB was administered at a concentration of 1.2 μM (Figure 6). In the case of Schaedler broth, a similar effect was reached by employing RB at a concentration 10 times higher than that for planktonic culture (3 μM). Since the total initial number of bacteria in biofilms was much lower than that for planktonic culture, the viability decrease was 4.5 and 5 \log_{10} units CFU/well for NYC and Schaedler broths, respectively. Similar to planktonic culture, light-only treatment did not cause any decrease in bacterial viability, and RB in the dark treatment exhibited limited toxicity in the dark (only in the case of biofilms formed in Schaedler broth), leading to a reduction in bacterial viability by ca. 1 \log_{10} unit CFU/well. The obtained data also indicate that the biofilm grown in Schaedler broth is much more tolerant to aPDI than that grown in NYC medium.

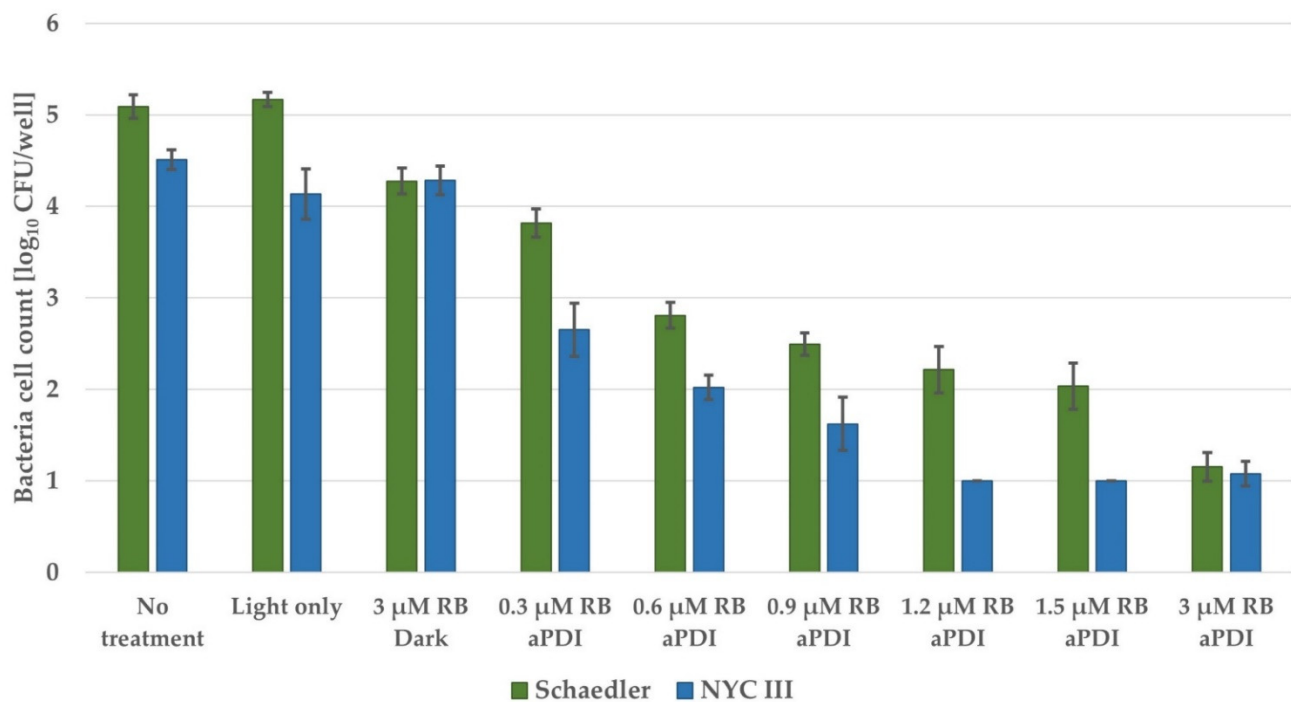


Figure 6. The antimicrobial effectiveness of aPDI with Rose Bengal on biofilm culture of *S. agalactiae* s. III grown on microtiter plates. An overnight culture was diluted in appropriate medium and incubated for 4 h. Then, the broth was changed, and incubation continued for 20 h. The biofilm was incubated with an appropriate concentration of RB. Then, the biofilm was washed, suspended in PBS, and illuminated with a 522 nm LED lamp. Dispersed biofilms were plated, and colonies were enumerated. The detection limit was 1 \log_{10} CFU/well. The values are the means of three separate experiments. Error bars represent the standard errors.

2.4.3. Photodynamic Inactivation of CDC Biofilm Reactor System Biofilm Culture

For biofilms grown in a continuous flow system, the three most effective RB concentrations were used. Since the coupon surface is 2.53 cm^2 , the limit of detection was 2.59 \log_{10} CFU/ cm^2 . aPDI with 3 μM RB caused a bacterial viability reduction of 3.6 \log_{10} unit CFU/ cm^2 (Figure 7), reaching the limit of detection. Similar to biofilm culture on microtiter plates, light-only treatment did not cause a decrease in bacterial viability, and RB treatment in the dark caused a toxicity effect reaching a viability reduction of

1.8 log₁₀ unit CFU/cm². This is the first time that toxicity of RB in the dark has been observed, and its explanation requires further investigation.

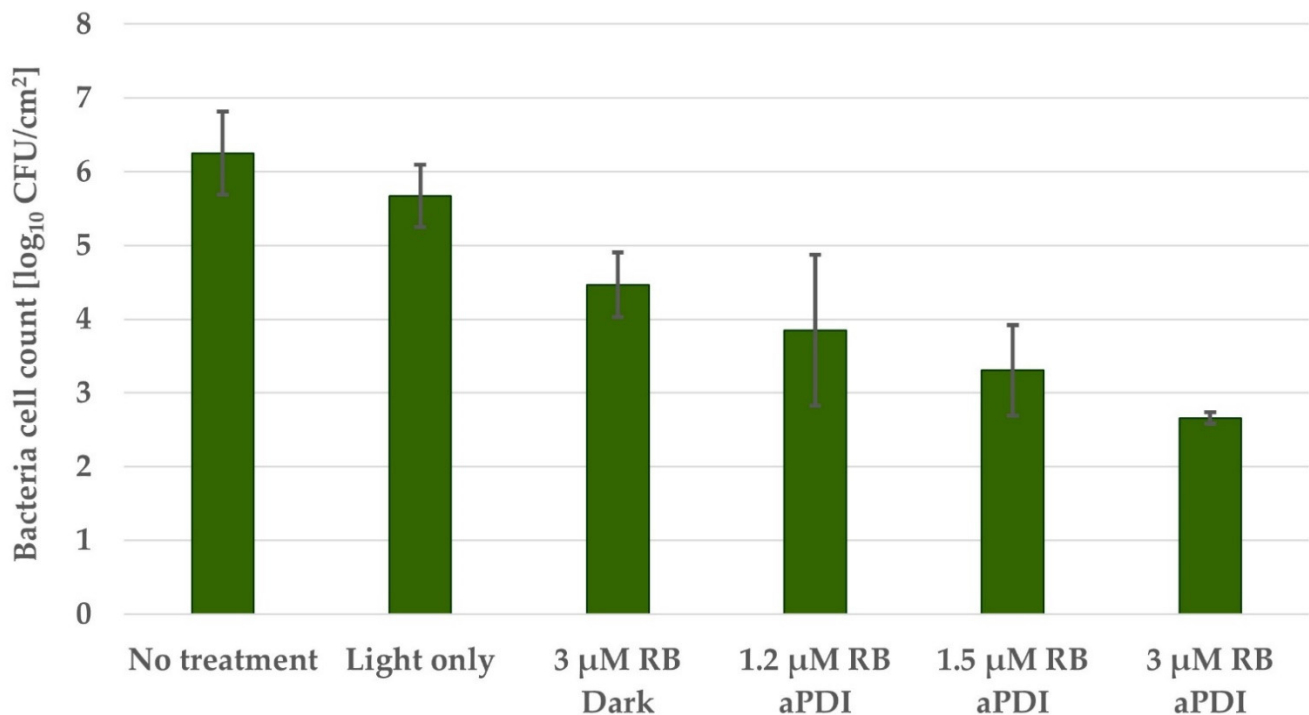


Figure 7. The antimicrobial effectiveness of aPDI with Rose Bengal on biofilm culture of *S. agalactiae* s. III grown in Schaedler medium on polypropylene coupons in the CDC Biofilm Reactor System. The reactor with full-strength broth was inoculated with overnight culture. After 24 h of incubation with mixing, a flow of 5× diluted broth was started and continued for 24 h. Coupons were removed and incubated with an appropriate concentration of RB. Then, the biofilm was washed, suspended in PBS, and illuminated with a 522 nm LED lamp. Coupons were then sonicated. Bacteria were plated, and colonies were enumerated. The detection limit was 2.59 log₁₀ CFU/cm². The values are the means of three separate experiments. Error bars represent the standard errors.

3. Discussion

There is no single recommended method for *S. agalactiae* biofilm growth experiments. *S. agalactiae* biofilms are usually grown on polystyrene 96-well plates in TSB [21–24] or THB [6,25–30]. Some deviations have been reported, such as THB supplemented with yeast extract [31], TSB supplemented with bovine serum [5], TSB supplemented with 3% BSA [32], RPMI [27], cation adjusted—Mueller Hinton broth (CA-MHB) [33] or CA-MHB supplemented with lysed horse broth [34]. Erika C. R. Bonsaglia et al. compared biofilm growth in four different broths, i.e., TSB, THB, LB, and BHI, among which growth in TSB was the greatest [8]. There has also been an attempt to culture *S. agalactiae* biofilms in simulated vaginal fluid, but biofilm growth was still better in TSB [7]. Therefore, our observation that *S. agalactiae* biofilm formation in NYC or Schaedler broth is greater than that in TSB should be beneficial for further model unification.

As the vaginal environment is affected by the frequent flow of fluids, we concluded that a biofilm model grown in continuous flow conditions, as in the CDC reactor, would better imitate the natural situation. Additionally, Buckingham–Meyer, Goeres, and Hamilton demonstrated that *Pseudomonas aeruginosa* and *Staphylococcus aureus* biofilms grown in a CDC reactor were more resistant to commonly used disinfectants than biofilms grown in static conditions [35]. They recommended this method as a model for the measurement of disinfectant efficacy. To date, *S. agalactiae* biofilms have been cultured only under static conditions on polystyrene plates or in a Calgary Biofilm Device [5], in which pegs are submerged in 96-well plates containing broth and can be exposed to shaking. In this

work, we undertook the first attempt to culture *S. agalactiae* biofilms under continuous flow conditions. Previously, biofilms of *Streptococcus pneumoniae* [36] and *Streptococcus mutans* [37] have been grown in a CDC reactor. *S. pneumoniae* biofilms have been grown on polycarbonate coupons in BHI broth supplemented with casein and yeast extract. The batch phase was set for 12 h, while the flow phase with 10% BHI broth with supplements was set for 24 h. For *S. mutans* biofilm culture, hydroxyapatite coupons were used, and 1% TSB was used in both phases. Both phases were also set for 24 h. In our protocol for *S. agalactiae* biofilm culture, we concluded that the use of polypropylene coupons and Schaedler broth leads to the growth of the highest number of bacteria. Both phases were set for 24 h, and in the flow phase, we used 20% Schaedler broth. Apart from the high number of bacterial cells, we also observed that in our model biofilms grew as mushroom-shaped microcolonies, which we previously described as indicative of biofilm maturity [38]. It was important for us to evaluate biofilm growth on different coupon materials because previous studies have shown that some surfaces allow for a better biofilm growth support i.e., Teflon for *Candida albicans* [39], zinc-galvanized steel for *Mycobacterium* sp. [40], or stainless steel for *Flavobacterium psychrophilum* [41]. Moreover, Dustin L. Williams et al. showed that change of coupon material from polycarbonate to collagen influences biofilm susceptibility to antibiotics, which can be an interesting direction for future biofilm model improvements [42]. Schaedler broth has a much richer composition than TSB. Schaedler has all the ingredients of TSB, but with a higher concentration of glucose (0.5% vs. 0.25%) which promotes biofilm growth of, i.e., *Staphylococcus aureus* and *Staphylococcus epidermidis* [43]; addition of animal tissue peptone which increases the content of available amino acids; addition of yeast extract which is necessary for biofilm growth of some bacteria, i.e., *Actinobacillus succinogenes* [44], but is also an additional source of vitamins; addition of cysteine, which is important for biofilm growth of i.e., *Streptococcus mutans* [45] and addition of haemin which is an iron source favoring more complex biofilm growth of i.e., *Actinobacillus actinomycetemcomitans* [46]. NYC is not as rich as Schaedler but has a richer composition than TSB. NYC, in comparison to TSB, has animal tissue peptone instead of tryptone (derived from casein) and soytone (derived from soya) but has additional yeast extract and the same glucose concentration as Schaedler broth. MRS also has a richer composition than TSB. A much higher concentration of glucose in MRS in comparison to TSB (2% vs 0.25%) may be the reason why biofilm growth is lower in MRS than in TSB. It was previously observed that high glucose concentration inhibits biofilm formation of, i.e., *Aeromonas hydrophila* [47].

Because of the high antibiotic resistance of biofilm-embedded cells, there is a tremendous demand for the evaluation of alternative approaches [5,31]. Against *S. agalactiae* biofilms, therapies based on human milk oligosaccharides [25,26], tea saponin [21], benzalkonium chloride [24], staphylococcal bacteriophage lysin CHAPk [32], or synthetic ellagic acid glycosides [29] have been proposed. Therapies based on the synergistic effect of antibiotics [34], synergistic effect of silver nanoparticles with eugenol [23], or silver nanoparticles with cinnamon oil [22] have also been proposed. We have previously summarized the use of photoinactivation against biofilms of ESKAPE pathogens [48], which cause numerous clinical infections. There have been few attempts of photoinactivation use against *S. agalactiae* planktonic culture [49–53]; however, there have been no reports of the use of photoinactivation against *S. agalactiae* biofilms. We are happy to report that Rose Bengal-mediated photoinactivation can be successfully used against *S. agalactiae* biofilms in both static and continuous flow models. As we expected, eradication of biofilm cultures requires the use of much higher concentrations of RB than planktonic culture. Additionally, biofilms grown in a continuous flow system require the use of higher RB concentrations than biofilms grown in static conditions, which confirms the success of biofilm culture optimization and new model introduction. The necessity of more rigorous photoinactivation conditions application for eradication of biofilm grown in Schaedler broth in comparison to NYC broth may result from the presence of L-cystine in Schaedler broth. L-cysteine is a reducing agent and plays role in the detoxification of hydrogen peroxide [54]. Nevertheless,

in our opinion presence of L-cysteine mimics a better vaginal environment, because it is present in healthy women's vaginas and is crucial for the growth of physiological flora, i.e., *Lactobacillus iners* [55]. Since RB-mediated aPDI is safe for human keratinocytes, it is a promising therapeutic approach against *S. agalactiae* biofilms, which should be investigated in-depth in the future.

4. Materials and Methods

4.1. Bacterial Strains and Culture Media

In this study, 4 strains of *Streptococcus agalactiae* were used (ATCC 27956 and 3 clinical strains: 1030/06, 2306/06, and 2974/07, representing serotypes IA, III, and V, respectively). The clinical strains were kindly provided by Izabela Sitkiewicz, National Medicines Institute, Warsaw, Poland). Columbia blood agar plates (Biomérieux, Craponne, France) were used for colony-forming unit (CFU) determination. Tryptic soy broth (TSB) (Biomérieux, Craponne, France) was used for overnight planktonic culture, and TSB, De Man, Rogosa and Sharpe (MRS) broth (BTL, Lodz, Poland), New York City III broth (NYC), and Schaedler (Oxoid, Basingstoke, UK) broth were used for biofilm culture. NYC broth was prepared on-site, containing HEPES (Sigma Aldrich, Saint Louis, MO, USA), proteose peptone (Sigma Aldrich, USA), yeast extract (Pol-Aura, Roznowo, Poland), sodium chloride (Stanlab, Lublin, Poland), and anhydrous glucose (Chempur, Piekary Slaskie, Poland).

4.2. Photosensitizing Agents

4,5,6,7-Tetrachloro-2',4',5',7'-tetraiodofluorescein disodium salt (Rose Bengal, RB) powder was purchased from Sigma (Sigma-Aldrich, Saint Louis, MO, USA). A stock solution (10 mM) was prepared in Millipore distilled water and kept in the dark at 4 °C.

4.3. Light Source

A custom constructed LED-based light source was used, which emitted λ_{max} 522 nm light with a radiosity of 10.6 mW/cm² (FWDH (full width half maximum): 34 nm) (Cezos, Gdynia, Poland).

4.4. Microtiter Plate Biofilm Culture

Biofilms were cultured on 96-well flat-bottom microtiter plates (Nest Biotechnology, Wuxi, Jiangsu, China). Four different broths (TSB, MRS, NYC, and Schaedler) were used in complete formula or diluted two times in double-distilled water. An overnight *S. agalactiae* culture was diluted 20 times in the appropriate broth (initial bacterial inoculum 10⁷ CFU/mL), and 200 μ L aliquots were transferred into plates in three technical repetitions. The negative control was broth without bacteria. The plate was covered with sealing tape and incubated at 37 °C for 4 h. Then, the medium was removed, replaced with 200 μ L of fresh appropriate broth, and incubated at 37 °C for 20 h. The experiment was conducted in three replicates.

4.5. Crystal Violet Staining

Biofilm cultures were washed three times with phosphate-buffered saline (PBS) (Sigma-Aldrich, Saint Louis, MO, USA) and fixed with 2% sodium acetate for 15 min. Then, the cells were stained with 0.1% crystal violet for 20 min and washed three times with distilled water. After drying, the precipitate was resolved in freshly prepared 33% acetic acid, and the absorbance at 570 nm was measured using an EnVision plate reader (Perkin Elmer, Waltham, MA, USA). The optical density of the samples (OD), which corresponds to the adhesion ability of the biofilm, was compared with the optical density of the negative control (ODc). The ODc was calculated as the mean of the negative control absorbance with the addition of three times the SD value. The following classification was used for the determination of biofilm production: nonadherent ($OD \leq ODc$), weakly adherent ($ODc < OD \leq 2 ODc$), moderately adherent ($2 ODc < OD \leq 4 ODc$), and strongly adherent ($4 ODc < OD$).

4.6. CDC Biofilm Reactor System Biofilm Culture

For biofilm culture, a CDC biofilm reactor model (BioSurface Technologies, Bozeman, MT, USA) was used. Coupons made of glass, polypropylene, polycarbonate, and porous polycarbonate were used. Before each culture, a whole setup was prepared as previously described [56]. Sterile broth (NYC or Schaedler) in the reactor was inoculated with 1 mL of 2.4 McFarland units (Densi-La-Meter II, ERBA Lachema, Brno, Czech Republic) adjusted overnight culture of *S. agalactiae*. The reactor was placed onto a magnetic stirrer with a heater set at 80 rpm and 37 °C for 24 h, which was the batch phase. Before starting the flow phase, 1 L of 4× concentrated sterile broth (NYC or Schaedler) was added to a 20 L carboy containing 19 L of distilled water autoclaved for 2 h at 14.7 psi. The final concentration of broth was five times lower than that recommended by the manufacturer. The carboy was connected to the reactor by silicone tubing and connected to a peristaltic pump (Watson–Marlow Fluid Technology Group, Falmouth, UK). The flow rate was set to 10.8 mL/min, and the reactor volume was 335 mL, which resulted in a residence time of 31 min, which was shorter than the *S. agalactiae* generation time. The time of the flow phase was set for 24 h. For CFU determination, the coupons were transferred to 15 mL Falcon tubes containing 10 mL of PBS. The coupons were sonicated for 1 min (Ulsonix, Proclean 3.0 DSP, Expando, Berlin, Germany), vortexed for 1 min and incubated on ice for 1 min. The whole procedure was repeated three times. Then, bacteria dispersed from the coupons were serially diluted in PBS and transferred onto Columbia blood agar plates. After 18 h of incubation at 37 °C, colonies were enumerated, and CFU/mL values were determined. The experiment was conducted in three replicates.

4.7. Biofilm Visualization

Biofilm growth on coupons was visualized using confocal microscopy. Visualization of biofilms was performed with SYBR Green staining. Coupons were washed in PBS and transferred to a 12-well glass-bottom plate containing 500 µL of PBS and incubated in the presence of 2 µL of 100× concentrated SYBR Green for 15 min in the dark at RT. Specimens were imaged using a confocal laser scanning microscope (Leica SP8X) with a 10× lens (Leica Biosystems, Nussloch, Germany). During observation, the excitation wavelength was 488 nm, and the emission wavelength range used for detecting SYBR Green was 501–548 nm. Photographs were obtained and then analyzed with Leica LAS X software.

4.8. Photodynamic Inactivation of Planktonic Cultures

An overnight culture (1 colony transferred into 5 mL of TSB and incubated for 18 h at 37 °C with shaking at 150 rpm) of *S. agalactiae* was adjusted to 2.4 McFarland units in PBS, which corresponds to a cell density of approx. 10⁸ CFU/mL. Working solutions of RB were prepared in Millipore distilled water. A total of 180 µL of bacterial suspension and 20 µL of photosensitizer solution were mixed in Eppendorf tubes and incubated in the dark at 37 °C for 15 min. Then, the samples were washed twice, centrifuged (10,000× *g*, 3 min), and resuspended in PBS. Aliquots of 100 µL of each sample were transferred into a 96-well plate (Nest Biotechnology, Wuxi, Jiangsu, China) and illuminated with a 522 nm LED lamp for 6 min (3.8 J/cm²). Afterward, samples were serially diluted in PBS and transferred onto Columbia blood agar plates. After 18 h of incubation at 37 °C, the colonies were counted, and CFU/mL values were determined. The experiment was conducted in three replicates.

4.9. Photo- and Cytotoxicity Assays Based on MTT

Photo- and cytotoxicity assays were previously described [57]. Briefly, HaCaT cells (CLS 300493) were seeded the day before treatment in three biological replicates for each condition in two 96-well plates (for light and dark conditions). The cells were grown in a humidified incubator at 37 °C and in a 5% CO₂ atmosphere in supplemented high-glucose DMEM (Life Technologies/Thermo Fisher Scientific, Waltham, MA, USA). RB was added directly to the medium and incubated for 15 min at 37 °C. Then, the cells were washed twice with PBS, and 100 µL of fresh medium was added. Next, the cells were illuminated

with a 522 nm LED lamp for 6 min (3.8 J/cm²). Cell survival was measured after 24 h of incubation at 37 °C by an MTT [3-(4,5-dimethylthiazol-2-yl)-2,5-diphenyltetrazolium bromide] assay. Briefly, 10 µL of an MTT solution (12 mM) was applied to each well and incubated for 4 h at 37 °C. The cells were then lysed in DMSO (Sigma-Aldrich, Saint Louis, MO, USA), and the absorbance of the formazan was measured at 550 nm using an EnVision plate reader (Perkin Elmer, Waltham, MA, USA).

4.10. Photodynamic Inactivation of Microtiter Plate Biofilm Cultures

Biofilms cultured in NYC or Schaedler broth were washed with PBS and then incubated with different RB concentrations in PBS in the dark at 37 °C for 15 min. Then, the biofilms were washed twice with PBS and illuminated for 6 min. After illumination, the biofilms were dispersed by scraping with a pipette tip and thorough pipetting. Afterward, samples were serially diluted in PBS and transferred onto Columbia blood agar plates. After 18 h of incubation at 37 °C, the colonies were counted, and CFU/mL values were determined. The experiment was conducted in three replicates.

4.11. Photodynamic Inactivation of CDC Biofilm Reactor System Biofilm Culture

Coupons were washed in PBS and transferred to a 12-well plate containing 1.5 mL of PBS with/without RB and incubated in the dark for 15 min at 37 °C. Then, the coupons were transferred to another 12-well plate containing 1.5 mL of PBS and illuminated on both sides for 6 min on each side. Then, the coupons were transferred to 15 mL Falcon tubes containing 10 mL of PBS. The coupons were sonicated for 1 min, vortexed for 1 min, and incubated on ice for 1 min. The whole procedure was repeated three times. Then, bacteria dispersed from the coupons were serially diluted in PBS and transferred onto Columbia blood agar plates. After 18 h of incubation at 37 °C, colonies were enumerated, and CFU/mL values were determined. The experiment was conducted in three replicates.

4.12. Statistical Analysis

The statistical analyses were performed using Excel. The quantitative variables were characterized by the arithmetic mean of standard deviation. Statistical significance of differences between two groups was processed with the Student's *t*-test. In all calculations, a statistical significance level of $p < 0.05$ was used.

5. Conclusions

Streptococcus agalactiae biofilm formation depends on the used medium and surface material. We believe that a continuous flow biofilm model is a better representation of the vaginal environment than a static biofilm model and we recommend the application of this model in future antibacterial studies. This model was successfully applied in photoinactivation studies and allowed to show its effectiveness. RB-mediated photoinactivation is effective in the eradication of both planktonic and biofilm cultures of *S. agalactiae*. It is also safe for human keratinocytes which makes it a promising antimicrobial therapy.

Author Contributions: Conceptualization, M.G.; methodology, M.K.P., M.R. and M.G.; software, M.R.; validation, M.K.P., M.R. and M.G.; formal analysis, M.K.P.; investigation, M.K.P. and M.R.; resources, M.G.; data curation, M.K.P., M.R. and M.G.; writing—original draft preparation, M.K.P.; writing—review and editing, M.G.; visualization, M.R.; supervision, M.G.; project administration, M.G.; funding acquisition, M.G. All authors have read and agreed to the published version of the manuscript.

Funding: This research was funded by the National Science Centre, grant number 2016/23/B/NZ7/03236. Biofilm visualization was supported by the National Science Centre, grant number 2018/30/Q/NZ7/00281.

Institutional Review Board Statement: Not applicable.

Informed Consent Statement: Not applicable.

Data Availability Statement: The datasets generated and/or analyzed during the current study are available from the corresponding author on reasonable request.

Acknowledgments: Clinical strains of *S. agalactiae* were kindly provided by Izabela Sitkiewicz, (National Medicines Institute, Warsaw, Poland).

Conflicts of Interest: The authors declare no conflict of interest.

References

1. Shet, A.; Ferrieri, P. Neonatal & maternal group B streptococcal infections: A comprehensive review. *Indian J. Med. Res.* **2004**, *120*, 141–150.
2. Kaminska, D.; Ratajczak, M.; Szumała-Kąkol, A.; Długaszewska, J.; Nowak-Malczewska, D.M.; Gajecka, M. Increasing resistance and changes in distribution of serotypes of *Streptococcus agalactiae* in Poland. *Pathogens* **2020**, *9*, 526. [[CrossRef](#)] [[PubMed](#)]
3. Ulett, K.B.; Benjamin, W.H.; Zhuo, F.; Xiao, M.; Kong, F.; Gilbert, G.L.; Schembri, M.A.; Ulett, G.C. Diversity of group B streptococcus serotypes causing urinary tract infection in adults. *J. Clin. Microbiol.* **2009**, *47*, 2055–2060. [[CrossRef](#)]
4. Muzny, C.A.; Schwebke, J.R. Biofilms: An Underappreciated Mechanism of Treatment Failure and Recurrence in Vaginal Infections. *Clin. Infect. Dis.* **2015**, *61*, 601–606. [[CrossRef](#)]
5. Olson, M.E.; Ceri, H.; Morck, D.W.; Buret, A.G.; Read, R.R. Biofilm bacteria: Formation and comparative susceptibility to antibiotics. *Can. J. Vet. Res.* **2002**, *66*, 86–92. [[PubMed](#)]
6. D'Urzo, N.; Martinelli, M.; Pezzicoli, A.; De Cesare, V.; Pinto, V.; Margarit, I.; Telford, J.L.; Maione, D.; Melin, P.; Decheva, A.; et al. Acidic pH strongly enhances in vitro biofilm formation by a subset of hypervirulent ST-17 *Streptococcus agalactiae* strains. *Appl. Environ. Microbiol.* **2014**, *80*, 2176–2185. [[CrossRef](#)] [[PubMed](#)]
7. Borges, S.; Silva, J.; Teixeira, P. Survival and biofilm formation by Group B streptococci in simulated vaginal fluid at different pHs. *Antonie Van Leeuwenhoek* **2012**, *101*, 677–682. [[CrossRef](#)]
8. Bonsaglia, E.C.R.; Latosinski, G.S.; Rossi, R.S.; Rossi, B.F.; Possebon, F.S.; Pantoja, J.C.F.; Fernandes Júnior, A.; Rall, V.L.M. Biofilm production under different atmospheres and growth media by *Streptococcus agalactiae* isolated from milk of cows with subclinical mastitis. *Arch. Microbiol.* **2020**, *202*, 209–212. [[CrossRef](#)]
9. Hinderfeld, A.S.; Simoes-Barbosa, A. Vaginal dysbiotic bacteria act as pathobionts of the protozoal pathogen *Trichomonas vaginalis*. *Microb. Pathog.* **2020**, *138*, 103820. [[CrossRef](#)]
10. Rosca, A.S.; Castro, J.; Cerca, N. Evaluation of different culture media to support in vitro growth and biofilm formation of bacterial vaginosis-associated anaerobes. *PeerJ* **2020**, *8*, e9917. [[CrossRef](#)]
11. Thellin, O.; Zorzi, W.; Zorzi, D.; Delvenne, P.; Heinen, E.; Elmoualij, B.; Quatresooz, P. Lysozyme as a cotreatment during antibiotics use against vaginal infections: An in vitro study on *Gardnerella vaginalis* biofilm models. *Int. Microbiol.* **2016**, *19*, 101–107. [[CrossRef](#)] [[PubMed](#)]
12. Martinez, S.; Garcia, J.G.; Williams, R.; Elmassry, M.; West, A.; Hamood, A.; Hurtado, D.; Gudenkauf, B.; Ventolini, G.; Schlabritz-Loutsevitch, N.; et al. *Lactobacilli* spp.: Real-time evaluation of biofilm growth. *BMC Microbiol.* **2020**, *20*, 1–9. [[CrossRef](#)] [[PubMed](#)]
13. Clabaut, M.; Suet, A.; Racine, P.J.; Tahrioui, A.; Verdon, J.; Barreau, M.; Maillot, O.; Le Tirant, A.; Karsybayeva, M.; Kremser, C.; et al. Effect of 17 β -estradiol on a human vaginal *Lactobacillus crispatus* strain. *Sci. Rep.* **2021**, *11*, 1–16. [[CrossRef](#)]
14. Machado, A.; Jefferson, K.K.; Cerca, N. Interactions between *Lactobacillus crispatus* and bacterial vaginosis (BV)-associated bacterial species in initial attachment and biofilm formation. *Int. J. Mol. Sci.* **2013**, *14*, 12004–12012. [[CrossRef](#)]
15. Rapacka-Zdończyk, A.; Woźniak, A.; Michalska, K.; Pierański, M.; Ogonowska, P.; Grinholc, M.; Nakonieczna, J. Factors Determining the Susceptibility of Bacteria to Antibacterial Photodynamic Inactivation. *Front. Med.* **2021**, *8*, 617. [[CrossRef](#)]
16. Pérez-Laguna, V.; García-Luque, I.; Ballesta, S.; Pérez-Artiaga, L.; Lampaya-Pérez, V.; Samper, S.; Soria-Lozano, P.; Rezusta, A.; Gilaberte, Y. Antimicrobial photodynamic activity of Rose Bengal, alone or in combination with Gentamicin, against planktonic and biofilm *Staphylococcus aureus*. *Photodiagn. Photodyn. Ther.* **2018**, *21*, 211–216. [[CrossRef](#)] [[PubMed](#)]
17. Silva, A.F.; Borges, A.; Freitas, C.F.; Hioka, N.; Mikcha, J.M.G.; Simões, M. Antimicrobial Photodynamic Inactivation Mediated by Rose Bengal and Erythrosine Is Effective in the Control of Food-Related Bacteria in Planktonic and Biofilm States. *Molecules* **2018**, *23*, 2288. [[CrossRef](#)]
18. Neckers, D.C. Rose Bengal. *J. Photochem. Photobiol. A Chem.* **1989**, *47*, 1–29. [[CrossRef](#)]
19. Dubey, T.; Gorantla, N.V.; Chandrashekhara, K.T.; Chinnathambi, S. Photodynamic exposure of Rose-Bengal inhibits Tau aggregation and modulates cytoskeletal network in neuronal cells. *Sci. Rep.* **2020**, *10*, 1–16. [[CrossRef](#)]
20. Pieranski, M.; Sitkiewicz, I.; Grinholc, M. Increased photoinactivation stress tolerance of *Streptococcus agalactiae* upon consecutive sublethal phototreatments. *Free Radic. Biol. Med.* **2020**, *160*, 657–669. [[CrossRef](#)]
21. Shang, F.; Wang, H.; Xue, T. Anti-biofilm effect of tea saponin on a *Streptococcus agalactiae* strain isolated from bovine mastitis. *Animals* **2020**, *10*, 1713. [[CrossRef](#)] [[PubMed](#)]
22. Abd El-Aziz, N.K.; Ammar, A.M.; El-Naenaey, E.; Sayed, Y.M.; El Damaty, H.M.; Elazazy, A.A.; Hefny, A.A.; Shaker, A.; Eldesoukey, I.E. Antimicrobial and antibiofilm potentials of cinnamon oil and silver nanoparticles against *Streptococcus agalactiae* isolated from bovine mastitis: New avenues for countering resistance. *BMC Vet. Res.* **2021**, *17*, 1–14. [[CrossRef](#)]

23. Perugini Biasi-Garbin, R.; Saori Otaguiri, E.; Morey, A.T.; Fernandes Da Silva, M.; Belotto Morguette, A.E.; Armando Contreras Lancheros, C.; Kian, D.; Perugini, M.R.E.; Nakazato, G.; Durán, N.; et al. Effect of eugenol against streptococcus agalactiae and synergistic interaction with biologically produced silver nanoparticles. *Evid.-Based Complement. Altern. Med.* **2015**, *2015*, 861497. [[CrossRef](#)] [[PubMed](#)]
24. Ebrahimi, A.; Hemati, M.; Shabanpour, Z.; Habibian Dehkordi, S.; Bahadoran, S.; Lotalian, S.; Khoibani, S. Effects of Benzalkonium Chloride on Planktonic Growth and Biofilm Formation by Animal Bacterial Pathogens. *Jundishapur J. Microbiol.* **2015**, *8*, e16058. [[CrossRef](#)] [[PubMed](#)]
25. Craft, K.M.; Townsend, S.D. 1-Amino-2'-fucosyllactose inhibits biofilm formation by *Streptococcus agalactiae*. *J. Antibiot. (Tokyo)* **2019**, *72*, 507–512. [[CrossRef](#)] [[PubMed](#)]
26. Ackerman, D.L.; Craft, K.M.; Doster, R.S.; Weitkamp, J.H.; Aronoff, D.M.; Gaddy, J.A.; Townsend, S.D. Antimicrobial and Antibiofilm Activity of Human Milk Oligosaccharides against *Streptococcus agalactiae*, *Staphylococcus aureus*, and *Acinetobacter baumannii*. *ACS Infect. Dis.* **2018**, *4*, 315–324. [[CrossRef](#)]
27. Silvestre, I.; Borrego, M.J.; Jordão, L. Biofilm formation by ST17 and ST19 strains of *Streptococcus agalactiae*. *Res. Microbiol.* **2020**, *171*, 311–318. [[CrossRef](#)]
28. Miranda, P.S.D.; Lannes-Costa, P.S.; Pimentel, B.A.S.; Silva, L.G.; Ferreira-Carvalho, B.T.; Menezes, G.C.; Mattos-Guaraldi, A.L.; Hirata, R.; Mota, R.A.; Nagao, P.E. Biofilm formation on different pH conditions by *Streptococcus agalactiae* isolated from bovine mastitic milk. *Lett. Appl. Microbiol.* **2018**, *67*, 235–243. [[CrossRef](#)] [[PubMed](#)]
29. Chambers, S.A.; Gaddy, J.A.; Townsend, S.D. Synthetic Ellagic Acid Glycosides Inhibit Early Stage Adhesion of *Streptococcus agalactiae* Biofilms as Observed by Scanning Electron Microscopy. *Chem.-A Eur. J.* **2020**, *26*, 9923–9928. [[CrossRef](#)]
30. Yang, Q.; Porter, A.J.; Zhang, M.; Harrington, D.J.; Black, G.W.; Sutcliffe, I.C. The impact of pH and nutrient stress on the growth and survival of streptococcus agalactiae. *Antonie Van Leeuwenhoek.* **2012**, *102*, 277–287. [[CrossRef](#)]
31. Boonyayatra, S.; Pata, P. Antimicrobial Resistance of Biofilm-Forming *Streptococcus agalactiae* Isolated from Bovine Mastitis. *J. Vet. Sci. Technol.* **2016**, *7*, 374. [[CrossRef](#)]
32. Shan, Y.; Yang, N.; Teng, D.; Wang, X.; Mao, R.; Hao, Y.; Ma, X.; Fan, H.; Wang, J. Recombinant of the staphylococcal bacteriophage lysin CHAPk and its elimination against streptococcus agalactiae biofilms. *Microorganisms* **2020**, *8*, 216. [[CrossRef](#)]
33. Butini, M.E.; Cabric, S.; Trampuz, A.; Di Luca, M. In vitro anti-biofilm activity of a biphasic gentamicin-loaded calcium sulfate/hydroxyapatite bone graft substitute. *Colloids Surf. B Biointerfaces* **2018**, *161*, 252–260. [[CrossRef](#)] [[PubMed](#)]
34. Moreno, M.G.; Trampuz, A.; Di Luca, M. Synergistic antibiotic activity against planktonic and biofilmembedded *Streptococcus agalactiae*, *Streptococcus pyogenes* and *Streptococcus oralis*. *J. Antimicrob. Chemother.* **2017**, *72*, 3085–3092. [[CrossRef](#)] [[PubMed](#)]
35. Buckingham-Meyer, K.; Goeres, D.M.; Hamilton, M.A. Comparative evaluation of biofilm disinfectant efficacy tests. *J. Microbiol. Methods* **2007**, *70*, 236–244. [[CrossRef](#)]
36. Trappetti, C.; Gualdi, L.; Di Meola, L.; Jain, P.; Korir, C.C.; Edmonds, P.; Iannelli, F.; Ricci, S.; Pozzi, G.; Oggioni, M.R. The impact of the competence quorum sensing system on *Streptococcus pneumoniae* biofilms varies depending on the experimental model. *BMC Microbiol.* **2011**, *11*, 236–244. [[CrossRef](#)] [[PubMed](#)]
37. Pérez-Díaz, M.A.; Boegli, L.; James, G.; Velasquillo, C.; Sánchez-Sánchez, R.; Martínez-Martínez, R.E.; Martínez-Castañón, G.A.; Martínez-Gutierrez, F. Silver nanoparticles with antimicrobial activities against *Streptococcus mutans* and their cytotoxic effect. *Mater. Sci. Eng. C* **2015**, *55*, 360–366. [[CrossRef](#)]
38. Taraszkievicz, A.; Fila, G.; Grinholc, M.; Nakonieczna, J. Innovative strategies to overcome biofilm resistance. *Biomed. Res. Int.* **2013**, *2013*, 150653. [[CrossRef](#)]
39. Frade, J.P.; Arthington-Skaggs, B.A. Effect of serum and surface characteristics on *Candida albicans* biofilm formation. *Mycoses* **2011**, *54*, e154–e162. [[CrossRef](#)] [[PubMed](#)]
40. Mullis, S.N.; Falkinham, J.O. Adherence and biofilm formation of *Mycobacterium avium*, *Mycobacterium intracellulare* and *Mycobacterium abscessus* to household plumbing materials. *J. Appl. Microbiol.* **2013**, *115*, 908–914. [[CrossRef](#)]
41. Vidal, J.M.; Miranda, C.D.; De la Fuente, M.; Alarcón, M.; Aroca, G.; Sossa, K.; Ruiz, P.; Urrutia, H. Formation of biofilms of the salmon pathogen *Flavobacterium psychrophilum* in different surfaces using the CDC biofilm reactor. *Aquaculture* **2020**, *514*, 734459. [[CrossRef](#)]
42. Williams, D.L.; Smith, S.R.; Peterson, B.R.; Allyn, G.; Cadenas, L.; Epperson, R.T.; Looper, R.E. Growth substrate may influence biofilm susceptibility to antibiotics. *PLoS ONE* **2019**, *14*, e0206774. [[CrossRef](#)]
43. Waldrop, R.; McLaren, A.; Calara, F.; McLemore, R. Biofilm Growth Has a Threshold Response to Glucose In Vitro. *Clin. Orthop. Relat. Res.* **2014**, *472*, 3305–3310. [[CrossRef](#)] [[PubMed](#)]
44. Urbance, S.E.; Pometto, A.L., III; DiSpirito, A.A.; Demirci, A. Medium Evaluation and Plastic Composite Support Ingredient Selection for Biofilm Formation and Succinic Acid Production by *Actinobacillus succinogenes*. *Food Biotechnol.* **2003**, *17*, 53–65. [[CrossRef](#)]
45. Kim, J.; Senadheera, D.B.; Lévesque, C.M.; Cvitkovitch, D.G. TcyR regulates l-cystine uptake via the TcyABC transporter in *Streptococcus mutans*. *FEMS Microbiol. Lett.* **2012**, *328*, 114–121. [[CrossRef](#)]
46. Rhodes, E.R.; Shoemaker, C.J.; Menke, S.M.; Edelmann, R.E.; Actis, L.A. Evaluation of different iron sources and their influence in biofilm formation by the dental pathogen *Actinobacillus actinomycetemcomitans*. *J. Med. Microbiol.* **2007**, *56*, 119–128. [[CrossRef](#)] [[PubMed](#)]

47. Jahid, I.K.; Lee, N.-Y.; Kim, A.; Ha, S.-D. Influence of Glucose Concentrations on Biofilm Formation, Motility, Exoprotease Production, and Quorum Sensing in *Aeromonas hydrophila*. *J. Food Prot.* **2013**, *76*, 239–247. [[CrossRef](#)] [[PubMed](#)]
48. Nakonieczna, J.; Wozniak, A.; Pieranski, M.; Rapacka-Zdonczyk, A.; Ogonowska, P.; Grinholc, M. Photoinactivation of ESKAPE pathogens: Overview of novel therapeutic strategy. *Future Med. Chem.* **2019**, *11*, 443–461. [[CrossRef](#)] [[PubMed](#)]
49. Matějka, Z.; Adámková, V.; Šmucler, R.; Svobodová, J.; Hubálková, H. Photodynamic therapy (PDT) for disinfection of oral wounds. In vitro study. *Open Med.* **2012**, *7*, 118–123. [[CrossRef](#)]
50. Sellera, F.P.; Sabino, C.P.; Ribeiro, M.S.; Gargano, R.G.; Benites, N.R.; Melville, P.A.; Pogliani, F.C. In vitro photoinactivation of bovine mastitis related pathogens. *Photodiagn. Photodyn. Ther.* **2016**, *13*, 276–281. [[CrossRef](#)]
51. Yi, M.; Wang, H.; Wang, M.; Cao, J.; Gao, F.; Ke, X.; Liu, Z.; Liu, Y.; Lu, M. Efficient Inhibition of *Streptococcus agalactiae* by AI-Egen-Based Fluorescent Nanomaterials. *Front. Chem.* **2021**, *9*, 715565. [[CrossRef](#)] [[PubMed](#)]
52. Bumah, V.V.; Morrow, B.N.; Cortez, P.M.; Bowman, C.R.; Rojas, P.; Masson-Meyers, D.S.; Suprpto, J.; Tong, W.G.; Enwemeka, C.S. The importance of porphyrins in blue light suppression of *Streptococcus agalactiae*. *J. Photochem. Photobiol. B Biol.* **2020**, *212*, 111996. [[CrossRef](#)] [[PubMed](#)]
53. Bumah, V.V.; Cortez, P.M.; Morrow, B.N.; Rojas, P.; Bowman, C.R.; Masson-Meyers, D.S.; Enwemeka, C.S. Blue light absorbing pigment in *Streptococcus agalactiae* does not potentiate the antimicrobial effect of pulsed 450 nm light. *J. Photochem. Photobiol. B Biol.* **2021**, *216*, 112149. [[CrossRef](#)]
54. Ohtsu, I.; Kawano, Y.; Suzuki, M.; Morigasaki, S.; Saiki, K.; Yamazaki, S.; Nonaka, G.; Takagi, H. Uptake of L-cystine via an ABC transporter contributes defense of oxidative stress in the L-cystine export-dependent manner in *Escherichia coli*. *PLoS ONE* **2015**, *10*, e0120619. [[CrossRef](#)]
55. Bloom, S.M.; Mafunda, N.A.; Woolston, B.M.; Hayward, M.R.; Frempong, J.F.; Abai, A.B.; Xu, J.; Mitchell, A.J.; Westergaard, X.; Hussain, F.A.; et al. Cysteine dependence in *Lactobacillus iners* constitutes a novel therapeutic target to modify the vaginal microbiota. *bioRxiv* **2021**. [[CrossRef](#)]
56. Woźniak, A.; Kruszewska, B.; Pierański, M.K.; Rychłowski, M.; Grinholc, M. Antimicrobial Photodynamic Inactivation Affects the Antibiotic Susceptibility of *Enterococcus* spp. Clinical Isolates in Biofilm and Planktonic Cultures. *Biomolecules* **2021**, *11*, 693. [[CrossRef](#)]
57. Nakonieczna, J.; Wolnikowska, K.; Ogonowska, P.; Neubauer, D.; Bernat, A.; Kamysz, W. Rose Bengal-Mediated Photoinactivation of Multidrug Resistant *Pseudomonas aeruginosa* Is Enhanced in the Presence of Antimicrobial Peptides. *Front. Microbiol.* **2018**, *9*, 1949. [[CrossRef](#)]

Chapter V

Antimicrobial photodynamic inactivation: an alternative for Group B *Streptococcus* vaginal colonization in a murine experimental model

1. Summary of the publication

While thousands of publications report the antimicrobial effectiveness of different ROS-based therapies against planktonic cultures, there are much less reporting effectiveness against biofilm culture and even less reporting effectiveness *in vivo*. Implementation of animal models during an investigation of new therapeutic approaches seems to irreplaceable.

In this publication, the effectiveness of RB-mediated aPDI was presented in both planktonic and biofilm models. Besides, the effect on human vaginal flora *Lactobacilli* was evaluated and it was the very first report of a multispecies biofilm with *S. agalactiae* included in the composition. Safety of aPDI was assessed with the use of a commonly used line of human immortalized keratinocytes, but also a human vaginal epithelial cell line. Moreover, the mutagenicity of aPDI was assessed in both prokaryotic and eukaryotic models. In *in vivo* experiments mice colonized with *S. agalactiae* were treated with aPDI and then its impact on GBS and other bacterial species was assessed with the use of both microbiological and bioinformatical methods. Finally, histopathological analysis was performed. RB-mediated aPDI was proven to be effective against *S. agalactiae* and its impact on vaginal tissue was not significant.

In this publication with the use of 7 different *S. agalactiae* strains Aim 1. was finally reached. In *in vitro* part of the experiments Aims 2., 4. and 5. were reached as well. At last with the use of the murine model Aims 7., 8. and 9. were also achieved.

2. Publication



Article

Antimicrobial Photodynamic Inactivation: An Alternative for Group B *Streptococcus* Vaginal Colonization in a Murine Experimental Model

Michał K. Pierański ^{1,*} , Jan G. Kosiński ² , Klaudia Szymczak ¹ , Piotr Sadowski ³
and Mariusz Grinholc ^{1,*}

¹ Laboratory of Photobiology and Molecular Diagnostics, Intercollegiate Faculty of Biotechnology University of Gdańsk and Medical University of Gdańsk, University of Gdańsk, 80-307 Gdańsk, Poland

² Department of Computational Biology, Institute of Molecular Biology and Biotechnology, Faculty of Biology, Adam Mickiewicz University in Poznań, 61-712 Poznań, Poland

³ Department of Pathomorphology, University Hospital in Kraków, 31-501 Kraków, Poland

* Correspondence: michal.pieranski@phdstud.ug.edu.pl (M.K.P.); mariusz.grinholc@biotech.ug.edu.pl (M.G.)

Abstract: Background: *Streptococcus agalactiae*, referred to as Group B *Streptococcus* (GBS), is a prominent bacterium causing life-threatening neonatal infections. Although antibiotics are efficient against GBS, growing antibiotic resistance forces the search for alternative treatments and/or prevention approaches. Antimicrobial photodynamic inactivation (aPDI) appears to be a potent alternative non-antibiotic strategy against GBS. Methods: The effect of rose bengal aPDI on various GBS serotypes, *Lactobacillus* species, human eukaryotic cell lines and microbial vaginal flora composition was evaluated. Results: RB-mediated aPDI was evidenced to exert high bactericidal efficacy towards *S. agalactiae* in vitro (>4 log₁₀ units of viability reduction for planktonic and >2 log₁₀ units for multispecies biofilm culture) and in vivo (ca. 2 log₁₀ units of viability reduction in mice vaginal GBS colonization model) in microbiological and metagenomic analyses. At the same time, RB-mediated aPDI was evidenced to be not mutagenic and safe for human vaginal cells, as well as capable of maintaining the balance and viability of vaginal microbial flora. Conclusions: aPDI can efficiently kill GBS and serve as an alternative approach against GBS vaginal colonization and/or infections.

Keywords: *Streptococcus agalactiae*; biofilm; murine model; photoinactivation; rose bengal; vaginal microbiome; metagenomics



Citation: Pierański, M.K.; Kosiński, J.G.; Szymczak, K.; Sadowski, P.; Grinholc, M. Antimicrobial Photodynamic Inactivation: An Alternative for Group B *Streptococcus* Vaginal Colonization in a Murine Experimental Model. *Antioxidants* **2023**, *12*, 847. <https://doi.org/10.3390/antiox12040847>

Academic Editor: Alessandra Napolitano

Received: 25 February 2023

Revised: 24 March 2023

Accepted: 30 March 2023

Published: 1 April 2023



Copyright: © 2023 by the authors. Licensee MDPI, Basel, Switzerland. This article is an open access article distributed under the terms and conditions of the Creative Commons Attribution (CC BY) license (<https://creativecommons.org/licenses/by/4.0/>).

1. Introduction

Group B *Streptococcus* (GBS) is the leading cause of invasive infections among neonates and accounts (together with *Escherichia coli*) for at least 60% of all deaths from neonatal bacterial meningitis [1]. It is a Gram-positive, commensal organism of adult humans' genitourinary and gastrointestinal tracts, which asymptotically colonizes the vaginal tract of 15–40% of pregnant women [1]. The most common cause of neonatal GBS disease is maternal colonization with *Streptococcus agalactiae* and its transmission to the fetus and newborns, leading to pneumonia, septicemia and meningitis [2]. The current prevention strategy is intrapartum antibiotic prophylaxis (IAP), applicable for pregnant women at risk of GBS transmission to newborns, which substantially reduces incidences of pneumonia and septicemia; however, the emergence of GBS meningitis, though stable over the past two decades, appears to increase [3,4]. Still, morbidity rates resulting from GBS infection remain unacceptably high, and up to 50% of surviving infants suffer from neurodevelopmental impairment [5]. Moreover, current antibiotic prophylaxis may be characterized by many shortcomings, especially in the case of women who deliver before being screened for GBS colonization and do not comply with the indications regarding the rules for taking or dosing the antibiotic, do not complete antibiotic therapy or are allergic to antibiotics. Obviously,

the development of antibiotic resistance is the next important issue. Penicillin-tolerant strains of GBS have been already identified, and resistance to other antibiotics has also been demonstrated [2]. Without alternative prevention strategies, IAP using first-line antibiotics would likely become useless. The issues mentioned above indicate the urgent need for new preventive and/or therapeutic strategies.

Antimicrobial photodynamic inactivation (aPDI) has recently gained increasing importance as a novel, non-antibiotic method targeting a wide variety of both Gram-positive and Gram-negative microbes [6–10]. In principle, the photochemical mechanism of aPDI is based on the excitation of a photosensitive compound by the light of a proper wavelength, resulting in the production of reactive oxygen species (ROS), which lead to damage to the cellular structures that are fundamental to the survival of microorganisms. The formation of singlet oxygen as the most important cytotoxic molecule leads to the oxidation of lipids, proteins and nucleic acids, which results in cell death [11]. In addition to singlet oxygen, other ROS, i.e., hydroxyl radicals, hydrogen peroxide and superoxide anions, were also demonstrated to be formed upon aPDI and to exert bactericidal effects [12]. The most crucial advantage of aPDI that needs to be highlighted is the fact that its bactericidal efficacy is not affected by the antibiotic resistance of the targeted microorganisms. Moreover, no aPDI-resistant microorganisms have been reported [13–15].

One of the most important advantages of rose bengal (RB), which was used in this study as a photosensitizer, is its water solubility and low cost. RB is a type II photosensitizer, which means that it can transfer energy directly to ground-state molecular oxygen, which results in the formation of singlet oxygen. RB singlet oxygen quantum yields range between 0.6 and 0.8 [16]. It has both photosensitive and sono-sensitive properties. RB is already approved by FDA as a vital stain to assess the ocular surface. RB was previously reported to be useful in photochemical tissue bonding, photodynamic inactivation (antimicrobial and anticancer), photothrombotic animal models and other applications [17–20].

In the view of the above data and the antimicrobial properties of aPDI, the current study aimed to assess photodynamic inactivation as an alternative for GBS vaginal colonization. Here, we present an in vitro (planktonic and biofilm culture), in vivo and bioinformatic study demonstrating the high bactericidal efficacy of aPDI towards *S. agalactiae*. The applied treatment was evidenced to be non-mutagenic and safe for human vaginal cells, while also leading to the maintenance of the balance and vitality of vaginal microbial flora.

2. Materials and Methods

2.1. Bacterial Strains and Culture Media

In this study, 7 strains of *Streptococcus agalactiae* were used, including ATCC 27956 and 6 clinical strains, namely 1030/06, 1029/06, 2306/06, 1153/07, 2974/07 and 3301/08, representing serotypes IA, IB, III, IV, V and IX, respectively. Izabela Sitkiewicz, Translational Medicine Center, Warsaw University of Life Sciences, Warsaw, Poland kindly provided the clinical strains. Additionally, 3 *Lactobacillus* species were included in the analysis, specifically *L. gasseri* LMG13134, *L. crispatus* LMG 12005 and *L. jensenii* LMG 06414, which were purchased from BCCM/LMG. Columbia blood agar plates (GRASO, Starogard Gdanski, Poland) were used for colony-forming unit (CFU) determination. Tryptic soy broth (TSB) (Biomerieux, Craaponne, France) was used for overnight planktonic culture of *S. agalactiae* and Schaedler broth (Oxoid, Basingstoke, UK) with a 10% addition of horse serum (Sigma Aldrich, Saint Louis, MO, USA) for *Lactobacilli*.

2.2. Photosensitizing Agents

4,5,6,7-Tetrachloro-20-,40-,50-,70- tetraiodofluorescein disodium salt (Rose Bengal, RB) powder was purchased from Sigma (Sigma-Aldrich, Saint Louis, MO, USA). A stock solution (10 mM) was prepared in Millipore distilled water and kept in the dark at 4 °C.

2.3. Light Sources

For in vitro studies, a custom-constructed LED-based light source was used, which emitted λ_{\max} 522 nm light with a radiosity of 10.6 mW/cm² (FWHM (full-width half-maximum): 34 nm) (Cezos, Gdynia, Poland). For in vivo studies, a custom-constructed LED-based light source, coupled with a spherical light distributor, model SD200 (Medlight S.A., Écublens, Switzerland), was used. This light source emitted λ_{\max} 555 nm light with a radiosity of 77.2 mW/cm² at the output and a radiosity of 1.8 mW/cm² with a spherical light distribution (FWHM (full-width half-maximum): 50 nm) (Cezos, Gdynia, Poland).

2.4. Photodynamic Inactivation of Planktonic Cultures

Photodynamic inactivation protocol was previously described [21]. In short, overnight cultures of *S. agalactiae* or *Lactobacilli* were adjusted to 2.4 or 2.0 McFarland units, respectively, which corresponds to a cell density of approx. 10⁸ CFU/mL. Bacterial suspensions were mixed with the photosensitizer solution and incubated in the dark at 37 °C for 15 min. Then, samples were washed and resuspended in PBS. Aliquots of 100 µL of each sample were transferred into a 96-well plate and illuminated with a 522 nm LED lamp for 6 min (3.8 J/cm²). Afterward, samples were serially diluted in PBS and transferred to Columbia blood agar plates. After 18 h of incubation at 37 °C, the colonies were counted, and CFU/mL values were determined. The experiment was conducted in three replicates.

2.5. Microtiter Plate Multispecies Biofilm Culture and Photodynamic Inactivation

Biofilm culture and photodynamic inactivation of biofilm were previously described [21]. In short, biofilms were cultured on 96-well flat-bottom microtiter plates. Overnight *S. agalactiae* culture was concentrated 8 times, *L. jensenii* was adjusted to 2.0 McFarland units (initial bacterial inoculum 10⁸ CFU/mL) and 10 µL aliquots of each bacterium were mixed in a well with 180 µL of Schaedler broth with a 5% addition of horse serum. The plate was covered and incubated at 37 °C and 5% CO₂ for 4 h. Then, the medium was removed, replaced with 200 µL of fresh medium and incubated at 37 °C and 5% CO₂ for 20 h. Then, biofilms were incubated with RB, washed and illuminated. After dispersing and serial dilutions, samples were plated on Columbia blood agar plates for *S. agalactiae* enumeration and on Columbia blood agar plates with 4 µg/mL of ciprofloxacin for *L. jensenii*. The experiment was conducted in three replicates.

2.6. Photo- and Cytotoxicity Assays Based on MTT

Photo- and cytotoxicity assays were previously described [15]. Briefly, HaCaT cells (CLS 300493) or human vaginal epithelial cells VK2E6E7 (ATCC CRL-2616, Washington, USA) cells were seeded 24 or 48 h before the treatment, respectively, in two 96-well plates (under light and dark conditions). The cells were grown in a humidified incubator at 37 °C and in a 5% CO₂ atmosphere in supplemented high-glucose DMEM (HaCaT) or Keratinocyte SFM, supplemented with L-glutamine, EGF and BPE (VK2E6E7) (Life Technologies/Thermo Fisher Scientific, Waltham, MA, USA). RB was added directly to the medium and incubated for 15 min at 37 °C. Then, the cells were washed with PBS, and 100 µL of fresh medium was added. Next, the cells were illuminated with the 3.8 J/cm² dose of a 522 nm light. Cell survival was measured after 24 h of incubation at 37 °C by an MTT [3-(4,5-dimethylthiazol-2-yl)-2,5-diphenyltetrazolium bromide] assay. Briefly, 10 µL of MTT solution (12 mM) was added to each well and incubated for 4 h at 37 °C. The cells were then lysed in DMSO (Sigma-Aldrich, Saint Louis, MO, USA), and the absorbance of the formazan was measured at 550 nm using an EnVision plate reader (Perkin Elmer, Waltham, MA, USA). In order to ensure that during the MTT test the absorbance signal came from formazan, not from the RB remaining in the cells, a spectral scan (450–700 nm) using an EnVision plate reader was performed for HaCaT cells treated with 30 µM RB in the dark and then treated with or without MTT prior to lysis in DMSO. The experiment was conducted in three replicates.

2.7. Analysis of Real-Time Cell-Growth Dynamics

Real-time cell-growth analysis on the RTCA device (Roche, Basel, Switzerland) was performed as described previously [22]. Briefly, human keratinocytes (HaCaT) were seeded before treatment at a density of 10^4 cells per well of E-plate (ACEA Biosciences Inc., San Diego, CA, USA). Treatments were performed when cells reached the exponential growth phase, reflected by cell index (CI) = 1.5–2. The RB at a concentration of 0, 5 or 30 μM was added and left for 15 min incubation at 37 °C in the dark. Next, cells were washed with PBS, and the medium was changed. Plates were illuminated with the 3.8 J/cm² dose of 522 nm light or left in the dark for the corresponding time. Plates were placed in the device, where the CI was measured every 10 min until all treated cells reached the plateau phase of growth. The experiment was conducted in three replicates.

2.8. Prokaryotic Mutagenicity Assay—Ames Test

Prokaryotic mutagenicity assay was performed using the commercial kit Ames Penta 2 (Xenometrix, Allschwil, Switzerland) according to the manufacturer's protocol. Briefly, 16 h overnight cultures of *Salmonella Typhimurium* [TA98, TA1535] and *Escherichia coli* [uvrA] were diluted in an exposure medium, incubated for 15 min with various concentrations of RB and exposed to the 522 nm light. As positive controls, 2-Nitrofluorene (TA98 and TA1535) and 4-Nitroquinoline-*N*-oxide (*E. coli* uvrA) were added to the cultures to induce mutations. All samples were then incubated for 90 min in an orbital shaker at 37 °C. Afterward, the exposure medium was added to the incubated cultures, and samples were partitioned into the 384-well plates. Then, microplates were covered with adhesive film, incubated for 48 h at 37 °C in the incubator and the number of revertants was assessed. The experiment was conducted in three replicates.

2.9. Eucaryotic Mutagenicity Assay—Comet Test

Eukaryotic mutagenicity assay was performed using the commercial kit CometAssay (Trevigen, Gaithersburg, MD, USA) according to the manufacturer's protocol for alkaline comet assay. Briefly, VK2E6E7 cells were seeded 48 h before treatment at a density of 2×10^5 cells per well on a 12-well plate. Cells were treated with RB-mediated aPDI the same way as for the MTT test or incubated for 20 min at 4 °C with 0.1% H₂O₂ was used as a positive control. Cells were then detached using the TrypLE Express Enzyme (Thermo Fisher Scientific, Waltham, MA, USA), washed with PBS and resuspended in PBS to obtain 10^5 cells/mL. Then, cells were mixed with molten LMAgarose and spread on glass slides. After drying, slides were immersed in lysis solution overnight at 4 °C. The next day, slides were incubated in an alkaline unwinding solution for 1 h at 4 °C and alkaline electrophoresis was performed (21 V, 30 min). Slides were washed twice in H₂O and once in 70% ethanol. After drying, samples were dyed with SYBR Gold and observed under a Nikon Eclipse TE300 Inverted Fluorescence Microscope using a green fluorescence filter. The experiment was performed in 3 independent repetitions. For each repetition, at least 80 comets were analyzed for each group. Comet images were analyzed using CometScore version 2.0 software created by Rex Hoover.

2.10. In Vivo Experiments

BALB/c mice (36 animals) were purchased from Charles River laboratories (Saffron Walden, Great Britain, UK). The mice were housed in the Infectious Animal Facility ABSL3 (Malopolska Centre of Biotechnology, Krakow, Poland). Animals were housed (6 per cage) and maintained on a 12 h light–dark cycle with access to water and food ad libitum. Female mice aged 8-weeks old were divided randomly into 6 groups (1. *S. agalactiae* + 555 nm light; 2. *S. agalactiae* + 5 μM RB aPDI; 3. *S. agalactiae* + 30 μM RB aPDI; 4. *S. agalactiae* + 5 μM RB; 5. *S. agalactiae* + 30 μM RB; and 6. *S. agalactiae* only). On the first day, all mice were subcutaneously given β -Estradiol 3-benzoate (0.02 mg/100 μL of sesame oil/mouse) for the induction of the estrus phase. On the second day, all mice were given 10 μL of *S. agalactiae* (10^5 CFU/mL) vaginally. On the third day, the vaginal wash with PBS (7 \times 50 μL) was

performed for bacteria enumeration. On the fourth day, illumination of vaginas was performed for group 1. Meanwhile, for groups 2 and 3, RB was provided vaginally to and after 30 min, vaginas were illuminated (50 min, 5.4 J/cm²). Similarly, RB was given vaginally to groups 4 and 5, but no illumination was provided, and group 6 was not treated at all. A vaginal wash was performed after 3 h for all groups. Furthermore, on the 5th day, a vaginal wash was performed for all groups. Afterward, mice were euthanized and vaginal tissue with the cervix was taken for analysis.

2.11. Microbiological Analysis of In Vivo Experiments

Vaginal washes were divided into two parts: the first was used immediately for microbiological analysis, while the second was frozen for later DNA isolation. Vaginal wash was serially diluted and plated onto the following 12 different culture media: Columbia blood agar (suitable for all aerobic bacteria culture); mannitol salt agar (for *Staphylococcus* culture); CHROMagar Strep B (for *S. agalactiae* enumeration); Edwards agar (for *Streptococcus* culture); Columbia agar with potassium tellurite (enabling *Enterococcus* culture); potato dextrose agar (for fungi and molds); Levine eosin methylene blue agar (for *Enterobacteriaceae* enumeration); CHROMagar Pseudomonas (promoting *Pseudomonas* growth); MRS Agar (for *Lactobacillus* culture); Schaedler blood agar with vit. K (enabling all anaerobic bacteria growth); Schaedler blood agar (dedicated to Gram-positive anaerobic bacteria); and Schaedler blood agar with kanamycin and vancomycin (used for Gram-negative anaerobic bacteria). All plates were purchased from GRASO, Starogard Gdanski, Poland. Plates for the cultivation of anaerobic bacteria were placed into plastic bags with an AnaeroGen sachet (Oxoid/Argenta Sp. Z.o.o., Poznan, Poland) and sealed. All plates were incubated at 37 °C for 48 h.

2.12. Preparation of Samples for DNA Sequencing Analysis

A total of 4 mice from group 3 (*S. agalactiae* + 30 µM RB aPDI) were chosen for sequencing library preparation. After defrosting the vaginal wash samples, total DNA was isolated using the DNeasy PowerSoil Pro Kit (Qiagen, Venlo, The Netherlands) according to the manufacturer's protocol. For sample enrichment, the 16S rRNA region was amplified using PCR. The oligonucleotide primer sequences used in the library preparation step were 5' AGTTTGATCCTGGCTCAG 3' (forward) and 5' AGGCCCGGGAACGTATTCAC 3' (reverse). PCR was carried out using Taq polymerase according to the manufacturer's protocol (Thermo Scientific™, Kansas City, Kansas, USA) for 5 min at 94 °C and 40 cycles of 1 min at 94 °C, 1 min at 55 °C and 2 min at 72 °C, followed by 10 min at 72 °C. Amplification products were then purified using the Syngen PCR Mini Kit (Syngen, Wroclaw, Poland) and sequenced by Genomed (Genomed S. A., Warszawa, Poland). Amplicons of the V3–V4 fragment of the 16S rRNA gene were sequenced using the Illumina MiSeq platform in paired-end mode with two readings of 300 bases [PE 300], assuming min. 50,000 pairs of reads per sample.

2.13. Analysis of Sequencing Data

The quality of raw sequencing reads was assessed using FastQC (version 0.11.9) [23] and MultiQC (version 1.14) [24]. Afterward, reads were imported into Qiime2 software (version 2022.11) [25]. However, due to a significant drop in quality of the 3' ends, only the first 240 and 200 nucleotides from the 5' ends were selected from the forward and reverse reads, respectively, and were subject to further analysis.

Preprocessed reads were merged, denoised, dereplicated and filtered using the Qiime2 implementation of the dada2 algorithm [26] with default settings. The filtering step was designed to remove low-quality reads and chimera sequences. All the steps were performed using the Qiime2 dada2 module, resulting in the amplicon sequence variants (ASV) observed in the analyzed samples.

Taxonomic classification of the ASVs was accomplished using a BLAST⁺-based classifier [27] called classify-consensus-blast, available in the feature-classifier module [28].

BLAST querying was performed against the QIIME2-compatible version of the SILVA database (release 138) [29,30] containing full-length 16S rRNA sequences preprocessed with RESCRIPt [31] and downloaded from the QIIME2 website (<https://docs.qiime2.org/>, accessed on 24 January 2023). Relative frequencies of identified taxa abundances are presented in the Supplementary Materials—file (Table S1): *rel_freq.xlsx*.

Additionally, LEfSe [32] analysis was employed to find significant differences in taxa abundances between D3, D4 and D5. LEfSe (version 1.0) was run using the Galaxy platform [33]. LDA scores were calculated using thresholds set to an alpha value of 0.05 and a logarithmic LDA score for discriminative features of 2. Furthermore, the “strategy for multi-class analyses” option was set to “One against all”.

2.14. Histopathological Analysis

Tissues suspended in 10% buffered formalin solution were sent to the Department of Pathomorphology, University Hospital, Krakow. After taking representative sections, the material was dehydrated in a series of increasing ethanol concentrations, cleared in xylene and impregnated with liquid paraffin in a vacuum tissue processor. After embedding in a paraffin block, microscopic preparations were made. The blocks were cut on a rotary microtome at a thickness of 2.5 μm . After drying, slides were stained with hematoxylin and eosin using an automated staining system. Histopathological analysis of the specimens was performed by an experienced pathologist (P.S.) who did not know the status of the examined material. Measurements were made using an Olympus BX53 microscope equipped with Olympus SWH10X-H eyepieces number 26.5 and an Olympus UPlanFLN 40 \times /0.75 objective. Three measurements were taken, specifically the intensity of the inflammatory infiltration in the proximal 2/3 of the vagina, the distal 1/3, and the degree of neutrophil involvement of the vaginal epithelium. The intensity measurement results were assessed semi-quantitatively using the following scale: 0—none; 0.5—minimum intensity; 1—very weak intensity, 1.5—weak intensity; 2—moderate intensity; 2.5—moderately strong intensity; and 3—strong intensity. In addition, the amount of purulent content within the vaginal lumen was measured. The results of the intensity of purulent content measurements within the vaginal lumen were evaluated semi-quantitatively using the following scale: 0—none; 1—moderately abundant purulent content; and 2—very abundant purulent content.

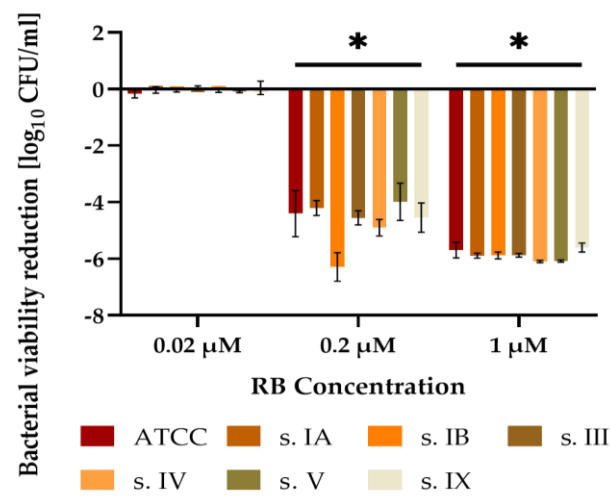
2.15. Statistical Analysis

GraphPad Prism version 9.5.0 for Windows (GraphPad Software, Inc., San Diego, CA, USA) was used to perform statistical analysis. Quantitative variables were characterized by the arithmetic mean and the standard deviation of the mean. Quantitative variables were characterized by the arithmetic mean and the standard deviation of the mean. One-way ANOVA followed by Dunnett’s multiple-comparisons test was used for data analysis. A *p* value of <0.05 was determined as an indicator of a significant difference.

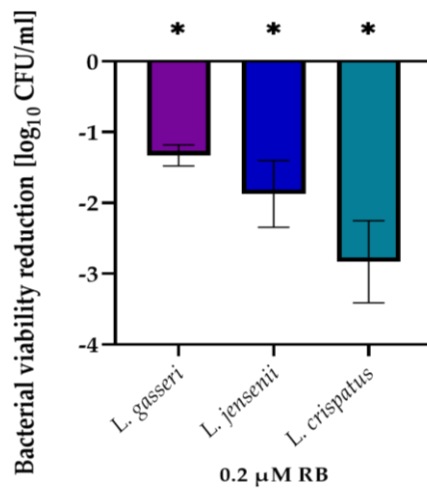
3. Results

3.1. *Streptococcus Agalactiae* Can Be Eradicated with RB-Mediated aPDI in Planktonic Culture In Vitro

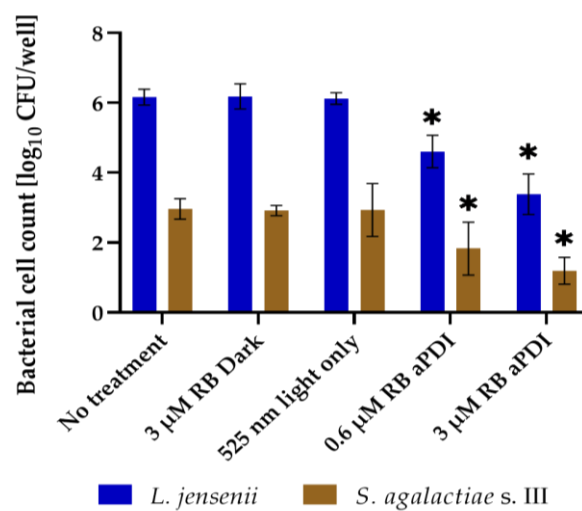
To verify if RB-mediated aPDI has potential in *S. agalactiae* eradication, the optimization of RB concentration and light dose had to be performed. The main goal was to obtain a lethal dose of aPDI, i.e., viability reduction by >3 \log_{10} CFU/mL. These parameters were chosen according to the previous experiments [21] using the ATCC strain. Figure 1A presents viability reduction in *S. agalactiae* caused by aPDI with different RB concentrations for the ATCC strain and six clinical isolates representing six different serotypes. aPDI with 0.2 μM RB was assessed as a lethal dose as it caused 4–6.3 \log_{10} units of viability reduction, while aPDI with 1 μM RB caused complete eradication of all strains in vitro.



(A)



(B)



(C)

Figure 1. Effect of RB-mediated aPDI on: (A) planktonic culture of *S. agalactiae*; (B) planktonic culture of human vaginal *Lactobacilli*; (C) multispecies biofilm culture of *S. agalactiae* and *L. jensenii*. Significance at the respective *p*-values is marked with asterisk (* *p* < 0.05) with respect to the “No treatment” group.

3.2. RB-Mediated aPDI Is Less Effective against Human Vaginal Lactobacilli Than against *S. agalactiae* In Vitro

Three representatives of the most common vaginal *Lactobacillus* species were chosen to assess the aPDI effect on human physiological vaginal flora. The viability reduction caused by aPDI with 0.2 μM RB was lower for all three *Lactobacillus* species than for *S. agalactiae* and varied between 1.3 to 2.8 \log_{10} units (Figure 1B).

3.3. RB-Mediated aPDI Inactivates *S. agalactiae* in Multispecies Biofilm Culture

The culture of multispecies biofilms of *S. agalactiae* and vaginal *Lactobacillus* is presented in Figure 1C. Serotype III of *S. agalactiae* was chosen as a strong biofilm producer. Multispecies biofilms were cultured for *S. agalactiae* with *L. gasseri*, *L. crispatus* or *L. jensenii*. For each combination, both species were inoculated in the same initial cell number. After 24 h of biofilm culture, fewer *S. agalactiae* cells were observed than *Lactobacillus* cells. Only multispecies biofilms of *S. agalactiae* and *L. jensenii* were presented as representative. As expected, biofilm culture requires use of a much higher concentration of RB than used for planktonic culture. To obtain viability reduction close to the detection limit for *S. agalactiae*, 3 μM RB was used for aPDI. The effectiveness (viability reduction) of aPDI was similar for both species in this multispecies biofilm. However, as for *L. jensenii* the initial cell number was much higher than for *S. agalactiae*; there was still a high number of viable *Lactobacillus* cells after photoinactivation.

3.4. RB-Mediated aPDI with Low Concentrations of RB Is Not Toxic for Eukaryotic Cells

To assess the RB-mediated aPDI effect on eukaryotic cells, the MTT test was performed. Human keratinocytes (HaCaT) (Figure 2A) and human vaginal epithelial cells (VK2E6E7) (Figure 2B) were used to investigate the cytotoxicity and phototoxicity of different RB concentrations used for in vitro (0.2, 0.6, 3 μM) and in vivo (5, 30 μM) studies. No cytotoxic effect was observed for any of the above concentrations. Except for 30 μM RB, no concentration caused any significant phototoxicity for HaCaT cells. For VK2E6E7 cells, a small phototoxic effect (<20%) was observed for 3 and 5 μM RB and significant phototoxicity was observed for 30 μM RB, similar to HaCaT cells. Because the MTT test assesses cell viability at only one timepoint (24 h post-treatment), for the highest RB concentrations, real-time cell-growth dynamics of HaCaT cells were also evaluated (Figure 2C). For 5 μM RB aPDI, a slight delay in growth curve was observed in comparison to the control (0 μM RB, dark). However, both groups reached a plateau at a similar time (ca. 60 h from seeding). For cells treated with 30 μM RB aPDI, a decrease in viability was observed shortly after photoinactivation, which is consistent with previous MTT results. Although proliferation was delayed, the cells reached a plateau about 150 h after seeding. This indicates that despite the fact that 30 μM RB aPDI exhibits some phototoxicity, the cells still manage to grow and divide to reach the plateau phase. In order to ensure that during the MTT test, the absorbance signal comes from formazan and not from the RB remaining in the cells, a spectral scan was performed (Figure 2D). It revealed that at 550 nm, the signal from cells treated with RB without MTT is at the background level.

3.5. RB-Mediated aPDI in the Ames Test Does Not Show Mutagenicity in Prokaryotic Cells

Two strains of *Salmonella Typhimurium* [TA98, TA1535] and one strain of *Escherichia coli* [uvrA] were used to assess the mutagenicity of RB and RB-mediated aPDI in the Ames test. These strains possess mutations that do not allow them to grow in the medium with a minimal amount of histidine. When mutations occur, revertant cells are able to grow in a medium with a minimal amount of histidine, which allows us to assess the mutagenicity of the tested compound. Strong mutagens specific for each strain were used as a positive control. In Figure 2E, it can be observed that none of the tested conditions showed significant mutagenicity for any of the tested strains. aPDI of 5 and 30 μM RB had a lethal effect on all tested strains. Consequently, the assessment of these conditions' mutagenicity in the prokaryotic model was not possible.

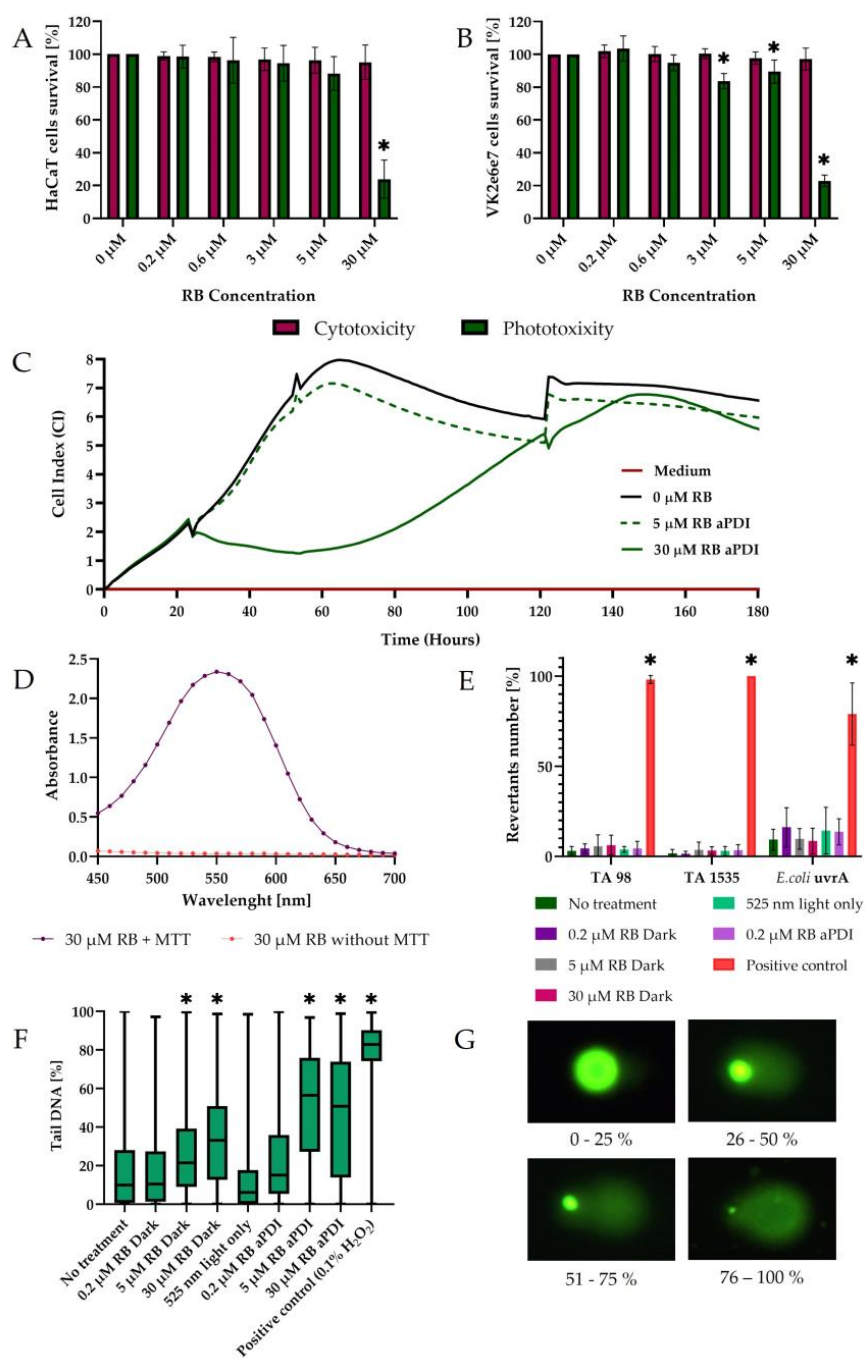


Figure 2. Analysis of RB-mediated aPDI toxicity: (A) Effect on human keratinocytes (HaCaT) with MTT test; (B) Effect on vaginal epithelial cells (VK2E6E7) with MTT test; (C) Effect on real-time Cell-growth dynamics (HaCaT); (D) Absorbance spectrum measurement of HaCaT cells after MTT test; (E) Mutagenic effect on prokaryotic cells via Ames test; (F) Mutagenic effect on eucaryotic cells (VK2E6E7) via comet assay; (G) Examples of obtained comets in comet assay with different percentage of DNA in comet tail, 100× magnification. Significance at the respective *p*-values is marked with asterisk (* *p* < 0.05) with respect to the “No treatment” group.

3.6. RB-Mediated aPDI in Comet Assay Does Not Show High Mutagenicity in Eucaryotic Cells

VK2E6E7 cells were used to assess RB-mediated aPDI mutagenicity in eucaryotic cells. After treatment, cells were mixed with agarose and dried on glass slides and alkaline electrophoresis was performed. In this process, DNA from cells containing DNA breaks (as a result of mutagenicity) was able to migrate from the nucleus and form comet tails, which were possible to observe under the fluorescence microscope after DNA staining. In Figure 2G, examples of obtained comets with different percentages of DNA in comet tails are presented. Figure 2F shows the mean percentage of DNA in comet tails for different experimental groups. Light only, 0.2 μM RB and 0.2 μM RB aPDI did not display any mutagenicity compared to the not treated group. Groups 5 and 30 μM RB in the dark showed a slight increase in tail DNA percentage. Groups 5 and 30 μM RB aPDI exhibited moderate mutagenic effects in eucaryotic cells; however, this effect is still much lower than for the positive control (0.1% H_2O_2).

3.7. RB-Mediated aPDI Can Inactivate *S. agalactiae* In Vivo in the Murine Model

To assess the efficacy of RB-mediated aPDI in vivo, the mouse model of vaginal colonization with *S. agalactiae* was used. The estrus phase was induced in BALB/c mice with β -estradiol. Then, their vaginas were inoculated with *S. agalactiae* (Figure 3A). Vaginal wash was performed the day after inoculation and 3 and 24 h post-treatment. Mice were treated with light only, RB only or RB-mediated aPDI, or they were not treated at all. Figure 3B explains how the vagina was irradiated with a spherical light distributor while the mouse was sedated. The presence of *S. agalactiae* in the vaginal wash was assessed with a microbiological approach, i.e., plating on CHROMagar Strep B (Figure 3C) with a metagenomic approach, as well as isolation and sequencing of DNA (Figure 3D). In the microbiological approach, all tested groups were investigated. For all control groups (no treatment, light only, RB in the dark), a slight reduction in *S. agalactiae* presence in the vagina was observed. For the 5 μM RB aPDI group, the change in *S. agalactiae* presence was comparable to the control groups. In the group treated with 30 μM RB aPDI, the reduction in *S. agalactiae* viability was the highest and reached ca. 2 \log_{10} units both 3 and 24 h post-treatment on day four and day five of the experiment, respectively (Figure 3C). For the metagenomic approach, washes from four mice from the group treated with 30 μM RB aPDI were sequenced. The relative frequency of *S. agalactiae* significantly decreased on days four (3 h post-treatment) and five (24 h post-treatment) (Figure 3D). Therefore, this confirms the results obtained using the microbiological approach.

3.8. The Histopathological Analysis Does Not Indicate the Negative Impact of RB-Mediated aPDI

After a vaginal wash on day five, all mice were euthanized and vaginal tissues with cervix were collected for histopathological analysis. Slides were searched for inflammation (Figure 4A), purulent content and invasion of epithelium by granulocytes (Figure 4B). Inflammation was assessed in the distal 1/3 of the vaginal wall and in 2/3 proximal of the vaginal wall (Figure 4C,D). No significant differences were observed in this parameter. However, as the invasion of epithelium by granulocytes was evaluated, although with no statistical significance, the score was the lowest for the group treated with 30 μM RB aPDI (Figure 4E). This may indicate that aPDI has a local negative impact on granulocytes and decreases the number of granulocytes on the site of treatment. For the last evaluated parameter, purulent content (mixed with exfoliated stratum corneum), in the vaginal lumen, no significant differences were observed (Figure 4F).

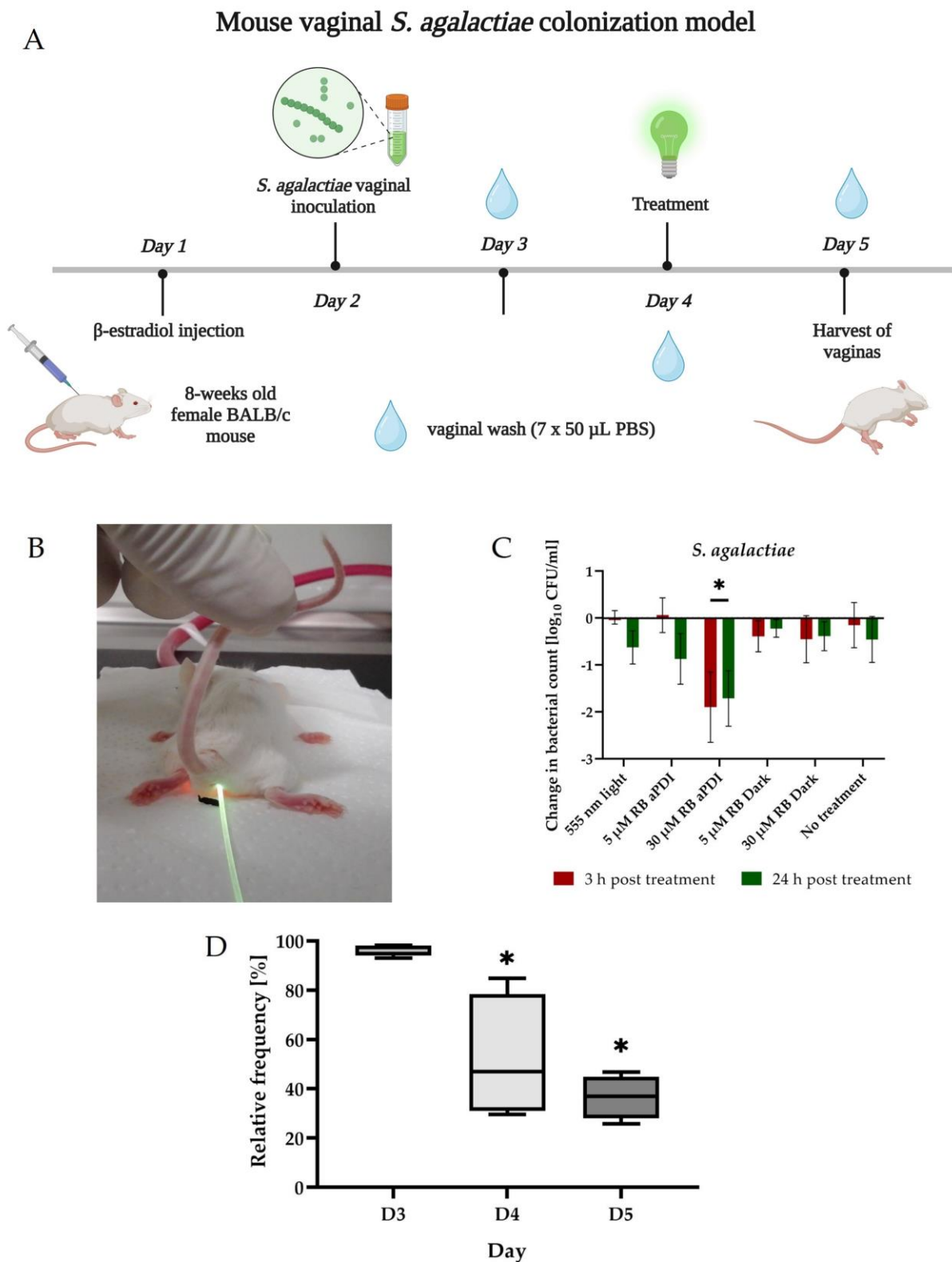


Figure 3. In vivo studies of *S. agalactiae* eradication efficacy with RB-mediated aPDI on murine model: (A) Scheme of mouse vaginal *S. agalactiae* colonization model, created with BioRender.com; (B) Irradiation of mouse vagina with spherical light distributor; (C) Change in *S. agalactiae* bacterial count obtained using microbiological approach in murine model; (D) *S. agalactiae* relative abundance in mice treated with 30 µM RB aPDI obtained with metagenomic analysis. Significance at the respective *p*-values is marked with asterisk (* *p* < 0.05) with respect to the “No treatment” group, or with respect to the day 3 group in Figure 3D.

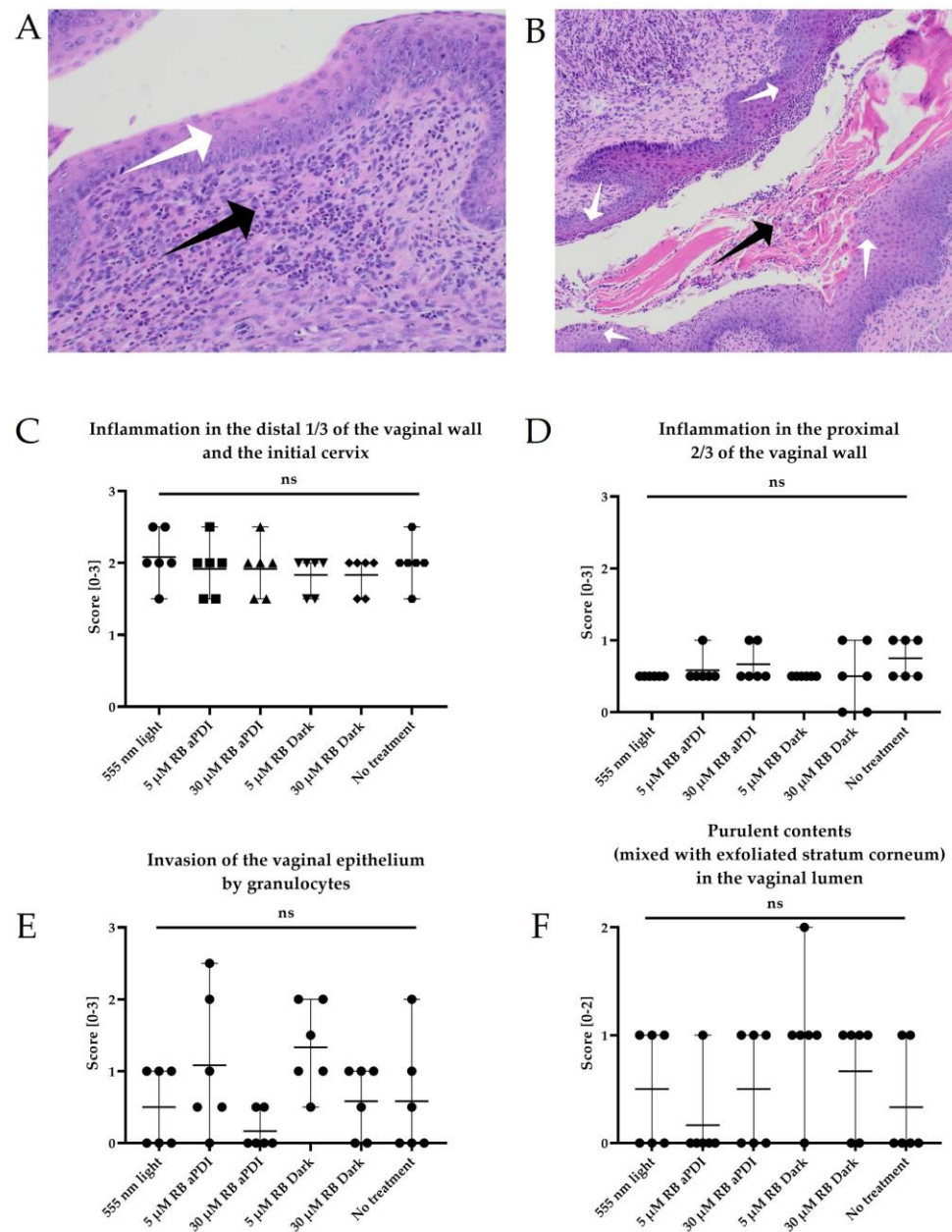


Figure 4. In vivo studies on *S. agalactiae* eradication efficacy with RB-mediated aPDI on murine model via histopathological analysis: (A) The distal 1/3 of the vaginal wall, white arrow: stratified squamous epithelium of the vaginal mucosa; black arrow: inflammatory infiltration focus, 200 \times magnification; (B) The distal 1/3 of the vaginal wall, black arrow: purulent content within the lumen of the vagina; white arrows: foci of invasion of the vaginal paraepidermoid epithelium by granulocytes, 100 \times magnification; (C) Inflammation score in the distal 1/3 of the vaginal wall; (D) Inflammation score in the proximal 2/3 of the vaginal wall; (E) Score of invasion of epithelium by granulocytes; (F) Score of purulent content in vaginal lumen. ns, not significant.

3.9. *S. agalactiae* Colonization Affects the Vaginal Microbiome Composition

To assess the impact of RB-mediated aPDI on vaginal flora, vaginal wash samples were serially diluted and spread on 12 different media. No colonies were observed on plates intended for the cultivation of *Pseudomonas* or fungi and molds. Changes in *S. agalactiae* growth are described above (Figure 3C). Changes in growth in the rest the groups are presented in Figure 5. Counts of Gram-negative anaerobic bacteria did not change significantly during the experiment. The number of all aerobic bacteria, *Strepto-*

coccus, *Enterococcus*, and *Lactobacillus*, as well as all anaerobic bacteria and Gram-positive anaerobic bacteria, changed similarly during the experiment. All of these bacterial group counts slightly decreased in most of the treatment groups compared to the non-treated group. Although for *Streptococcus*, *Lactobacillus* and Gram-positive anaerobic bacteria, changes in bacterial counts were significantly different for 30 μM RB aPDI in comparison to the non-treated group, these changes were lower than in *S. agalactiae* (Figure 3C). The most noticeable change was observed in *Enterobacteriaceae* and *Staphylococcus*. The counts of these two groups increased significantly in all tested groups of mice with no significant differences between groups.

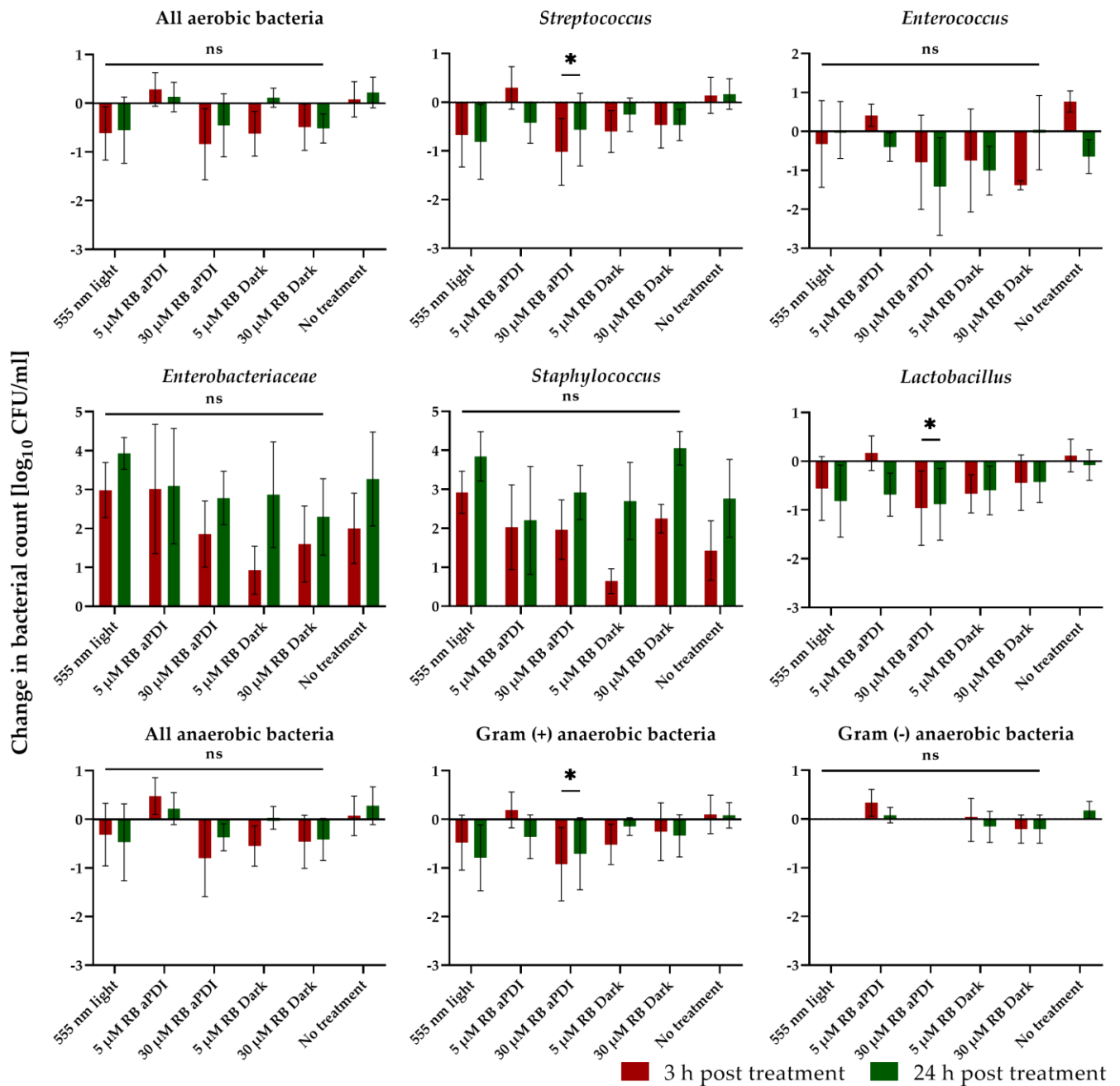


Figure 5. Changes in the bacterial counts obtained using the microbiological approach in a murine model. Significance at the respective p -values is marked with asterisk ($* p < 0.05$) with respect to the “No treatment” group; ns, not significant.

3.10. aPDI Impacts the Abundance of the Most Prevalent Species in Mouse Vaginas

As a result of the 16S rRNA gene-sequencing data analysis, we observed the significant impact of aPDI on the microbial communities of the mouse vaginas. The most striking effect was observed in the *S. agalactiae* abundance, during which D3 in all the biological replicates corresponded to more than 90% of identified amplicon sequence variants (ASVs). The relative abundance (Figure 6A,C) of *S. agalactiae* decreased more than two-fold from D3 to D4 and D5, ultimately reaching lows of ~25–45%. In contrast, the relative frequency of *Staphylococcus sciuri* increased at D4 and D5. *S. sciuri* represented less than 1% of all ASVs on D3, while the prevalence of the species increased significantly to ~1–64% on D4, finally reaching 44–64% on D5. To a lesser extent, we observed a significant increase in the relative abundance of *Corynebacterium* from D3 (~6%) to D4 (~27%) and D5 (~29%) in the mice designated 669. In the remaining samples, the share of *Corynebacterium* ASVs did not exceed 1%. Furthermore, the prevalence of the *Escherichia-Shigella* group changed between D3 (up to ~2%), D4 (up to ~16%) and D5 (up to ~3%). Additionally, the presence of *Escherichia coli* (D3: <1%, D4: <1%~2%, D5: <1%~5%) and *Methylobacterium-Methylobacterium* (D3: <1%, D4: <1%~1%, D5: <1%) groups are worthy of mention.

LEfSe analysis (Figure 6B) was performed to determine the most significant differences in taxon abundance between the subsequent days of in vivo experiment. The study has shown that the decreasing trend in *Streptococcus* and the increasing trend in *Staphylococcus* genera abundances between D3 and D5 were statistically significant in terms of the LDA scores shown in Figure 6B.

Further analysis of the heatmap displaying the relative abundances of the observed genera (Figure 6C) suggests that vaginal microbiome composition is similar between analyzed mice. The most significant differences in frequency were observed in *Streptococcus*, *Staphylococcus*, *Escherichia-Shigella*, *Corynebacterium*, *Methylobacterium-Methylobacterium*, and *Microbacterium* genera.

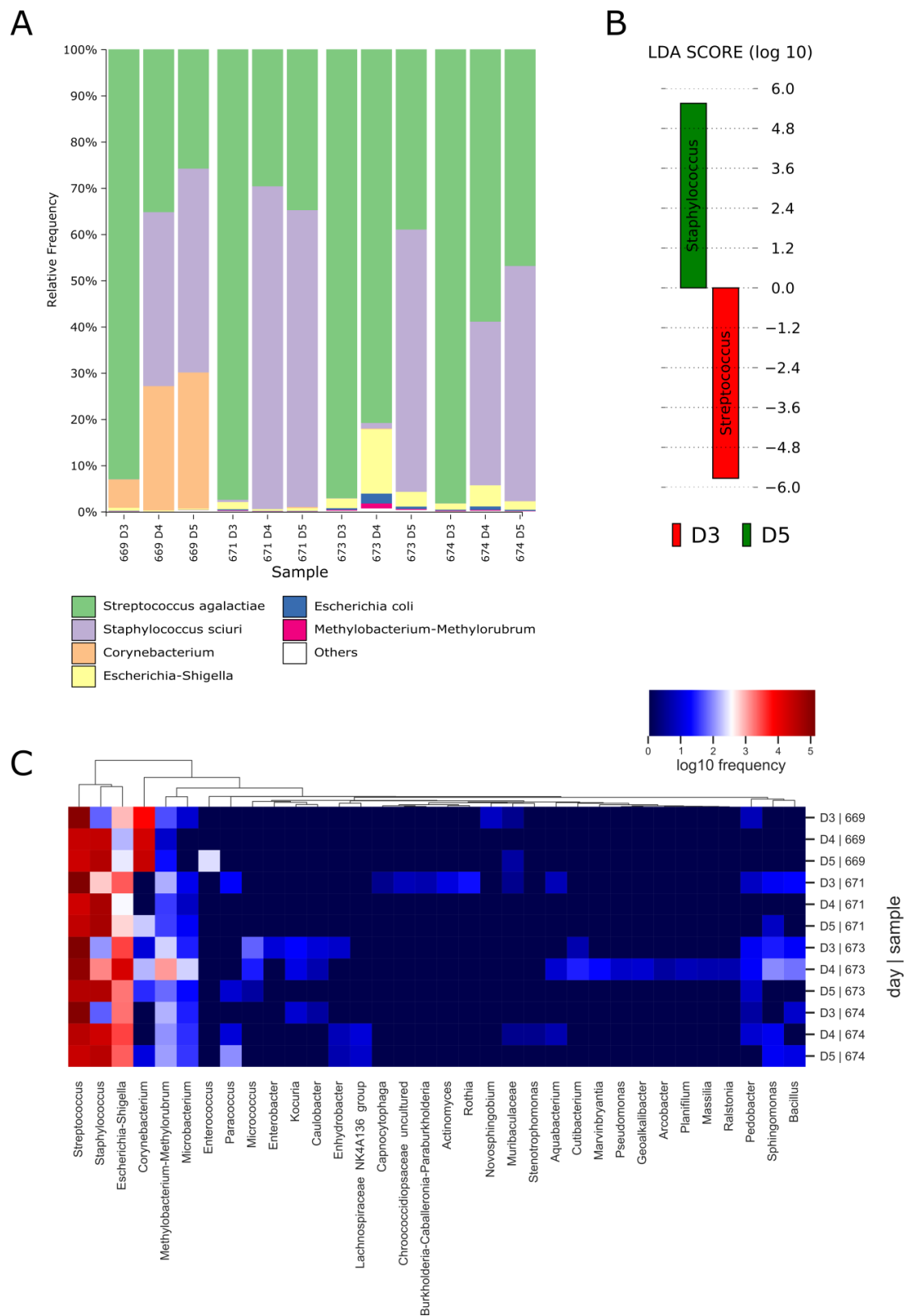


Figure 6. Metagenomic analysis of V3-V4 fragment of 16S rRNA gene sequencing from vaginal wash obtained from mice treated with 30 μ M RB aPDI: (A) Relative frequency of most abundant bacterial species. Numbers 669, 671, 673 and 674 represent four different mice, while D3, D4, and D5 abbreviations correspond to the day of the experiment; (B) Results of LfSe analysis representing significant differences in taxa abundances between D3, D4 and D5; (C) The genus level abundance of vaginal microbiota in each mouse on different days.

4. Discussion

Recently, several alternatives to current IAP, aiming to prevent or limit maternal GBS colonization, have been explored. These, first of all, include strategies that assume applying compounds with specific antimicrobial activity toward GBS, i.e., plant-derived crude extracts and phytochemicals [34] and plant-based lipids from *Aristolochia longa* and *Bryonia dioica* [35], octylglycerol [36] or synthetic peptides mimicking human C5a, which was demonstrated in in vivo mouse vaginal colonization models to be bactericidal toward GBS [37]. Although these compounds reveal some efficacy against GBS in animal models, it is still to be established if any of them are suitable for human use. As a next alternative to antibiotic treatment, intrapartum chlorhexidine vaginal washes have been considered and confirmed to significantly lower neonatal colonization [38]. Finally, the use of probiotic agents limiting pathogen overgrowth and promoting native vaginal flora has been proposed [39,40]. The most promising probiotic candidates demonstrating beneficiary activity against GBS include the *Lactobacillus* genus, i.e., *L. rhamnosus*, *L. gasseri* or *L. reuteri*.

Here, we describe the use of novel antimicrobial photodynamic inactivation as an attractive and highly effective antimicrobial approach that could potentially lead to control of GBS vaginal colonization with respect to the harmless effect on host cells and the mild influence on viability and composition of vaginal flora. Regardless of the abundant literature regarding the use of aPDI against human microbial pathogens (most recently reviewed by Nakonieczna et al. (2019) [7]), there is only one single report by Sellera et al. (2016) that demonstrates the efficacy of classical aPDI in the inactivation of pathogens associated with bovine mastitis (*S. aureus*, *Streptococcus agalactiae*, *S. dysgalactiae*, *Corynebacterium bovis*, and the alga *Prototheca zopfii*), indicating that aPDI could be an interesting tool for inactivating *S. agalactiae* as a source of veterinary infections [41]. Nevertheless, no studies have yet described the use of aPDI against *S. agalactiae*, which is involved in the etiology of neonatal infections. Moreover, no studies have demonstrated the potential of using aPDI to control GBS vaginal colonization, which emphasizes the novelty of this investigation.

The current study describes aPDI employing a harmless photoactive compound, i.e., rose bengal (RB), which was used in our previous mechanistic studies concerning aPDI treatment [21,42,43]. RB is a xanthene dye, which has been widely applied as a photoactive compound in photodynamic treatment [15,44–51]. Among xanthene dyes, which are potent producers of ROS, such as singlet oxygen [52], RB is one of the most efficient and widely used source of $^1\text{O}_2$ in polar solvents, such as water [53]. Moreover, it is considered a molecule with high biocompatibility (necessary criteria for therapeutic agent) and a low level of cytotoxicity, even at higher concentrations [15,48]. Although most bacteria have advanced systems for ROS neutralization and repair of ROS-induced damage, there are no adequate defenses for singlet oxygen and hydroxyl radicals, so even small amounts of these may be fatal [54]. We have previously shown that *S. agalactiae* responds to aPDI-induced oxidative stress with increased expression of major oxidative stress response elements, such as *sodA*, *ahpC*, *npx*, *cylE*, *tpx* or *recA*. Moreover, even though we observed increased photoinactivation stress tolerance after consecutive treatments in *S. agalactiae*, a slight increase in RB concentration was sufficient to eradicate tolerant strains [43].

The results of the current study demonstrate that various pathogenic GBS serotypes were susceptible to the action of aPDI both in planktonic and multispecies biofilm culture while leaving high viability of main representatives of human vaginal flora, i.e., *Lactobacillus* species. As far as GBS biofilm development appears to support vaginal colonization [55] by effective protection from antimicrobials and host defense factors, the results concerning effective inactivation activity of aPDI toward *S. agalactiae* growing in multispecies biofilm culture should be considered to be of high importance. The human vaginal flora was clustered into five different groups and four of them were evidenced to be dominated by *Lactobacillus* species [56]; thus, three different representatives of *Lactobacillus*, i.e., *L. gasseri*, *L. jensenii* and *L. crispatus* were selected for in vitro evaluation within the current study, indicating that employed aPDI could indeed lead to reduced viability of *Lactobacilli*.

However, the remaining portion of these microorganisms is still a two-order magnitude higher than targeted GBS, which enables the efficient recovery of the native vaginal flora.

When searching for alternative prevention and/or treatment approaches, the safety aspects of the strategy must be taken into account. Described aPDI was evidenced to be safe toward both human keratinocytes and vaginal epithelial cells regardless of cyto- and phototoxicity effects. Real-time growth dynamics confirmed that even when high RB concentrations were used (leading to eukaryotic cells inactivation by approximately 80%), treated human cells were capable of efficient recovery upon treatment. Moreover, the proposed approach under studied conditions was evidenced to exert no mutagenic effect (emphasized with the application of FDA-approved Ames methodology using three various microbial mutants) and mild genotoxic effect toward eukaryotic cell lines (much below the positive, genotoxic control). Overall, aPDI safety was also evidenced with the presented mice colonization model via histopathological analysis. Vaginal tissues with the cervix were collected and searched for inflammation, purulent content and invasion of epithelium by granulocytes. No significant differences were observed in these parameters, indicating the safe use of aPDI and exerting no aPDI-induced inflammation.

Finally, aPDI was assessed regarding its influence on the composition and viability of native vaginal flora. Employing a microbiological and bioinformatic approach, we have undoubtedly confirmed that aPDI leads to significant reduction in GBS load within the vaginal tract and the mild inactivation of all (except *Enterobacteriaceae* and *Staphylococcus* genus) microbial groups, i.e., aerobic (including *Streptococcus*, *Enterococcus*, *Lactobacillus*) and anaerobic bacteria (including Gram-positive and Gram-negative bacteria). In the case of *Enterobacteriaceae* and *Staphylococcus*, the increased load of these microbes was reported during the experiment; however, this effect was not dependent on the treatment used and was also observed for the not treated animals. Observed with bioinformatical analysis, *S. sciuri*, although considered pathogenic, commonly occurs in rodents [57,58] and can even have a positive effect, such as preventing asthma in mice [59]. The most probable cause for *Enterobacteriaceae* and *Staphylococcus* prevalence increase is the effect of *S. agalactiae* infection. A similar effect was previously observed in mice vaginas after HSV-2 infection [60]. Vaginal flora of mice in contrast to human vaginal flora is not dominated by *Lactobacilli* [61]. Therefore, it is not possible to predict outcome of aPDI in human vaginal flora based on the results from aPDI treatment of mouse vagina. This investigation is yet to be conducted. There is a possibility that the use of intravaginal probiotic treatment right after aPDI would prevent secondary infections of the urogenital tract.

5. Conclusions

In recent decades, GBS has remained a prominent concern for neonatal health. Although IAP has substantially reduced incidence of GBS infections, maternal and infant colonization rates remain a concern in modern medicine. The emergence of novel and beyond broad-spectrum antibiotic alternative strategies to control GBS vaginal colonization appears to be promising for the urgent need to prevent neonatal GBS infections. The present study showed that antimicrobial photodynamic inactivation may serve as a safe alternative option against GBS. Moreover, the global scenario of antibacterial resistance has been of great concern for public health, and novel non-antibiotic strategies could help us resolve this problem. Obviously, further detailed, preclinical studies assessing the bactericidal efficacy and toxicological aspects of aPDI are required to provide a basis for full clinical trials. However, we believe that photodynamic inactivation should be considered an important treatment and/or prevention option worthy of further investigations.

Supplementary Materials: The following supporting information can be downloaded at: <https://www.mdpi.com/article/10.3390/antiox12040847/s1>, Table S1: Relative frequencies of identified taxa abundances—file: rel_freq.xlsx.

Author Contributions: Conceptualization, M.G. and M.K.P.; methodology, M.K.P., J.G.K., K.S., P.S. and M.G.; software, J.G.K.; validation, M.K.P., J.G.K., K.S., P.S. and M.G.; formal analysis, M.K.P., K.S. and J.G.K.; investigation, M.K.P., K.S., J.G.K. and P.S.; resources, M.G.; data curation, M.K.P. and J.G.K.; writing—original draft preparation, M.K.P. and M.G.; writing—review and editing, M.K.P. and M.G.; visualization, M.K.P., J.G.K., K.S. and P.S.; supervision, M.G.; project administration, M.G.; funding acquisition, M.G. All authors have read and agreed to the published version of the manuscript.

Funding: This research received no external funding. The APC was funded by statutory activity no. 531-N119-D098-23.

Institutional Review Board Statement: The animal study protocol was approved by the 2nd Local Institutional Animal Care and Use Committee (IACUC) in Kraków (protocol code 2/2016; date of approval: 22 March 2016).

Informed Consent Statement: Not applicable.

Data Availability Statement: The data presented in this study are available in the article and supplementary materials.

Acknowledgments: We would like to thank Izabela Sitkiewicz (Translational Medicine Center, Warsaw University of Life Sciences, Warsaw, Poland) for kind donation of *S. agalactiae* strains; Inga Drebot and Katarzyna Guła (Malopolska Centre of Biotechnology, Krakow, Poland) for animal handling; Michał Rychłowski (Laboratory of Virus Molecular Biology, Intercollegiate Faculty of Biotechnology University of Gdansk and Medical University of Gdansk) for assistance in fluorescence microscopy; Agnieszka Bernat-Wójtowska (Laboratory of Photobiology and Molecular Diagnostics, Intercollegiate Faculty of Biotechnology University of Gdansk and Medical University of Gdansk) for substantive support with handling of eucaryotic cell cultures; Agata Pawlikowska-Woźniak (Laboratory of Photobiology and Molecular Diagnostics, Intercollegiate Faculty of Biotechnology University of Gdansk and Medical University of Gdansk) for substantive support with Ames and Comet assays; and Beata Kruszewska-Naczka (Laboratory of Photobiology and Molecular Diagnostics, Intercollegiate Faculty of Biotechnology University of Gdansk and Medical University of Gdansk) for preparation of Figure 3A. Figure 3A and graphical abstract were created with BioRender.com.

Conflicts of Interest: The authors declare no conflict of interest. The funders had no role in the design of the study; in the collection, analyses, or interpretation of data; in the writing of the manuscript; or in the decision to publish the results.

References

1. Infectious Diseases of the Fetus and Newborn E-Book—Jack S. Remington, Christopher B. Wilson, Victor Nizet, Jerome O. Klein, Yvonne Maldonado—Google Książki. Available online: https://books.google.pl/books?hl=pl&lr=&id=5ECgVBNQDUMC&oi=fnd&pg=PP1&dq=Wilson,+C.+B.,+Nizet,+V.,+Maldonado,+Y.,+Remington,+J.+S.+%26+Klein+J.+O.+Infectious+Diseases+of+the+Fetus+and+Newborn+Infant+8th+edn+Saunders+Elsevier,+2016&ots=TJfboIzo_5&sig=BRNSI7zhywMyrr22bC1MVMNAu90&redir_esc=y#v=onepage&q&f=false (accessed on 22 February 2023).
2. Prevention of Group B Streptococcal Early-Onset Disease in Newborns: ACOG Committee Opinion, Number 797. *Obstet. Gynecol.* **2020**, *135*, e51–e72. [[CrossRef](#)] [[PubMed](#)]
3. Lamagni, T.L.; Keshishian, C.; Efstratiou, A.; Guy, R.; Henderson, K.L.; Broughton, K.; Sheridan, E. Emerging Trends in the Epidemiology of Invasive Group B Streptococcal Disease in England and Wales, 1991–2010. *Clin. Infect. Dis.* **2013**, *57*, 682–688. [[CrossRef](#)] [[PubMed](#)]
4. Okike, I.O.; Ribeiro, S.; Ramsay, M.E.; Heath, P.T.; Sharland, M.; Ladhani, S.N. Trends in bacterial, mycobacterial, and fungal meningitis in England and Wales 2004–11: An observational study. *Lancet Infect. Dis.* **2014**, *14*, 301–307. [[CrossRef](#)]
5. Kohli-Lynch, M.; Russell, N.J.; Seale, A.C.; Dangor, Z.; Tann, C.J.; Baker, C.J.; Bartlett, L.; Cutland, C.; Gravett, M.G.; Heath, P.T.; et al. Neurodevelopmental Impairment in Children after Group B Streptococcal Disease Worldwide: Systematic Review and Meta-analyses. *Clin. Infect. Dis.* **2017**, *65*, S190–S199. [[CrossRef](#)]
6. Wang, Y.; Wang, Y.; Wang, Y.; Murray, C.K.; Hamblin, M.R.; Hooper, D.C.; Dai, T. Antimicrobial blue light inactivation of pathogenic microbes: State of the art. *Drug Resist. Updat.* **2017**, *33*, 1–22. [[CrossRef](#)] [[PubMed](#)]
7. Nakonieczna, J.; Wozniak, A.; Pieranski, M.; Rapacka-Zdonczyk, A.; Ogonowska, P.; Grinholc, M. Photoinactivation of ESKAPE pathogens: Overview of novel therapeutic strategy. *Future Med. Chem.* **2019**, *11*, 443–461. [[CrossRef](#)] [[PubMed](#)]
8. St. Denis, T.G.; Dai, T.; Izikson, L.; Astrakas, C.; Anderson, R.R.; Hamblin, M.R.; Tegos, G.P. All you need is light. *Virulence* **2011**, *2*, 509–520. [[CrossRef](#)]
9. Kharkwal, G.B.; Sharma, S.K.; Huang, Y.Y.; Dai, T.; Hamblin, M.R. Photodynamic therapy for infections: Clinical applications. *Lasers Surg. Med.* **2011**, *43*, 755–767. [[CrossRef](#)]

10. Wainwright, M.; Maisch, T.; Nonell, S.; Plaetzer, K.; Almeida, A.; Tegos, G.P.; Hamblin, M.R. Photoantimicrobials—Are we afraid of the light? *Lancet Infect. Dis.* **2017**, *17*, e49–e55. [CrossRef]
11. Wainwright, M. Photodynamic antimicrobial chemotherapy (PACT). *J. Antimicrob. Chemother.* **1998**, *42*, 13–28. [CrossRef]
12. Baptista, M.S.; Cadet, J.; Di Mascio, P.; Ghogare, A.A.; Greer, A.; Hamblin, M.R.; Lorente, C.; Nunez, S.C.; Ribeiro, M.S.; Thomas, A.H.; et al. Type I and Type II Photosensitized Oxidation Reactions: Guidelines and Mechanistic Pathways. *Photochem. Photobiol.* **2017**, *93*, 912–919. [CrossRef] [PubMed]
13. Grinholc, M.; Rapacka-Zdonczyk, A.; Rybak, B.; Szabados, F.; Bielawski, K.P. Multiresistant Strains Are as Susceptible to Photodynamic Inactivation as Their Naïve Counterparts: Protoporphyrin IX-Mediated Photoinactivation Reveals Differences between Methicillin-Resistant and Methicillin-Sensitive *Staphylococcus aureus* Strains. *Photomed. Laser Surg.* **2014**, *32*, 121–129. [CrossRef] [PubMed]
14. Fila, G.; Kawiak, A.; Grinholc, M.S. Blue light treatment of *Pseudomonas aeruginosa*: Strong bactericidal activity, synergism with antibiotics and inactivation of virulence factors. *Virulence* **2017**, *8*, 938–958. [CrossRef] [PubMed]
15. Nakonieczna, J.; Wolnikowska, K.; Ogonowska, P.; Neubauer, D.; Bernat, A.; Kamysz, W. Rose bengal-mediated photoinactivation of multidrug resistant *Pseudomonas aeruginosa* is enhanced in the presence of antimicrobial peptides. *Front. Microbiol.* **2018**, *9*, 1949. [CrossRef]
16. Wilkinson, F.; Helman, W.P.; Ross, A.B. Quantum Yields for the Photosensitized Formation of the Lowest Electronically Excited Singlet State of Molecular Oxygen in Solution. *J. Phys. Chem. Ref. Data* **2009**, *22*, 113. [CrossRef]
17. Kurosu, M.; Mitachi, K.; Yang, J.; Pershing, E.V.; Horowitz, B.D.; Wachter, E.A.; Lacey, J.W.; Ji, L.; Rodrigues, Y.; Antibacterial, D.J.; et al. Antibacterial Activity of Pharmaceutical-Grade Rose Bengal: An Application of a Synthetic Dye in Antibacterial Therapies. *Molecules* **2022**, *27*, 322. [CrossRef]
18. Nakonechny, F.; Barel, M.; David, A.; Koretz, S.; Litvak, B.; Ragozin, E.; Etinger, A.; Livne, O.; Pinhasi, Y.; Gellerman, G.; et al. Dark Antibacterial Activity of Rose Bengal. *Int. J. Mol. Sci.* **2019**, *20*, 3196. [CrossRef] [PubMed]
19. Vanerio, N.; Stijnen, M.; De Mol, B.A.J.M.; Kock, L.M. Biomedical Applications of Photo- and Sono-Activated Rose Bengal: A Review. *Photobiomodulation Photomed. Laser Surg.* **2019**, *37*, 383–394. [CrossRef]
20. Hirose, M.; Yoshida, Y.; Horii, K.; Hasegawa, Y.; Shibuya, Y. Efficacy of antimicrobial photodynamic therapy with Rose Bengal and blue light against cariogenic bacteria. *Arch. Oral Biol.* **2021**, *122*, 105024. [CrossRef]
21. Pieranski, M.K.; Rychłowski, M.; Grinholc, M. Optimization of *Streptococcus agalactiae* Biofilm Culture in a Continuous Flow System for Photoinactivation Studies. *Pathogens* **2021**, *10*, 1212. [CrossRef]
22. Michalska, K.; Rychłowski, M.; Krupińska, M.; Szewczyk, G.; Sarna, T.; Nakonieczna, J. Gallium Mesoporphyrin IX-Mediated Photodestruction: A Pharmacological Trojan Horse Strategy to Eliminate Multidrug-Resistant *Staphylococcus aureus*. *Mol. Pharm.* **2022**, *19*, 1434–1448. [CrossRef] [PubMed]
23. Simon Andrews Babraham Bioinformatics—FastQC a Quality Control Tool for High Throughput Sequence Data. Available online: <https://www.bioinformatics.babraham.ac.uk/projects/fastqc/> (accessed on 24 January 2023).
24. Ewels, P.; Magnusson, M.; Lundin, S.; Käller, M. MultiQC: Summarize analysis results for multiple tools and samples in a single report. *Bioinformatics* **2016**, *32*, 3047–3048. [CrossRef] [PubMed]
25. Bolyen, E.; Rideout, J.R.; Dillon, M.R.; Bokulich, N.A.; Abnet, C.C.; Al-Ghalith, G.A.; Alexander, H.; Alm, E.J.; Arumugam, M.; Asnicar, F.; et al. Reproducible, interactive, scalable and extensible microbiome data science using QIIME 2. *Nat. Biotechnol.* **2019**, *37*, 852–857. [CrossRef] [PubMed]
26. Callahan, B.J.; McMurdie, P.J.; Rosen, M.J.; Han, A.W.; Johnson, A.J.A.; Holmes, S.P. DADA2: High-resolution sample inference from Illumina amplicon data. *Nat. Methods* **2016**, *13*, 581–583. [CrossRef] [PubMed]
27. Camacho, C.; Coulouris, G.; Avagyan, V.; Ma, N.; Papadopoulos, J.; Bealer, K.; Madden, T.L. BLAST+: Architecture and applications. *BMC Bioinform.* **2009**, *10*, 1–9. [CrossRef]
28. Bokulich, N.A.; Kaehler, B.D.; Rideout, J.R.; Dillon, M.; Bolyen, E.; Knight, R.; Huttley, G.A.; Gregory Caporaso, J. Optimizing taxonomic classification of marker-gene amplicon sequences with QIIME 2's q2-feature-classifier plugin. *Microbiome* **2018**, *6*, 1–17. [CrossRef]
29. Quast, C.; Pruesse, E.; Yilmaz, P.; Gerken, J.; Schweer, T.; Yarza, P.; Peplies, J.; Glöckner, F.O. The SILVA ribosomal RNA gene database project: Improved data processing and web-based tools. *Nucleic Acids Res.* **2013**, *41*, D590–D596. [CrossRef]
30. Pruesse, E.; Quast, C.; Knittel, K.; Fuchs, B.M.; Ludwig, W.; Peplies, J.; Glöckner, F.O. SILVA: A comprehensive online resource for quality checked and aligned ribosomal RNA sequence data compatible with ARB. *Nucleic Acids Res.* **2007**, *35*, 7188–7196. [CrossRef]
31. Robeson, M.S.; O'Rourke, D.R.; Kaehler, B.D.; Ziemski, M.; Dillon, M.R.; Foster, J.T.; Bokulich, N.A. RESCRIPt: Reproducible sequence taxonomy reference database management. *PLoS Comput. Biol.* **2021**, *17*, e1009581. [CrossRef]
32. Segata, N.; Izard, J.; Waldron, L.; Gevers, D.; Miropolsky, L.; Garrett, W.S.; Huttenhower, C. Metagenomic biomarker discovery and explanation. *Genome Biol.* **2011**, *12*, 1–18. [CrossRef]
33. Afgan, E.; Nekrutenko, A.; Grünig, B.A.; Blankenberg, D.; Goecks, J.; Schatz, M.C.; Ostrovsky, A.E.; Mahmoud, A.; Lonie, A.J.; Syme, A.; et al. The Galaxy platform for accessible, reproducible and collaborative biomedical analyses: 2022 update. *Nucleic Acids Res.* **2022**, *50*, W345–W351. [CrossRef]
34. Abachi, S.; Lee, S.; Vasantha Rupasinghe, H.P.; Battino, M.; Niki, E.; Quiles, J.L. Molecular Mechanisms of Inhibition of *Streptococcus* Species by Phytochemicals. *Molecules* **2016**, *21*, 215. [CrossRef] [PubMed]

35. Dhouioui, M.; Boulila, A.; Jemli, M.; Schiets, F.; Casabianca, H.; Zina, M.S. Fatty Acids Composition and Antibacterial Activity of *Aristolochia longa* L. and *Bryonia dioica* Jacq. Growing Wild in Tunisia. *J. Oleo Sci.* **2016**, *65*, 655–661. [[CrossRef](#)] [[PubMed](#)]
36. Moncla, B.J.; Pryke, K.; Isaacs, C.E. Killing of *Neisseria gonorrhoeae*, *Streptococcus agalactiae* (group B streptococcus), *Haemophilus ducreyi*, and vaginal *Lactobacillus* by 3-O-octyl-sn-glycerol. *Antimicrob. Agents Chemother.* **2008**, *52*, 1577–1579. [[CrossRef](#)] [[PubMed](#)]
37. Cavaco, C.K.; Patras, K.A.; Zlamal, J.E.; Thoman, M.L.; Morgan, E.L.; Sanderson, S.D.; Dorana, K.S. A novel C5a-derived immunobiotic peptide reduces *Streptococcus agalactiae* colonization through targeted bacterial killing. *Antimicrob. Agents Chemother.* **2013**, *57*, 5492–5499. [[CrossRef](#)]
38. Ohlsson, A.; Shah, V.S.; Stade, B.C. Vaginal chlorhexidine during labour to prevent early-onset neonatal group B streptococcal infection. *Cochrane Database Syst. Rev.* **2014**, *12*, CD003520. [[CrossRef](#)]
39. Falagas, M.E.; Betsi, G.I.; Athanasiou, S. Probiotics for the treatment of women with bacterial vaginosis. *Clin. Microbiol. Infect.* **2007**, *13*, 657–664. [[CrossRef](#)]
40. Homayouni, A.; Bastani, P.; Ziyadi, S.; Mohammad-Alizadeh-Charandabi, S.; Ghalibaf, M.; Mortazavian, A.M.; Mehrabany, E.V. Effects of probiotics on the recurrence of bacterial vaginosis: A review. *J. Low. Genit. Tract Dis.* **2014**, *18*, 79–86. [[CrossRef](#)]
41. Sellera, F.P.; Sabino, C.P.; Ribeiro, M.S.; Gargano, R.G.; Benites, N.R.; Melville, P.A.; Pogliani, F.C. In vitro photoinactivation of bovine mastitis related pathogens. *Photodiagnosis Photodyn. Ther.* **2016**, *13*, 276–281. [[CrossRef](#)]
42. Brasel, M.; Pieranski, M.; Grinholc, M. An extended logistic model of photodynamic inactivation for various levels of irradiance using the example of *Streptococcus agalactiae*. *Sci. Rep.* **2020**, *10*, 14168. [[CrossRef](#)]
43. Pieranski, M.; Sitkiewicz, I.; Grinholc, M. Increased photoinactivation stress tolerance of *Streptococcus agalactiae* upon consecutive sublethal phototreatments. *Free Radic. Biol. Med.* **2020**, *160*, 657–669. [[CrossRef](#)] [[PubMed](#)]
44. Rapacka-Zdonczyk, A.; Wozniak, A.; Pieranski, M.; Wozniwodzka, A.; Bielawski, K.P.; Grinholc, M. Development of *Staphylococcus aureus* tolerance to antimicrobial photodynamic inactivation and antimicrobial blue light upon sub-lethal treatment. *Sci. Rep.* **2019**, *9*, 1–18. [[CrossRef](#)] [[PubMed](#)]
45. Grinholc, M.; Rodziewicz, A.; Forys, K.; Rapacka-Zdonczyk, A.; Kawiak, A.; Domachowska, A.; Golunski, G.; Wolz, C.; Mesak, L.; Becker, K.; et al. Fine-tuning recA expression in *Staphylococcus aureus* for antimicrobial photoinactivation: Importance of photo-induced DNA damage in the photoinactivation mechanism. *Appl. Microbiol. Biotechnol.* **2015**, *99*, 9161–9176. [[CrossRef](#)]
46. Sabbahi, S.; Ben Ayed, L.; Jemli, M. *Staphylococcus aureus* photodynamic inactivation mechanisms by rose bengal: Use of antioxidants and spectroscopic study. *Appl. Water Sci.* **2018**, *8*, 1–9. [[CrossRef](#)]
47. Silva, A.F.; Borges, A.; Freitas, C.F.; Hioka, N.; Mikcha, J.M.G.; Simões, M. Antimicrobial Photodynamic Inactivation Mediated by Rose Bengal and Erythrosine Is Effective in the Control of Food-Related Bacteria in Planktonic and Biofilm States. *Molecules* **2018**, *23*, 2288. [[CrossRef](#)] [[PubMed](#)]
48. Dubey, T.; Gorantla, N.V.; Chandrashekara, K.T.; Chinnathambi, S. Photodynamic exposure of Rose-Bengal inhibits Tau aggregation and modulates cytoskeletal network in neuronal cells. *Sci. Rep.* **2020**, *10*, 12380. [[CrossRef](#)] [[PubMed](#)]
49. Wang, B.; Wang, J.H.; Liu, Q.; Huang, H.; Chen, M.; Li, K.; Li, C.; Yu, X.F.; Chu, P.K. Rose-bengal-conjugated gold nanorods for in vivo photodynamic and photothermal oral cancer therapies. *Biomaterials* **2014**, *35*, 1954–1966. [[CrossRef](#)]
50. Panzarini, E.; Inguscio, V.; Fimia, G.M.; Dini, L. Rose Bengal Acetate PhotoDynamic Therapy (RBAC-PDT) Induces Exposure and Release of Damage-Associated Molecular Patterns (DAMPs) in Human HeLa Cells. *PLoS ONE* **2014**, *9*, e105778. [[CrossRef](#)]
51. Amescua, G.; Arboleda, A.; Nikpoor, N.; Durkee, H.; Relhan, N.; Aguilar, M.C.; Flynn, H.W.; Miller, D.; Parel, J.M. Rose Bengal Photodynamic Antimicrobial Therapy: A Novel Treatment for Resistant Fusarium Keratitis. *Cornea* **2017**, *36*, 1141. [[CrossRef](#)]
52. Komagoe, K.; Kato, H.; Inoue, T.; Katsu, T. Continuous real-time monitoring of cationic porphyrin-induced photodynamic inactivation of bacterial membrane functions using electrochemical sensors. *Photochem. Photobiol. Sci.* **2011**, *10*, 1181–1188. [[CrossRef](#)]
53. Alarcón, E.; Edwards, A.M.; Aspée, A.; Borsarelli, C.D.; Lissi, E.A. Photophysics and photochemistry of rose bengal bound to human serum albumin. *Photochem. Photobiol. Sci.* **2009**, *8*, 933–943. [[CrossRef](#)] [[PubMed](#)]
54. Vatansever, F.; de Melo, W.C.M.A.; Avci, P.; Vecchio, D.; Sadasivam, M.; Gupta, A.; Chandran, R.; Karimi, M.; Parizotto, N.A.; Yin, R.; et al. Antimicrobial strategies centered around reactive oxygen species—Bactericidal antibiotics, photodynamic therapy, and beyond. *FEMS Microbiol. Rev.* **2013**, *37*, 955–989. [[CrossRef](#)] [[PubMed](#)]
55. Rosini, R.; Margarit, I. Biofilm formation by *Streptococcus agalactiae*: Influence of environmental conditions and implicated virulence factor. *Front. Cell. Infect. Microbiol.* **2015**, *5*, 2013–2016. [[CrossRef](#)] [[PubMed](#)]
56. Ravel, J.; Gajer, P.; Abdo, Z.; Schneider, G.M.; Koenig, S.S.K.; McCulle, S.L.; Karlebach, S.; Gorle, R.; Russell, J.; Tacket, C.O.; et al. Vaginal microbiome of reproductive-age women. *Proc. Natl. Acad. Sci. USA* **2011**, *108*, 4680–4687. [[CrossRef](#)] [[PubMed](#)]
57. Hauschild, T.; Schwarz, S. Differentiation of *Staphylococcus sciuri* Strains Isolated from Free-Living Rodents and Insectivores. *J. Vet. Med. Ser. B* **2003**, *50*, 241–246. [[CrossRef](#)] [[PubMed](#)]
58. Nemeghaire, S.; Argudín, M.A.; Feßler, A.T.; Hauschild, T.; Schwarz, S.; Butaye, P. The ecological importance of the *Staphylococcus sciuri* species group as a reservoir for resistance and virulence genes. *Vet. Microbiol.* **2014**, *171*, 342–356. [[CrossRef](#)]
59. Hagner, S.; Harb, H.; Zhao, M.; Stein, K.; Holst, O.; Ege, M.J.; Mayer, M.; Matthes, J.; Bauer, J.; Von Mutius, E.; et al. Farm-derived Gram-positive bacterium *Staphylococcus sciuri* W620 prevents asthma phenotype in HDM- and OVA-exposed mice. *Allergy* **2013**, *68*, 322–329. [[CrossRef](#)]

60. Guerrero-Beltrán, C.; Garcia-Heredia, I.; Ceña-Diez, R.; Rodriguez-Izquierdo, I.; Serramía, M.J.; Martinez-Hernandez, F.; Lluesma-Gomez, M.; Martinez-Garcia, M.; Muñoz-Fernández, M.Á. Cationic Dendrimer G2-S16 Inhibits Herpes Simplex Type 2 Infection and Protects Mice Vaginal Microbiome. *Pharmaceutics* **2020**, *12*, 515. [[CrossRef](#)]
61. Noguchi, K.; Tsukumi, K.; Urano, T. Qualitative and quantitative differences in normal vaginal flora of conventionally reared mice, rats, hamsters, rabbits, and dogs. *Comp. Med.* **2003**, *53*, 404–412. Available online: <https://pubmed.ncbi.nlm.nih.gov/14524417/> (accessed on 24 March 2023).

Disclaimer/Publisher’s Note: The statements, opinions and data contained in all publications are solely those of the individual author(s) and contributor(s) and not of MDPI and/or the editor(s). MDPI and/or the editor(s) disclaim responsibility for any injury to people or property resulting from any ideas, methods, instructions or products referred to in the content.

Summary

Before the implementation of the results from *in vitro* experiments into clinical settlement several aspects need to be considered. Optimal future therapy should have a strong antibacterial effect not only against the planktonic culture of the species of interest but also against biofilm. It should have a limited effect on other bacterial species, especially on physiological flora. It should maintain its antibacterial properties not only in monoculture but also in multispecies environments. If the above requirements are fulfilled, the next step should include verification if the development of resistance to examined therapy is highly probable, or unlikely. Further, this therapy should not be toxic for human tissues and should not have a mutagenic effect, which would increase the probability of side effects. Then, if the results of all *in vitro* tests look promising, *in vivo* experimental models could be implemented. The transition from bench to clinic is always connected with some obstacles. Conversion of the experimental settings into another, a more complicated model often is exposed to unpredictable factors. Nevertheless, future therapy still should be effective and safe at the same time.

RB-mediated aPDI is highly effective in the eradication of *S. agalactiae* in both planktonic and biofilm cultures. It has a weaker impact on human vaginal *Lactobacilli* than on *S. agalactiae*. Its toxicity against human epithelial cells and mutagenic effect on both prokaryotic and eukaryotic cells are within reasonable limits. Development of tolerance due to multiple sub-lethal dose treatments was observed, but it was far from a resistance. Finally, despite being used as a single dose and with low power light source, RB-mediated aPDI turned out to significantly decrease the viability of *S. agalactiae* in the murine model of vaginal colonization, had no significant impact on the murine tissue and limited impact on physiological flora. Therefore, all assumed aims were reached and the assumed hypothesis was confirmed.

On that account, I conclude that with further investigation, and maybe use as a combined and not monotherapy, RB-mediated aPDI has a great potential to be routinely used in hospital settings.

Literature

1. Infectious Diseases of the Fetus and Newborn E-Book - Jack S. Remington, Christopher B. Wilson, Victor Nizet, Jerome O. Klein, Yvonne Maldonado - Google Książki Available online:
https://books.google.pl/books?hl=pl&lr=&id=5ECgVBNQDUMC&oi=fnd&pg=PP1&dq=Wilson,+C.+B.,+Nizet,+V.,+Malsonado,+Y.,+Remington,+J.+S.+%26+Klein+J.+O.+Infectious+Diseases+of+the+Fetus+and+Newborn+Infant+8th+edn+Saunder+Elsevier,+2016&ots=TJfboIZo_5&sig=BRNSI7zhywMyrr22bC1MVMNAu90&redir_esc=y#v=onepage&q&f=false (accessed on 22 February 2023).
2. Morgan, J.A.; Cooper, D.B. *Group B Streptococcus And Pregnancy*; StatPearls Publishing, 2018;
3. Shet, A.; Ferrieri, P. *Neonatal & Maternal Group B Streptococcal Infections: A Comprehensive Review*; 2004; Vol. 120;
4. Kohli-Lynch, M.; Russell, N.J.; Seale, A.C.; Dangor, Z.; Tann, C.J.; Baker, C.J.; Bartlett, L.; Cutland, C.; Gravett, M.G.; Heath, P.T.; et al. Neurodevelopmental Impairment in Children After Group B Streptococcal Disease Worldwide: Systematic Review and Meta-Analyses. *Clin. Infect. Dis.* **2017**, *65*, S190–S199, doi:10.1093/CID/CIX663.
5. Prevention of Group B Streptococcal Early-Onset Disease in Newborns: ACOG Committee Opinion, Number 797. *Obstet. Gynecol.* **2020**, *135*, e51–e72, doi:10.1097/AOG.0000000000003668.
6. Seki, T.; Kimura, K.; Reid, M.E.; Miyazaki, A.; Banno, H.; Jin, W.; Wachino, J.; Yamada, K.; Arakawa, Y. High Isolation Rate of MDR Group B Streptococci with Reduced Penicillin Susceptibility in Japan. *J. Antimicrob. Chemother.* **2015**, *70*, 2725–2728, doi:10.1093/jac/dkv203.
7. Navarro-Torné, A.; Curcio, D.; Moisi, J.C.; Jodar, L. Burden of Invasive Group B Streptococcus Disease in Non-Pregnant Adults: A Systematic Review and Meta-Analysis. *PLoS One* **2021**, *16*, e0258030, doi:10.1371/JOURNAL.PONE.0258030.
8. Koide, S.; Nagano, Y.; Takizawa, S.; Sakaguchi, K.; Soga, E.; Hayashi, W.; Tanabe, M.; Denda, T.; Kimura, K.; Arakawa, Y.; et al. Genomic Traits Associated with Virulence and Antimicrobial Resistance of Invasive Group B Streptococcus Isolates with Reduced Penicillin Susceptibility from Elderly Adults. *Microbiol. Spectr.* **2022**, *10*, doi:10.1128/SPECTRUM.00568-22/SUPPL_FILE/SPECTRUM.00568-22-S0001.PDF.
9. Phuoc, N.N.; Linh, N.T.H.; Crestani, C.; Zadoks, R.N. Effect of Strain and Environmental Conditions on the Virulence of Streptococcus Agalactiae (Group B Streptococcus; GBS) in Red Tilapia (*Oreochromis Sp.*). *Aquaculture* **2021**, *534*, 736256, doi:10.1016/J.AQUACULTURE.2020.736256.
10. Lakew, B.T.; Fayera, T.; Ali, Y.M. Risk Factors for Bovine Mastitis with the Isolation and Identification of Streptococcus Agalactiae from Farms in and

- around Haramaya District, Eastern Ethiopia. *Trop. Anim. Health Prod.* **2019**, *51*, 1507–1513, doi:10.1007/S11250-019-01838-W/TABLES/4.
11. Boonyayatra, S.; Wongsathein, D.; Tharavichitkul, P. Genetic Relatedness Among *Streptococcus Agalactiae* Isolated from Cattle, Fish, and Humans*. <https://home.liebertpub.com/afpd> **2020**, *17*, 137–143, doi:10.1089/FPD.2019.2687.
 12. Barkham, T.; Zadoks, R.N.; Azmai, M.N.A.; Baker, S.; Bich, V.T.N.; Chalker, V.; Chau, M.L.; Dance, D.; Deepak, R.N.; van Doorn, H.R.; et al. One Hypervirulent Clone, Sequence Type 283, Accounts for a Large Proportion of Invasive *Streptococcus Agalactiae* Isolated from Humans and Diseased Tilapia in Southeast Asia. *PLoS Negl. Trop. Dis.* **2019**, *13*, e0007421, doi:10.1371/JOURNAL.PNTD.0007421.
 13. Yao, Y.-Y.; Chen, D.-D.; Cui, Z.-W.; Zhang, X.-Y.; Zhou, Y.-Y.; Guo, X.; Li, A.-H.; Zhang, Y.-A. Oral Vaccination of Tilapia against *Streptococcus Agalactiae* Using *Bacillus Subtilis* Spores Expressing Sip. *Fish Shellfish Immunol.* **2019**, *86*, 999–1008, doi:10.1016/j.fsi.2018.12.060.
 14. Zhang, D.; Gao, Y.; Li, Q.; Ke, X.; Liu, Z.; Lu, M.; Shi, C. An Effective Live Attenuated Vaccine against *Streptococcus Agalactiae* Infection in Farmed Nile Tilapia (*Oreochromis Niloticus*). *Fish Shellfish Immunol.* **2020**, *98*, 853–859, doi:10.1016/J.FSI.2019.11.044.
 15. Tsang, R.S.W. A Narrative Review of the Molecular Epidemiology and Laboratory Surveillance of Vaccine Preventable Bacterial Meningitis Agents: *Streptococcus Pneumoniae*, *Neisseria Meningitidis*, *Haemophilus Influenzae* and *Streptococcus Agalactiae*. *Microorganisms* **2021**, *9*, 1–19, doi:10.3390/microorganisms9020449.
 16. van der Linden, M.; Jaschek, M.; Junker, J.; Levina, N.; Weidenhaupt, B. Evaluation of the “HG Group B *Streptococcus*” Loop-Mediated Isothermal Amplification Assay for Accurate Identification of *Streptococcus Agalactiae*. *J. Med. Microbiol.* **2022**, *71*, 001609, doi:10.1099/JMM.0.001609/CITE/REFWORKS.
 17. Khan, U.B.; Jauneikaite, E.; Andrews, R.; Chalker, V.J.; Spiller, O.B. Identifying Large-Scale Recombination and Capsular Switching Events in *Streptococcus Agalactiae* Strains Causing Disease in Adults in the UK between 2014 and 2015. *Microb. Genomics* **2022**, *8*, 000783, doi:10.1099/MGEN.0.000783/CITE/REFWORKS.
 18. Bacterial Biofilms - Google Książki Available online: https://books.google.pl/books?hl=pl&lr=&id=5pUtEAAAQBAJ&oi=fnd&pg=PA135&dq=biofilm+antibiotic+penetration&ots=HKWLpase1p&sig=rOqqR8o-eXxs79W_Gzu9YvDpFus&redir_esc=y#v=onepage&q=biofilm+antibiotic+penetration&f=false (accessed on 30 March 2023).
 19. Muzny, C.A.; Schwebke, J.R. Biofilms: An Underappreciated Mechanism of Treatment Failure and Recurrence in Vaginal Infections. *Clin. Infect. Dis.* **2015**, *61*, 601–606, doi:10.1093/cid/civ353.
 20. D’Urzo, N.; Martinelli, M.; Pezzicoli, A.; De Cesare, V.; Pinto, V.; Margarit, I.;

- Telford, J.L.; Maione, D.; Melin, P.; Decheva, A.; et al. Acidic PH Strongly Enhances in Vitro Biofilm Formation by a Subset of Hypervirulent ST-17 *Streptococcus Agalactiae* Strains. *Appl. Environ. Microbiol.* **2014**, *80*, 2176–2185, doi:10.1128/AEM.03627-13.
21. Ventolini, G. Vaginal Lactobacillus: Biofilm Formation in Vivo – Clinical Implications. *Int. J. Womens. Health* **2015**, *7*, 243–247, doi:10.2147/IJWH.S77956.
 22. Vatansever, F.; de Melo, W.C.M.A.; Avci, P.; Vecchio, D.; Sadasivam, M.; Gupta, A.; Chandran, R.; Karimi, M.; Parizotto, N.A.; Yin, R.; et al. Antimicrobial Strategies Centered around Reactive Oxygen Species – Bactericidal Antibiotics, Photodynamic Therapy, and Beyond. *FEMS Microbiol. Rev.* **2013**, *37*, 955–989, doi:10.1111/1574-6976.12026.
 23. Cieplik, F.; Deng, D.; Crielaard, W.; Buchalla, W.; Hellwig, E.; Al-Ahmad, A.; Maisch, T. Antimicrobial Photodynamic Therapy – What We Know and What We Don't. *Crit. Rev. Microbiol.* **2018**, *44*, 571–589, doi:10.1080/1040841X.2018.1467876.
 24. Wang, X.; Zhao, X.; Malik, M.; Drlica, K. Contribution of Reactive Oxygen Species to Pathways of Quinolone-Mediated Bacterial Cell Death. *J. Antimicrob. Chemother.* **2010**, *65*, 520–524, doi:10.1093/JAC/DKP486.
 25. Vanerio, N.; Stijnen, M.; De Mol, B.A.J.M.; Kock, L.M. Biomedical Applications of Photo- and Sono-Activated Rose Bengal: A Review. <https://home.liebertpub.com/photob> **2019**, *37*, 383–394, doi:10.1089/PHOTOB.2018.4604.
 26. Nakonieczna, J.; Wozniak, A.; Pieranski, M.; Rapacka-Zdonczyk, A.; Ogonowska, P.; Grinholc, M. Photoinactivation of ESKAPE Pathogens: Overview of Novel Therapeutic Strategy. *Future Med. Chem.* **2019**, *11*, 443–461, doi:10.4155/fmc-2018-0329.
 27. Maclean, M.; MacGregor, S.J.; Anderson, J.G.; Woolsey, G. Inactivation of Bacterial Pathogens Following Exposure to Light from a 405-Nanometer Light-Emitting Diode Array. *Appl. Environ. Microbiol.* **2009**, *75*, 1932–1937, doi:10.1128/AEM.01892-08/ASSET/94803841-F356-4D49-ABBE-7097E5D6828B/ASSETS/GRAPHIC/ZAM0070997720004.JPEG.
 28. Hirose, M.; Yoshida, Y.; Horii, K.; Hasegawa, Y.; Shibuya, Y. Efficacy of Antimicrobial Photodynamic Therapy with Rose Bengal and Blue Light against Cariogenic Bacteria. *Arch. Oral Biol.* **2021**, *122*, 105024, doi:10.1016/J.ARCHORALBIO.2020.105024.
 29. Maraccini, P.A.; Wenk, J.; Boehm, A.B. Photoinactivation of Eight Health-Relevant Bacterial Species: Determining the Importance of the Exogenous Indirect Mechanism. *Environ. Sci. Technol.* **2016**, *50*, 5050–5059, doi:10.1021/ACS.EST.6B00074/SUPPL_FILE/ES6B00074_SI_001.PDF.
 30. Spesia, M.B.; Durantini, E.N. Photodynamic Inactivation Mechanism of *Streptococcus Mitis* Sensitized by Zinc(II) 2,9,16,23-Tetrakis[2-(N,N,N-Trimethylamino)Ethoxy]Phthalocyanine. *J. Photochem. Photobiol. B Biol.* **2013**,

- 125, 179–187, doi:10.1016/J.JPHOTOBIOLOG.2013.06.007.
31. Moreira, L.H.; de Souza, J.C.P.; de Lima, C.J.; Salgado, M.A.C.; Fernandes, A.B.; Andreani, D.I.K.; Villaverde, A.B.; Zângaro, R.A. Use of Photodynamic Therapy in the Treatment of Bovine Subclinical Mastitis. *Photodiagnosis Photodyn. Ther.* **2018**, *21*, 246–251, doi:10.1016/J.PDPDT.2017.12.009.
 32. Bumah, V.V.; Morrow, B.N.; Cortez, P.M.; Bowman, C.R.; Rojas, P.; Masson-Meyers, D.S.; Suprpto, J.; Tong, W.G.; Enwemeka, C.S. The Importance of Porphyrins in Blue Light Suppression of *Streptococcus Agalactiae*. *J. Photochem. Photobiol. B Biol.* **2020**, *212*, 111996, doi:10.1016/J.JPHOTOBIOLOG.2020.111996.
 33. Sellera, F.P.; Sabino, C.P.; Ribeiro, M.S.; Gargano, R.G.; Benites, N.R.; Melville, P.A.; Pogliani, F.C. In Vitro Photoinactivation of Bovine Mastitis Related Pathogens. *Photodiagnosis Photodyn. Ther.* **2016**, *13*, 276–281, doi:10.1016/j.pdpdt.2015.08.007.
 34. Li, R.; Yuan, L.; Jia, W.; Qin, M.; Wang, Y. Effects of Rose Bengal- and Methylene Blue-Mediated Potassium Iodide-Potentiated Photodynamic Therapy on *Enterococcus Faecalis*: A Comparative Study. *Lasers Surg. Med.* **2021**, *53*, 400–410, doi:10.1002/LSM.23299.
 35. Siddiqui, S.H.; Awan, K.H.; Javed, F. Bactericidal Efficacy of Photodynamic Therapy against *Enterococcus Faecalis* in Infected Root Canals: A Systematic Literature Review. *Photodiagnosis Photodyn. Ther.* **2013**, *10*, 632–643, doi:10.1016/J.PDPDT.2013.07.006.
 36. Rapacka-Zdonczyk, A.; Wozniak, A.; Pieranski, M.; Woziwodzka, A.; Bielawski, K.P.; Grinholc, M. Development of *Staphylococcus Aureus* Tolerance to Antimicrobial Photodynamic Inactivation and Antimicrobial Blue Light upon Sub-Lethal Treatment. *Sci. Rep.* **2019**, *9*, 1–18, doi:10.1038/s41598-019-45962-x.

Attachments

1. Statements of contribution

Gdańsk, 17.05.2022 r.

MSc Eng Michał Brasel
Faculty of Electrical Engineering
West Pomeranian University of Technology
26 Kwietnia 10
71-126, Szczecin

Co-authorship statement

I hereby declare my contribution to the publication:

Brasel, M., Pieranski, M., & Grinholc, M. (2020). **An extended logistic model of photodynamic inactivation for various levels of irradiance using the example of Streptococcus agalactiae.** Scientific Reports, 10(1), 1-17; <https://doi.org/10.1038/s41598-020-71033-7>.

As follows:

	Ideas	Work	Writing	Stewardship	Adjusted Authorship contribution
Co-author	10%	40%	40%	10%	%
M. Brasel	50	60	70	45	60
M. Pieranski	30	40	10	20	30
M. Grinholc	20	0	20	35	10

Michał Brasel

Signature

Gdańsk, 13.05.2022 r.

MSc Michał Pierański
Laboratory of Photobiology and Molecular Diagnostics
Intercollegiate Faculty of Biotechnology
University of Gdansk and Medical University of Gdansk
Abrahama 58
80-307 Gdańsk

Co-authorship statement

I hereby declare my contribution to the publication:

Brasel, M., Pieranski, M., & Grinholc, M. (2020). **An extended logistic model of photodynamic inactivation for various levels of irradiance using the example of *Streptococcus agalactiae***. Scientific Reports, 10(1), 1-17; <https://doi.org/10.1038/s41598-020-71033-7>.

As follows:

	Ideas	Work	Writing	Stewardship	Adjusted Authorship contribution
Co-author	10%	40%	40%	10%	%
M. Brasel	50	60	70	45	60
M. Pieranski	30	40	10	20	30
M. Grinholc	20	0	20	35	10



Signature

Gdańsk, 16.05.2022 r.

Dr hab. Mariusz Grinholc, prof. UG
Laboratory of Photobiology and Molecular Diagnostics
Intercollegiate Faculty of Biotechnology
University of Gdansk and Medical University of Gdansk
Abrahama 58
80-307 Gdańsk

Co-authorship statement

I hereby declare my contribution to the publication:

Brasel, M., Pieranski, M., & Grinholc, M. (2020). **An extended logistic model of photodynamic inactivation for various levels of irradiance using the example of *Streptococcus agalactiae*.** Scientific Reports, 10(1), 1-17; <https://doi.org/10.1038/s41598-020-71033-7>.

As follows:

	Ideas	Work	Writing	Stewardship	Adjusted Authorship contribution
Co-author	10%	40%	40%	10%	%
M. Brasel	50	60	70	45	60
M. Pieranski	30	40	10	20	30
M. Grinholc	20	0	20	35	10

Zakład Fotobiologii i Diagnostyki
Molekularnej


dr hab. Mariusz Grinholc, prof. UG

.....
Signature

Gdańsk, 13.05.2022 r.

MSc Michał Pierański
Laboratory of Photobiology and Molecular Diagnostics
Intercollegiate Faculty of Biotechnology
University of Gdansk and Medical University of Gdansk
Abrahama 58
80-307 Gdańsk

Co-authorship statement

I hereby declare my contribution to the publication:

Pieranski, M., Sitkiewicz, I., & Grinholc, M. (2020). **Increased photoinactivation stress tolerance of *Streptococcus agalactiae* upon consecutive sublethal phototreatments.** Free Radical Biology and Medicine, 160, 657-669; <https://doi.org/10.1016/j.freeradbiomed.2020.09.003>.

As follows:

	Ideas	Work	Writing	Stewardship	Adjusted Authorship contribution
Co-author	10%	40%	40%	10%	%
M. Pieranski	40	100	20	40	60
I. Sitkiewicz	10	0	10	0	5
M. Grinholc	50	0	70	60	35



Signature

Warszawa, 17.05.2022 r.

Prof. Dr hab. Izabela Sitkiewicz
Center for Translational Medicine
Warsaw University of Life Sciences
Nowoursynowska 100
02-797 Warszawa

Co-authorship statement

I hereby declare my contribution to the publication:

Pieranski, M., Sitkiewicz, I., & Grinholc, M. (2020). **Increased photoinactivation stress tolerance of *Streptococcus agalactiae* upon consecutive sublethal phototreatments.** Free Radical Biology and Medicine, 160, 657-669; <https://doi.org/10.1016/j.freeradbiomed.2020.09.003>.

As follows:

	Ideas	Work	Writing	Stewardship	Adjusted Authorship contribution
Co-author	10%	40%	40%	10%	%
M. Pieranski	40	100	20	40	60
I. Sitkiewicz	10	0	10	0	5
M. Grinholc	50	0	70	60	35



Signature

Gdańsk, 16.05.2022 r.

Dr hab. Mariusz Grinholc, prof. UG
Laboratory of Photobiology and Molecular Diagnostics
Intercollegiate Faculty of Biotechnology
University of Gdansk and Medical University of Gdansk
Abrahama 58
80-307 Gdańsk

Co-authorship statement

I hereby declare my contribution to the publication:

Pieranski, M., Sitkiewicz, I., & Grinholc, M. (2020). **Increased photoinactivation stress tolerance of *Streptococcus agalactiae* upon consecutive sublethal phototreatments.** Free Radical Biology and Medicine, 160, 657-669; <https://doi.org/10.1016/j.freeradbiomed.2020.09.003>.

As follows:

	Ideas	Work	Writing	Stewardship	Adjusted Authorship contribution
Co-author	10%	40%	40%	10%	%
M. Pieranski	40	100	20	40	60
I. Sitkiewicz	10	0	10	0	5
M. Grinholc	50	0	70	60	35

Zakład Fotobiologii i Diagnostyki
Molekularnej



.....dr hab. Mariusz Grinholc, prof. UG.....

Signature

Gdańsk, 13.05.2022 r.

MSc Michał Pierański
Laboratory of Photobiology and Molecular Diagnostics
Intercollegiate Faculty of Biotechnology
University of Gdansk and Medical University of Gdansk
Abrahama 58
80-307 Gdańsk

Co-authorship statement

I hereby declare my contribution to the publication:

Pieranski, M. K., Rychlowski, M., & Grinholc, M. (2021). **Optimization of *Streptococcus agalactiae* biofilm culture in a continuous flow system for photoinactivation studies.** *Pathogens*, 10(9), 1212; <https://doi.org/10.3390/pathogens10091212>

As follows:

	Ideas	Work	Writing	Stewardship	Adjusted Authorship contribution
Co-author	10%	40%	40%	10%	%
M. Pieranski	40	85	80	30	70
M. Rychlowski	10	15	10	0	10
M. Grinholc	50	0	10	70	20



Signature

Gdańsk, 16.05.2022 r.

Dr Michał Rychłowski
Laboratory of Virus Molecular Biology
Intercollegiate Faculty of Biotechnology
University of Gdansk and Medical University of Gdansk
Abrahama 58
80-307 Gdańsk

Co-authorship statement

I hereby declare my contribution to the publication:

Pieranski, M. K., Rychłowski, M., & Grinholc, M. (2021). **Optimization of *Streptococcus agalactiae* biofilm culture in a continuous flow system for photoinactivation studies.** *Pathogens*, 10(9), 1212; <https://doi.org/10.3390/pathogens10091212>

As follows:

	Ideas	Work	Writing	Stewardship	Adjusted Authorship contribution
Co-author	10%	40%	40%	10%	%
M. Pieranski	40	85	80	30	70
M. Rychłowski	10	15	10	0	10
M. Grinholc	50	0	10	70	20



Signature

 UNIVERSITY OF GDAŃSK
MEDICAL UNIVERSITY OF GDAŃSK
Department of Virus Molecular Biology
Intercollegiate Faculty of Biotechnology
Antoniego Abrahama 58, 80-307 Gdańsk, Poland
T 58 523-63-35, F +48 58 523-64-31

Gdańsk, 16.05.2022 r.

Dr hab. Mariusz Grinholc, prof. UG
Laboratory of Photobiology and Molecular Diagnostics
Intercollegiate Faculty of Biotechnology
University of Gdansk and Medical University of Gdansk
Abrahama 58
80-307 Gdańsk

Co-authorship statement

I hereby declare my contribution to the publication:

Pieranski, M. K., Rychlowski, M., & Grinholc, M. (2021). Optimization of *Streptococcus agalactiae* biofilm culture in a continuous flow system for photoinactivation studies. *Pathogens*, 10(9), 1212; <https://doi.org/10.3390/pathogens10091212>

As follows:

	Ideas	Work	Writing	Stewardship	Adjusted Authorship contribution
Co-author	10%	40%	40%	10%	%
M. Pieranski	40	85	80	30	70
M. Rychlowski	10	15	10	0	10
M. Grinholc	50	0	10	70	20

Zakład Fotobiologii i Diagnostyki
Molekularnej



dr hab. Mariusz Grinholc, prof. UG

Signature

Gdańsk, 30.03.2023 r.

MSc Michał Pierański
Laboratory of Photobiology and Molecular Diagnostics
Intercollegiate Faculty of Biotechnology
University of Gdansk and Medical University of Gdansk
Abrahama 58
80-307 Gdańsk

Co-authorship statement

I hereby declare my contribution to the publication:

Michał K. Pierański; Jan G. Kosiński; Klaudia Szymczak; Piotr Sadowski; Mariusz Grinholc. „Antimicrobial photodynamic inactivation: an alternative for Group B Streptococcus vaginal colonization in a murine experimental model”. Antioxidants (ISSN 2076-3921).

As follows:

	Ideas	Work	Writing	Stewardship	Adjusted Authorship contribution
Co-author	10%	40%	40%	10%	%
M. Pierański	30	70	40	30	50
J. Kosiński	10	10	10	0	10
K. Szymczak	5	10	5	0	5
P. Sadowski	5	10	5	0	5
M. Grinholc	50	0	40	70	30



Signature

Poznań, 30.03.2023 r.

MSc Jan G. Kosiński
Department of Computational Biology
Institute of Molecular Biology and Biotechnology
Faculty of Biology, Adam Mickiewicz University in Poznań
Uniwersytetu Poznańskiego 6
61-614 Poznań

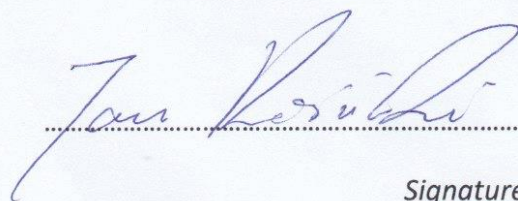
Co-authorship statement

I hereby declare my contribution to the publication:

Michał K. Pierański; Jan G. Kosiński; Klaudia Szymczak; Piotr Sadowski; Mariusz Grinholc. „*Antimicrobial photodynamic inactivation: an alternative for Group B Streptococcus vaginal colonization in a murine experimental model*”. *Antioxidants* (ISSN 2076-3921).

As follows:

	Ideas	Work	Writing	Stewardship	Adjusted Authorship contribution
Co-author	10%	40%	40%	10%	%
M. Pierański	30	70	40	30	50
J. Kosiński	10	10	10	0	10
K. Szymczak	5	10	5	0	5
P. Sadowski	5	10	5	0	5
M. Grinholc	50	0	40	70	30



.....

Signature

Gdańsk, 30.03.2023 r.

MSc Klaudia Szymczak
Laboratory of Photobiology and Molecular Diagnostics
Intercollegiate Faculty of Biotechnology
University of Gdansk and Medical University of Gdansk
Abrahama 58
80-307 Gdańsk

Co-authorship statement

I hereby declare my contribution to the publication:

Michał K. Pierański; Jan G. Kosiński; Klaudia Szymczak; Piotr Sadowski; Mariusz Grinholc. „*Antimicrobial photodynamic inactivation: an alternative for Group B Streptococcus vaginal colonization in a murine experimental model*”. Antioxidants (ISSN 2076-3921).

As follows:

	Ideas	Work	Writing	Stewardship	Adjusted Authorship contribution
Co-author	10%	40%	40%	10%	%
M. Pierański	30	70	40	30	50
J. Kosiński	10	10	10	0	10
K. Szymczak	5	10	5	0	5
P. Sadowski	5	10	5	0	5
M. Grinholc	50	0	40	70	30


.....

Signature

Kraków, 30.03.2023 r.

MD Piotr Sadowski
Department of Pathomorphology
University Hospital in Kraków
Kopernika 36
31-501 Kraków


Co-authorship statement

I hereby declare my contribution to the publication:

Michał K. Pierański; Jan G. Kosiński; Klaudia Szymczak; Piotr Sadowski; Mariusz Grinholc. „Antimicrobial photodynamic inactivation: an alternative for Group B Streptococcus vaginal colonization in a murine experimental model”. Antioxidants (ISSN 2076-3921).

As follows:

	Ideas	Work	Writing	Stewardship	Adjusted Authorship contribution
Co-author	10%	40%	40%	10%	%
M. Pierański	30	70	40	30	50
J. Kosiński	10	10	10	0	10
K. Szymczak	5	10	5	0	5
P. Sadowski	5	10	5	0	5
M. Grinholc	50	0	40	70	30


.....

Signature

Gdańsk, 30.03.2023 r.

Dr hab. Mariusz Grinholc, prof. UG
Laboratory of Photobiology and Molecular Diagnostics
Intercollegiate Faculty of Biotechnology
University of Gdansk and Medical University of Gdansk
Abrahama 58
80-307 Gdańsk

Co-authorship statement

I hereby declare my contribution to the publication:

Michał K. Pierański; Jan G. Kosiński; Klaudia Szymczak; Piotr Sadowski; Mariusz Grinholc. „Antimicrobial photodynamic inactivation: an alternative for Group B Streptococcus vaginal colonization in a murine experimental model”. Antioxidants (ISSN 2076-3921).

As follows:

	Ideas	Work	Writing	Stewardship	Adjusted Authorship contribution
Co-author	10%	40%	40%	10%	%
M. Pierański	30	70	40	30	50
J. Kosiński	10	10	10	0	10
K. Szymczak	5	10	5	0	5
P. Sadowski	5	10	5	0	5
M. Grinholc	50	0	40	70	30



.....
Signature